On-line partial discharges detection in conversion systems used in aeronautics

Benjamin Cella

Université Fédérale
Toulouse Midi-Pyrénées

THÈSE

En vue de l'obtention du

DOCTORAT DE L'UNIVERSITÉ DE TOULOUSE

Délivré par :

Université Toulouse 3 Paul Sabatier (UT3 Paul Sabatier)

Présentée et soutenue par :
Benjamin Cella

le mercredi 2 décembre 2015

Titre :

On-line partial discharges detection in conversion systems used in aeronautics

---

École doctorale et discipline ou spécialité :
ED GEET : Génie Electrique

Unité de recherche :
Laplace Laboratory, UMR CNRS/UPS/INP, MDCE

Directeur/trice(s) de Thèse :

M. Thierry Lebey, CNRS Senior Research Scientist

Jury :
M. Ian Cotton, PhD, Professor - Manchester University, UK, Rapporteur
M. Daniel Roger, PhD, Professor - LSEE, Bethune, France, Rapporteur
M. Rodolphe De Maglie, Dr.-Ing, Research Engineer - Liebherr Elektronik GmbH, Lindau, Germany, Examiner
M. Thierry Lebey, CNRS Senior Research Scientist - Laplace Laboratory, Toulouse, France
M. David Malec, PhD, Research Director - Laplace Laboratory, Toulouse, France
M. Jean-Pascal Cambronne, PhD, Research Director - Laplace Laboratory, Toulouse, France

Abstract:

The more electrical airplane concept led industrial companies to focus a part of their efforts on risks linked to the use of high voltage in a severe environment (Low pressure, wide range of temperature and humidity …). Associated risks are the existence and the growing of partial discharges ultimately leading to the breakdown of the system in which they occur. Considering this problematic, the Liebherr Elektronik GmbH group, in collaboration with the Laplace laboratory, launched the study of a method allowing partial discharges detection in converters intended to be used in aeronautical applications. The results of this work are the subject of this thesis. The first part brings the status of the current knowledge about partial discharges from their physical nature to the detection methods which are used. In the second part, three measurement phases assessing the efficiency of the studied method are introduced and their results discussed. Finally, in the third part, the conclusions of our works and their perspectives are presented.

Keywords: Partial discharges, On-line, Aeronautics, PWM voltage, Non-intrusive sensor

Abstract (French):

Le concept de l'avion plus électrique a conduit les industriels à focaliser une partie de leurs efforts sur les risques liés à l'utilisation de la haute tension dans un environnement sévère (Basse pression, large plage de température et d'humidité …). Les risques associés sont l'existence et le développement de décharges partielles conduisant à terme à la défaillance du système dans lequel, elles se produisent. Considérant cette problématique, le groupe Liebherr Elektronik GmbH, en collaboration avec le laboratoire Laplace, a lancé l'étude d'une méthode permettant de détecter les décharges partielles dans des convertisseurs destinés à des applications aéronautiques. Ce sont les résultats de ce travail qui font l'objet de cette thèse. La première partie fait état des connaissances actuelles sur les décharges partielles, de leur nature physique aux méthodes de détection utilisées. Dans la seconde partie, trois phases de mesures validant l'efficacité de la méthode étudiée sont présentées et leurs résultats sont discutés. Enfin, dans une troisième partie, les conclusions de nos travaux et leurs perspectives sont présentées.

Keywords: Décharges partielles, On-line, Aéronautique, Tension MLI, Capteur non-intrusif

À mes merveilleuses grands-mères, Yvette Sanvicens, Francine Cella.

À la mémoire de mes grands-pères, Albert Sanvicens, Mario Cella.

À tous ceux qui m'ont soutenu . . .

« Le doute est l'école de la vérité »
Francis Bacon

Acknowledgments

If it is true that a PhD thesis is not the work of only one person, this PhD thesis make clearly no exception considering the list of people who helped me and without whom this PhD would not have been possible.

First and foremost I wish to thank my supervisor, **Thierry Lebey**, head of research at CNRS and future director of the Laplace laboratory. If I should resume, in one word, his main virtue and his behavior regarding my work those last three years, I would say “patience”. Since the beginning of our relationship and despite the long distance between us, he always found out the time to guide me, the right words to teach me and an infinite tolerance to forgive my numerous ineptness. He has constantly been there when I was dealing with any problematics on the professional aspects as well as on other aspects of everyday life. A working session with him is always intensive but subtly sprinkle with happy times thanks to his unusual sense of humor which significantly metamorphoses the meaning of the term “working”. I definitely learned a lot by working with him, not only on my PhD subject aspects, but also on the rigor required by a scientific work. I wish one day, I will get the ability to smartly solve problems as he does. Those three years are already over, but this is just the beginning of a new step in my professional life, and thanks to him I feel ready to face it. Thierry, a huge and sincere “thank you” for everything you brought to me in barely three years.

The three years I spent in Germany would have been much more difficult and much less pleasant without the support of the one who can be considered as my second supervisor, **Rodolphe De Maglie**. He is the first one who encouraged me to do a PhD four years ago. Since then, he has been present for my integration in the Liebherr group, he supported me on every project related to the PhD or to Liebherr and he brought me reassurance when my brain was keeping saying “you will not succeed”. He taught me the aspects of an efficient engineer and researcher work in a constant happy ambiance. His ability to see the good sides on every problems has been a real asset that encouraged me to give the best of myself every time. He is always open to any subject and has an opinion on everything. I enjoyed spending time with him to discuss any topics during minutes or hours. He became more than a working colleague to me, he became a friend. I don’t know what the future will be made of, but I will not forget what I learned from him.

I would like to give a special thanks to **Alfred Engler**, head of the predevelopment department at Liebherr Elektronik GmbH. Since I was trainee at Liebherr four years ago, he never ceased to believe in me and he always pushed me to give the best of myself. He is a very intelligent and comprehensive leader who took me beyond my limits. I remember his first words when I started at Liebherr three years ago: “Mr. Cella, this is not a gift we are offering to you, this is a challenge!”. Today I clearly understand this sentence and I would like to answer: “Yes Mr. Engler, it was a real challenge! But nevertheless, thank you for this gift”.

I would like to thank **Ralph Cremer**, technical managing director of Liebherr Elektronik GmbH who welcomed me a first time, four years ago as a trainee and a second time, three years ago as an engineer and PhD student. Thanks to his support, I have spent a lot of time at the Laplace laboratory where the main results of my PhD came out. This PhD would not have been possible without his contribution.

I would like to sincerely and gratefully thank **Jean-Luc Maigne**, general director of Liebherr Toulouse who supported me for integrating the Liebherr group.

For this dissertation I would like to thank my reading committee members: **Ian Cotton** and **Daniel Robert**, for their time, interest, and relevant comments. I also would like to thanks the others members of this PhD jury, **Jean-Pascal Cambronne** and **David Malec**.

I would like to thank the members from the schools where I did my study before the PhD. **Eric Escande** and the complete team of the CESI engineer school in Toulouse. They always pushed me to give the best of myself. Thanks to them I realized that I had wings on my back. **Jean-Robert Gatonas**, physics teacher from the school Sainte Louise de Marillac in Perpignan, he brought me support to find an internship four years ago at Liebherr Elektronik GmbH. Thanks to him I discovered a wonderful country and I got the opportunity to do a PhD. **All my others teachers** from the school of Sainte Louise de Marillac in Perpignan. This school is the beginning of important things in my studies: my passion for electronics and the discovery that when I remove "the big hair in my hand" (French expression) I can achieve significant things.

I would like to thanks the different members of the **Liebherr company** I have worked with and especially from the **pre-development department**. Their professionalism and constant gladness brought me an ideal background to work. I also would like to thank the members of the **Laplace laboratory** for having being so friendly during my time in Toulouse. A special thanks to **Thibaut billard** and **Cerdic Abadie** for having helping me during some measurements phases and for their general friendship. Thanks to **Philippe Castelan** for his wise advices and for his general and so pleasant cheerfulness.

I would like to thank my family for its constant support and presence. **Audrey Cella** simply for being the ideal sister that anyone would like to have and for having being a model to me. My father, **Philippe Cella** who knows some parts of me better than myself and has always used it to push me up. My mother, **Florence Sanvicens** for her infinite patience with me and for being the spark who gave me the will to do scientific work with her cartesian mind. My wonderful grandmothers **Francine Cella** and **Yvette Sanvicens** who brought me and continue to bring me a quantity of love that has no equal. My mother and father in law **Chantal Arpajou** and **Jean-Francois Dalmau** for being the sweet treat which illuminates my days with their constant cheerfulness.

A special thanks to **George Bouvéry**, who brought me the taste of reading and warm moments in the narrow and mysterious streets of the old Perpignan. The constant happiness on his face is always a real pleasure. He is the proof that even the shadow can emit light.

I would like to thank **Marie-Aimée** and **Egon Eder** who helped me building my new life in Germany. Thanks to their constant kindness and patience, I succeeded to find my place in Lindau.

Finally, a unique thanks to my girlfriend, **Gaëlle Bouvéry**, who has been the closest person to me during these last three years. We lived this PhD together, the good and the bad sides, and she brought me the love and the comfort that I really needed in some "dark" situations. I am deeply grateful for the sacrifices she did and for the huge quantity of efforts she had to do to integrate the little Mediterranean girl to the Germanic country. Vielen Dank meine Liebe und … Blumen.

Benjamin Cella
Lindau, Germany
November 2015

Summary

1 INTRODUCTION

This chapter provides the background required to understand the context and purpose of this thesis. In the first section, we start by focusing on the evolution of electrical power embedded in airplanes. Then, we describe the concept of the "more electric aircraft." The last section describes the purpose of the work done for this thesis.

1.1 ENERGY EMBEDDED IN AIRPLANES

The most common architecture used in civil aircrafts is a combination of several kinds of energies, namely: pneumatic, mechanical, hydraulic and electrical. All of these secondary energies are created by the primary energy source based on the kerosene combustion in the main engines. Here is some example of the uses of these energies [Rosero]

- **Pneumatic**: This energy is mainly used to supply the Environmental Control System (ECS) and bring hot air for Wing-Anti-Icing (WAI) systems. The main drawbacks of pneumatic energy are its low efficiency and the difficulty to detect leaks.
- **Mechanical**: This energy is the link between the engines and hydraulic pumps, electrical generator, and other mechanically driven subsystems.
- **Hydraulic**: This energy is transferred from the central hydraulic pumps to the actuation systems for primary and secondary flight control, and to numerous other auxiliary systems. Hydraulic systems are very robust, but they are heavy and inflexible. Moreover, in the case of leakage, hydraulic fluid can degrade surrounding components due to its corrosive nature.
- **Electrical**: This energy is obtained through an electrical generator, supplying all electrical devices in an airplane (flight control actuation systems, lighting, entertainment systems, etc.). Electrical power require lighter infrastructure than hydraulic power and is more flexible. However, it has a lower power density than hydraulic power and the risk of fire is increased in the event of unexpected electrical discharges.

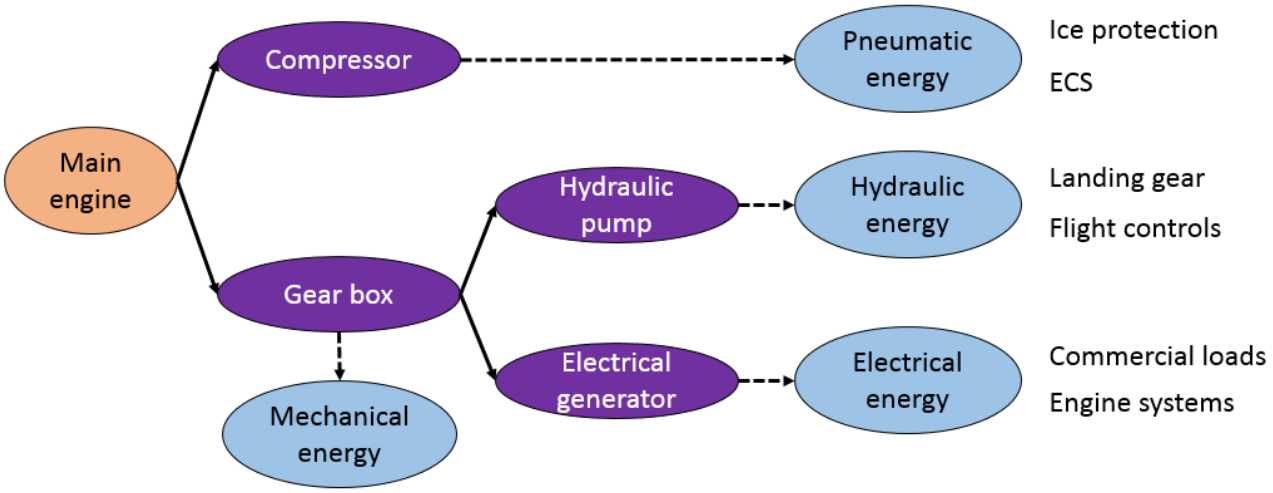

Figure 1: Example of conventional power distribution in airplanes

The electrical power embedded in airplanes has undergone constant evolution over recent decades. The main reasons for this include the general increase of electrical equipment on-board, and a desire to move towards a more electric aircraft overall.

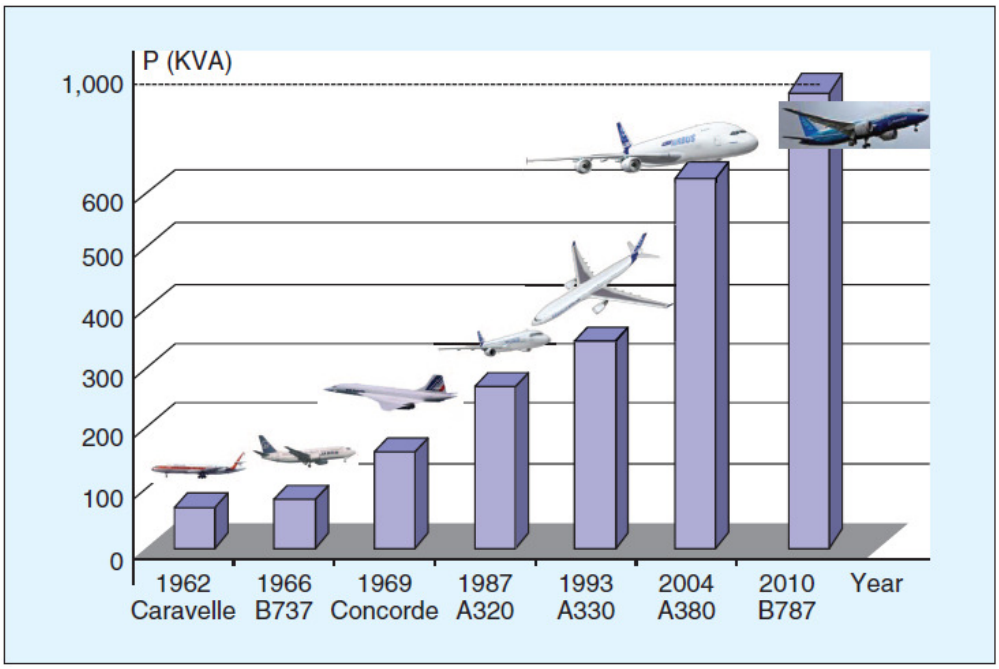

Figure 2: Evolution of the electrical power embedded in airplanes over recent decades [Roboam]

1.2 THE CONCEPT OF A "MORE ELECTRIC AIRCRAFT"

Considering the complexity of maintenance in conventional power distribution systems, it became clear that it would be advantageous to switch from a multi-power-source system to a system with mainly electrical power. As shown in Figure 3 the more electric concept simplifies the overall architecture. This explains why some airplane manufacturers are currently focusing on solutions which are more electric.

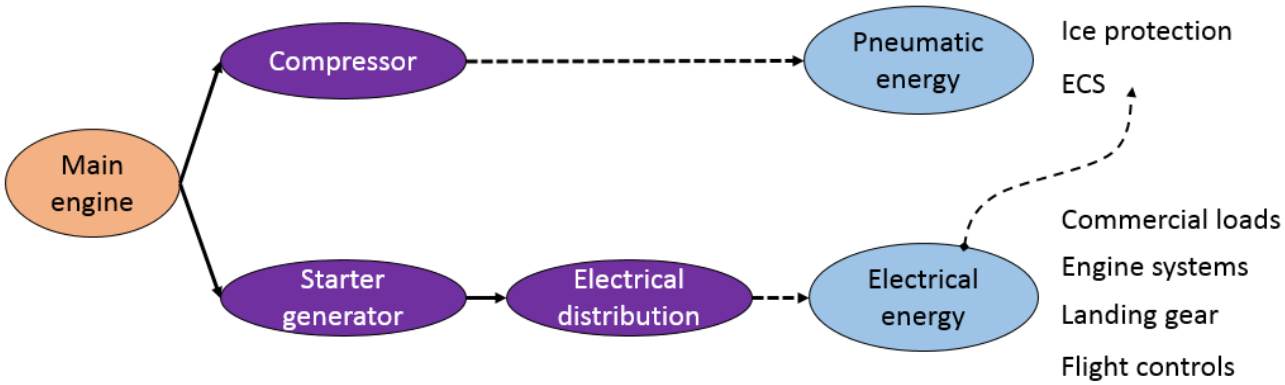

Figure 3: Schematic of distribution in a more electrical aircraft

As shown in Figure 3, most of the systems are supplied with electric power. Therefore the power demand is increased. Following this, increasing power means either increasing the voltage supplied by the power source, or increasing the maximum current that can be drawn from the power source. Increasing the latter element forces power cables to withstand greater amperage. This is achieved by increasing the diameter of cables. This change in dimension necessarily leads to an increase of the aircraft's weight. However, this is not an acceptable solution for industries who are trying, in parallel, to reduce the weight of the airplanes in order to minimize fuel consumption. Consequently the only acceptable way to increase available power in aircrafts is to increase the voltage of the power sources.

As an example, flight controls can be found on the wing of the airplane as shown in Figure 4. These systems drive, among other things, the FLAP and SLAT surfaces.

1.3 ISSUES AND PURPOSE OF THIS THESIS

Increasing the voltage to avoid burdening the aircraft, supresses one drawback and creates another one: increasing voltage may lead to the phenomenon of partial discharges. Consequently, many studies need to be performed in order to find out whether partial discharges exist in current power electronics systems.

In collaboration with the Laplace laboratory, the company Liebherr Elektronik GmbH has been focusing on this topic for several years. Their main objective was to develop a method capable of detecting partial discharges on-line in an aeronautic system.

1.3.1 LIEBHERR ELEKTRONIK GMBH

This division of the Liebherr group works on the electronic components in Liebherr systems, which includes the fields of construction machines and aircraft power electronics devices. The company developed, among other things, a power converter for the A350 airplane. This converter aims to control the flap assembly at the rear of the wings, as shown in Figure 4 and Figure 5.

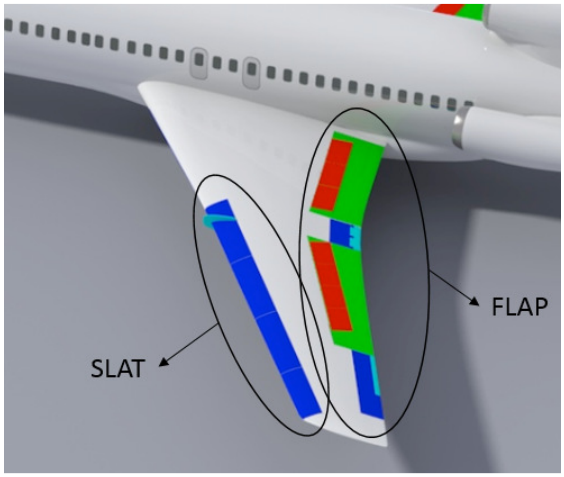

Figure 4: Slat and flap position on a wing

Figure 5: Controller for flight actuation in an A350 airplane

The controller in Figure 5 is part of the ADGB (Active Differential Gear Box) system. Two ADGBs are installed in each aircraft and are used to drive the FLAP on the wings. This system is comprised of a gear, power-off brake, various sensors, and a MCE (Motor Control Electronic). The MCE (Figure 5) operates a permanent magnet synchronous machine which drives the transmission for the outboard flap panel. Here is a description of the different elements of the MCE:

- PCE: The Power Control Electronic is an AC-to-PWM converter. It supplies the motor that controls the flap assembly at the rear of the wings.
- EPOB: The Electrical Power-Off Brake is a brake used to stabilize the flap.
- SEPOB: The Standby Electrical Power-Off Brake is a secondary EPOB.
- CU: The Controller Unit drives the MCE system.

This system is the platform which has been investigated for partial discharges detection in the frame of this PhD.

1.3.2 PURPOSE OF THE THESIS

The objective of this thesis, is to highlight whether or not partial discharges can occur in the PCE.

This target is reached by analyzing the electrical structure of the PCE and by applying a test methodology (*Figure 6*). The difficulty is to perform on-line partial discharges measurements in an aeronautical converter, since no efficient method has been developed at this time.

We therefore decided to focus on a relatively recent partial discharge detection method that has shown interesting results in the automotive field [Billard]. This new detection method was compared with the standard electrical method using a coupling capacitor and RLC filter. The objective of this collaboration work is two-fold, to:

- Validate the robustness of this new detection method in the aeronautical field.
- Determine whether PD can occur or be detected in a running PCE (on-line detection).

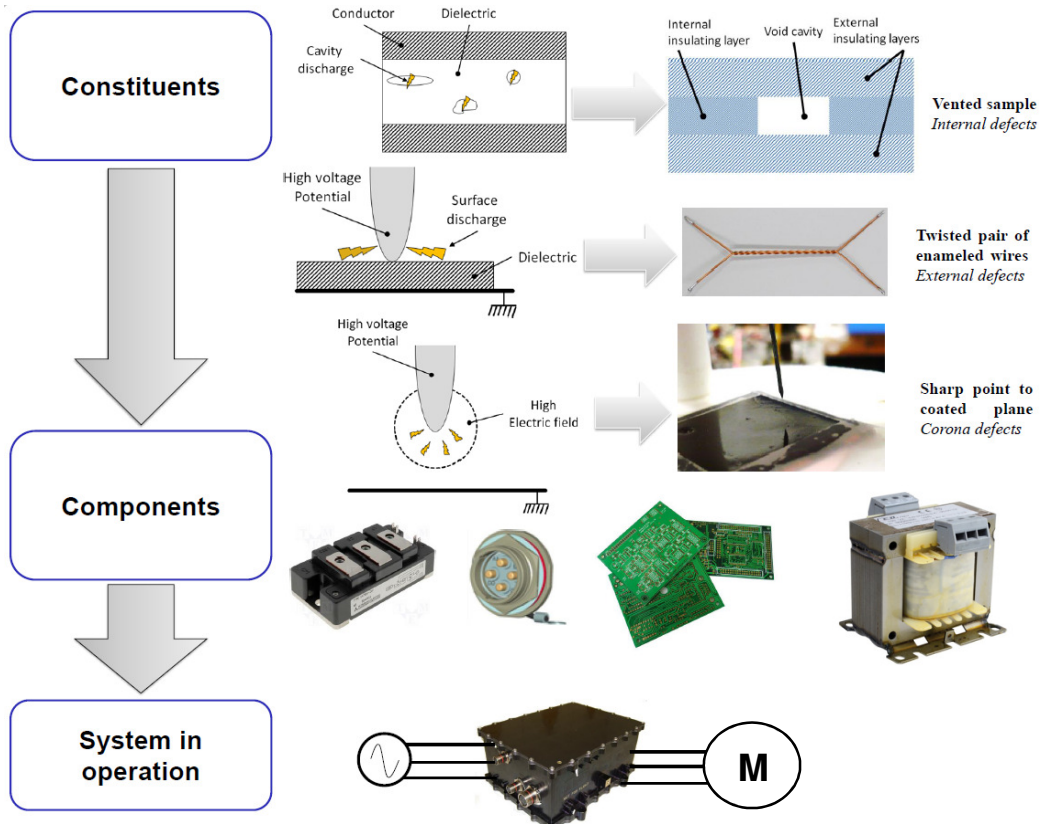

Figure 6: Test methodology applied during the complete study

The methodology used to reach these objectives is based on *Figure 6*. The first step consists of testing samples made with constituents or materials used in aerospace applications. Three types of defects are created and tested. A vented sample simulates an internal defect, a twisted pair of enamelled wire has external defects and a needle to plane sample has corona defects.
The second step is to test the individual components used in the PCE (IGBTs, diodes, connectors, PCBs, cabling etc.). The last step is to test the complete operating system (PCE + Cable + Motor). Each of these steps is described in the following chapters.

1.3.3 MAIN CONTRIBUTIONS

a) Scientific contributions

The most important contribution of this work is the on-line detection of partial discharges in an aeronautics converter. A partial discharge sensing method, using a non-intrusive sensor, has been used for this purpose. The studied method allows to make the distinction between partial discharges and the switching noise from the converter. Each tests have been done at low pressure to take into account altitude effects.

As a second contribution, this work allowed to draw a limitation of the sensing method. During the investigation of some samples submitted to low pressure, the nature of some discharges has changed from pulsed to pseudo-glow (c.f. 4.1.2.4) and no partial discharges were measurable although we proved that partial discharges were still occurring.

b) Industrial contributions

Thanks to this work, the company Liebherr Elektronik GmbH has now significant knowledges to lead deeper investigations around the partial discharges topic. With the development of the sensing method they have a tool allowing to assess their converters regarding partial discharges.

Another contribution is the development of a partial discharge free pulses generator which generates a voltage shape representative of the voltage used in aeronautical systems, namely an actual pulse width modulation. The maximum voltage can go up to 2kV. This laboratory tool will allow Liebherr to meet demand concerning the design of partial discharges free converters.

1.3.4 CONTENT

This document is organized into the following chapters:

Chapter 2: State of the art
This chapter brings the basics regarding the partial discharges topic. The different types of defects in which discharges may occur are described and the different natures of discharges that may exist are detailed. The influence of the environment on partial discharges is depicted and finally some detection and analysis methods are listed.

Chapter 3: An original method for detecting partial discharges in the aeronautical field
This chapter describes the method used to sense the partial discharges throughout this work. Physical aspects of the method are discussed and advantages and drawbacks are given.

Chapter 4: Experimental study
This chapter gathers the main results of the measurements. It is divided in three steps, first the measurements of some basic samples, second the measurements of some components from an aeronautics converter and third the measurement of a complete running converter. A detailed analysis of the results is made and interpretations are given.

Chapter 5: Conclusion
This chapter brings the conclusions of the overall works. The results of the previous chapters are gathered and analyzed. Futures potential works on the topic are detailed.

2 STATE OF THE ART

This chapter introduces the partial discharge phenomenon. To start, some basic definitions are provided, then the description of the discharge behaviour under different types of voltage (AC, PWM, DC) is investigated. Lastly, the effect of environmental conditions is studied.

2.1 SOME BASICS ABOUT PARTIAL DISCHARGES

2.1.1 DEFINITION

An electrical discharge that partially bridges the gap between two electrodes supplied by high voltage is called partial discharge. The occurrence of the phenomenon depends on factors such as temperature, pressure, humidity, insulation type and thickness, and of course, voltage magnitude and waveform applied between the electrodes.

Partial discharges are characterized by various parameters that are described below [IEC60270]:

The **partial discharge pulse** is the current or voltage pulse that results from a partial discharge that occurs within the object under test. The pulse is measured using suitable detector circuits, which are introduced into the test circuit for test purposes.

The **apparent charge (q)** is the charge (in Coulomb) that can be read by a measuring instrument at the terminals of the test sample. This value is different from the actual charge present in the discharge since not all the charges created in the defect reach the terminal of the sample where the measurement is performed.

The **pulse repetition frequency (N)** is the number of discharges measured in a second.

The **average discharge current (I)** is the sum of the absolute value of the charges in a period, divided by the period. $Tref$ is a chosen reference time interval.

$$I = \frac{1}{Tref} * \sum_{k=1}^{i} q_k$$

The **discharge power (P)** is the sum of the products of the value of the charges by voltage applied in a period, divided by the period. $Tref$ is a chosen reference time interval.

$$I = \frac{1}{Tref} * \sum_{k=1}^{i} (\mathrm{q_k} * u_k)$$

The **background noise** is the signal that can be measured when the test sample is not supplied by power. This characteristic must be measured before partial discharges measurements for calibration issue.

The **partial discharge inception voltage (PDIV)** is the applied voltage at which repetitive partial discharges are first observed in the test object, when the voltage applied to the object is gradually increased from a lower value at which no partial discharges are observed.

The **partial discharge extinction voltage (PDEV)** is the applied voltage at which repetitive partial discharges cease to occur in the test object, when the voltage applied to the object is decreased gradually from a higher value at which partial discharges pulse quantities are observed.

The **mean free path** is the average distance travelled by a moving particle between successive impacts, which modify its direction or energy.

2.1.2 TYPE OF DEFECTS

PD can be characterized by an extrinsic parameter: the type of defect allowing discharges to be ignited. Three types of defects can be specified: internal, external and corona.

a) Internal defect

The internal defect (Figure 7) is a void or cavity present in an insulating material. This can be the sheath of wires, the coating on PCBs, the enamelling part around transformers' wires, etc… This type of defect is generally created during the manufacturing process. When the insulating material is applied, some gas bubbles may be created until the material is completely dry. This type of defect allows discharges to occur inside the unwanted cavity. They are relatively difficult to obtain in the laboratory because of the small size of the defect which is hard to obtain. The vented sample is often used to simulate such a defect.

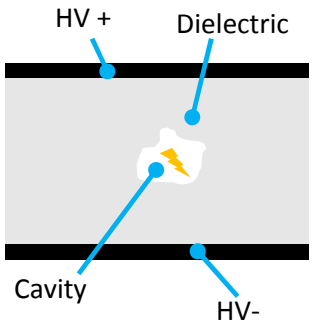

Figure 7: Representation of internal defects

b) External defect

The external defect, or surface defect, depends mostly on the physical shape of the component. An external space can be the location of intense discharges if it is situated between two electrodes (even if they are coated) supplied with high voltage. Recurring examples of external defects are the surrounding air close to the windings of high voltage motors or a twisted pair of enamelled wires (Figure 8).

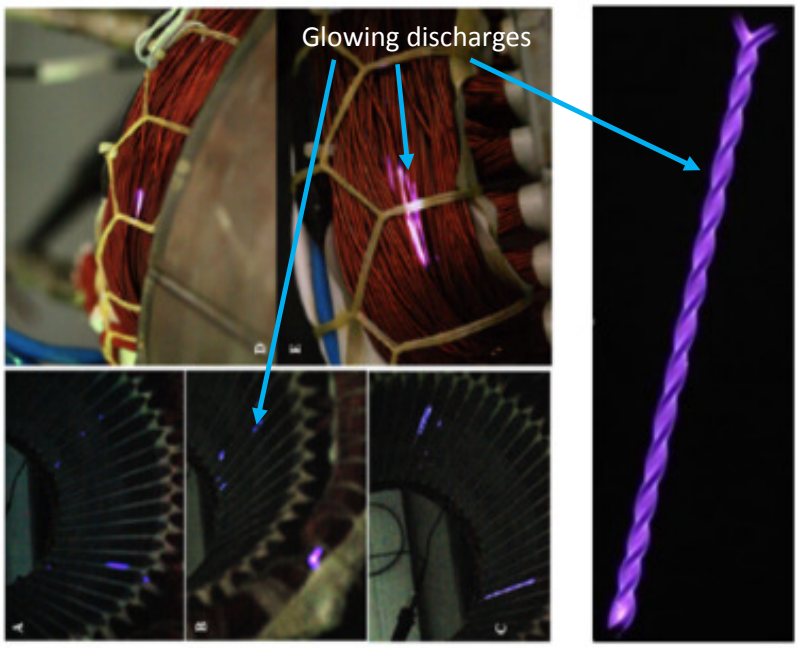

Figure 8: Example of external discharges in an electric stator [Billard] and a twisted pair of enamelled wire [Cella]

Discharges occurring in an external defect, and under particular conditions (such as low pressure), are characterized by a glowing light that make the phenomenon relatively easy to detect.

c) Corona defect

The corona defect (Figure 9) is created by the presence of a sharp needle or edge in the vicinity of a high voltage source. This sharp shape induces a phenomenon called the "needle effect," which increases the electric field around the sharp element. This creates an area in which electrons are accelerated and may ionize atoms. It leads to an electronic avalanche and thus an electrical discharge.

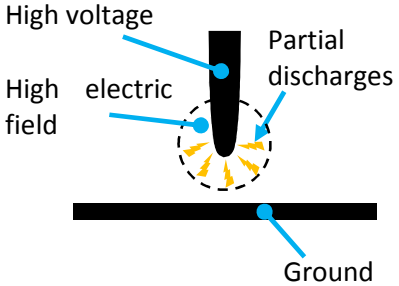

Figure 9: Representation of corona defects

2.1.3 NATURE OF DISCHARGES

Partial discharges are also characterized by the nature of the discharges. The nature of the discharges can vary, depending on voltage and current as shown in the voltage/current characteristic of discharges (Figure 10). [Povey]

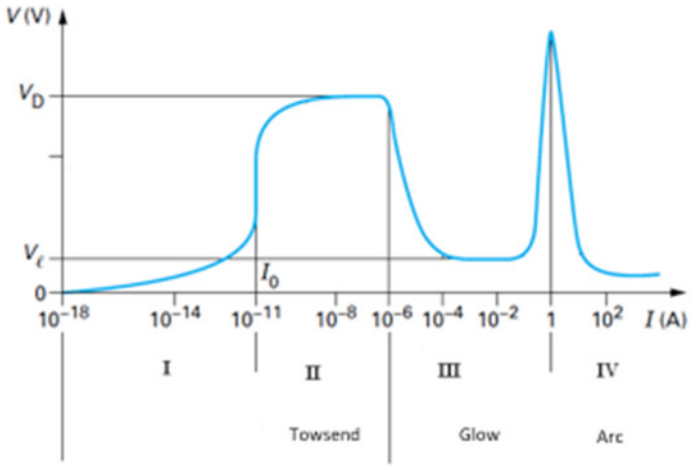

Figure 10: The different natures of the discharges in gas

At low voltage (Figure 10: Phase I), weak ionizations occur and low current is pulled. In the second phase, the voltage is high enough to allow the discharge to be self-sustained and the **Townsend mechanism** predominates. Under particular conditions (Voltage, pressure etc.), the discharge can switch to other characteristics and become glowing. According to [Bartnikas1], glowing discharges can be classified mainly into two types: **glow** and **pseudo-glow** discharges. The different states of these discharges is described below.

The **Townsend discharge** is an electrical breakdown process that takes place in uniform field, parallel-plane metallic electrode gaps. It undergoes the electron-avalanche concept, which is described as follows: when a single electron is accelerated by an electric field, it may collide with a neutral gas or atom or molecule and ionize it. This creates a second electron, both accelerated in the electric field direction and having a probability to ionize other atoms or molecules. The probability for an electron to ionize a neutral gas molecule over a travelled distance x is given by αdx. α being known as the first ionization coefficient, is equal to the number of ionizing impact per electron per unit distance.
This first step of the Townsend discharge is represented in Figure 11.

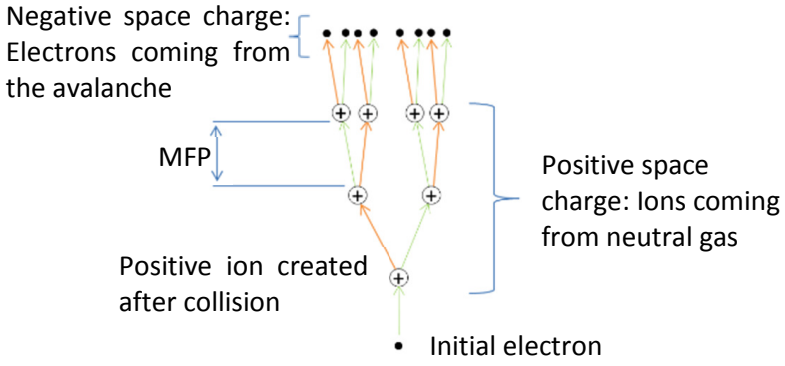

Figure 11: Representation of the avalanche mechanism. MFP being the Mean Free Path

As shown in Figure 11, this process creates a negative swarm of electrons at the front of the avalanche. This is explained by the fact that the electrons are faster than the positive ions (~100 times more). These electrons reach the anode quickly, while the slower moving ions drift towards the cathode. Upon impact, they may liberate additional electrons with a probability γ, which is the second ionization coefficient.

$$\gamma = \frac{1}{\exp(\propto d) - 1}$$

Equation 1: Townsend second coefficient

$\propto$ is the first Townsend ionization coefficient and d is the inter-electrode distance. Lastly, when the height of the positive ion avalanche becomes large enough, secondary electron emissions may lead to a self-sustained discharge.

The second step of the Townsend discharge is shown in Figure 12.

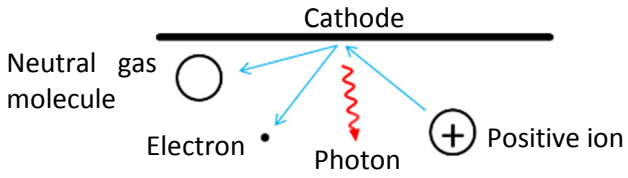

Figure 12: Secondary ion emission at the cathode

In the case of a non-uniform field, as it is often the case, there is a significant probability that the **streamer discharge** will predominate. The streamer theory, which was proposed independently by Meek and Raether [Meek], starts in the same way as in the Townsend mechanism, with a single electron being accelerated and igniting an electron avalanche. After the electrons have disappeared into the anode, a large positive space charge, comprised of positive ions, remains in the inter-electrode space and enhances the global electric field. At that point, any single electron in the vicinity will be accelerated in the direction of the positive ion swarm and will reinforce it. Afterwards, the number of auxiliary avalanches is increased and the streamer starts at the anode and grows up. When it reaches the cathode, the streamer becomes a highly conductive plasma channel. Figure 13 describes the complete streamer mechanism.

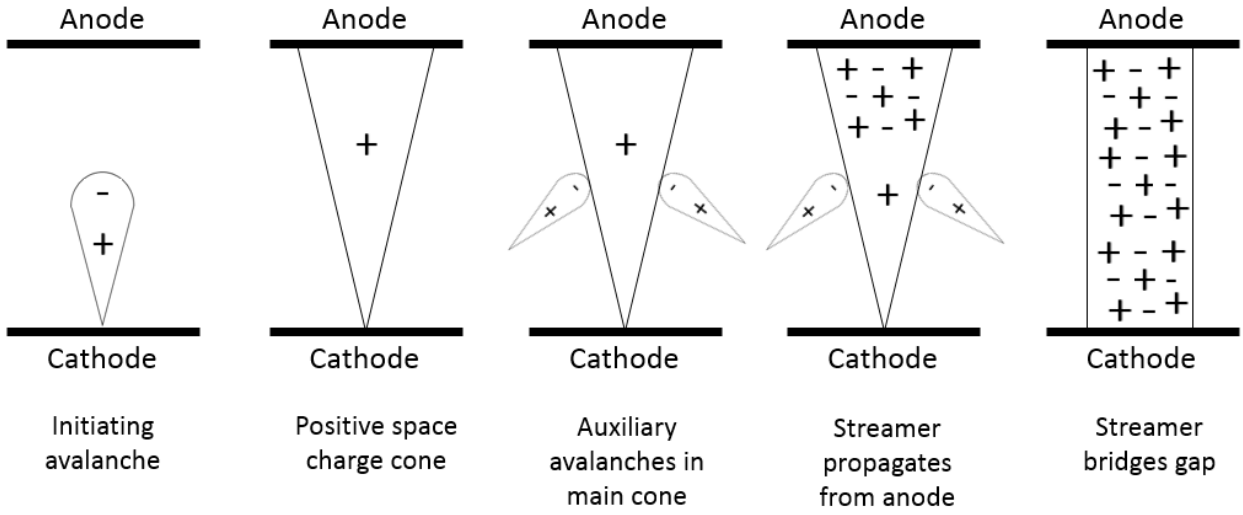

Figure 13: Representation of the streamer mechanism [Meek]

[Bartnikas2] offered a description of the discharge sequence. He explained that when a void is subject to AC voltage above its breakdown value, discharges will occur periodically at each half cycle of the sinusoid. The number of discharges is determined by an integer amount multiple of the void's breakdown voltage. For example, when the maximum voltage of the sinusoid (Ea) just reached the breakdown voltage (Eb), four discharges per half cycle occur, as shown in Figure 14.

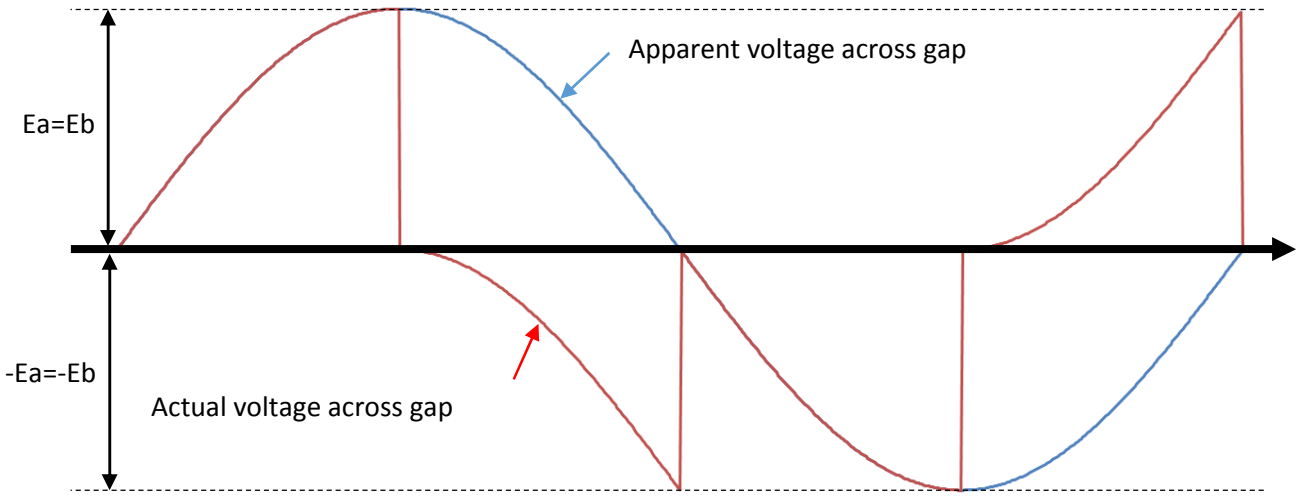

Figure 14: Voltage waveform across an idealized cavity subject to AC voltage (Ea=Eb)

The apparent voltage across the void may be considered as a fraction of the voltage applied to tested object since the object and its defect can be represented as a capacitive divider (Figure 21). It has consequently the same shape. However this voltage is theoretical since it is actually distorted by the discharges occurring inside the defect. Actually, the voltage across the void has a different shape than the voltage applied to the tested object. For this reason, both voltages are represented in Figure 14, Figure 15, Figure 16 and Figure 17.

If the maximum voltage of the sinusoid reaches twice the breakdown voltage (Ea=2*Eb), eight discharges per half cycle will occur, as shown in Figure 15.

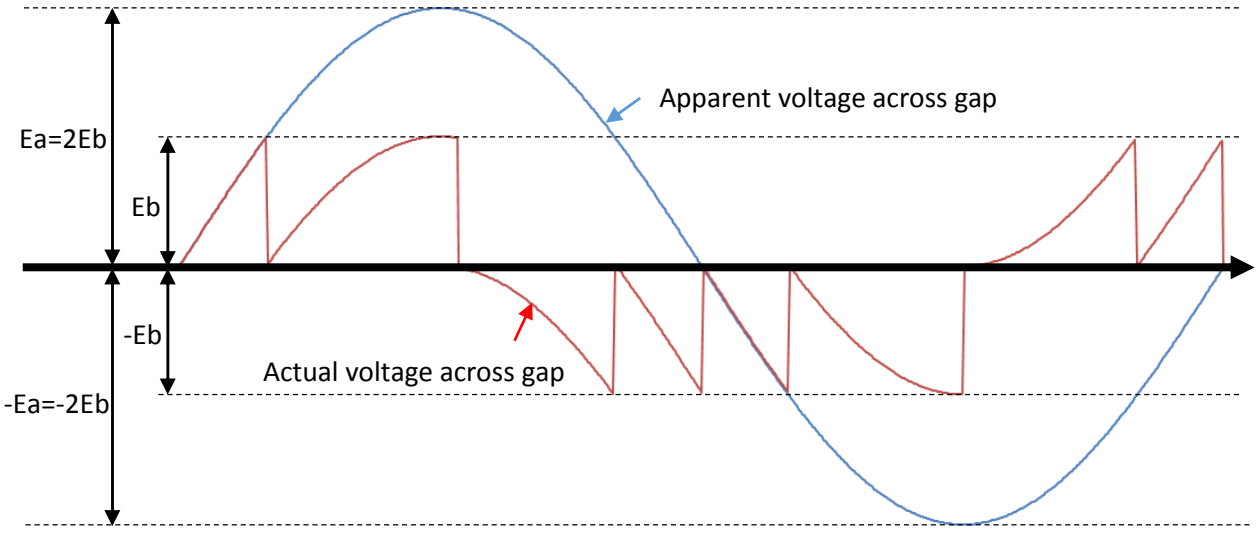

Figure 15: Voltage waveform across an idealized cavity submitted to AC voltage (Ea=2*Eb)

In particular cases, such as low pressure, the discharge can switch from a pulse-type, as Townsend or streamer, to another nature of discharge called glow and pseudo-glow, which were defined by [Bartnikas1] as following:

A test object that is undergoing a glow discharge emits light in the purple and ultraviolet spectrum. When this occurs, only two discharges per cycle (At θ1 and θ2) can be measured. The glow portion of the discharge is confined between π and θ1, and 2π and θ2. The Figure 16 represents the electrical behavior for an ideal glow discharge.

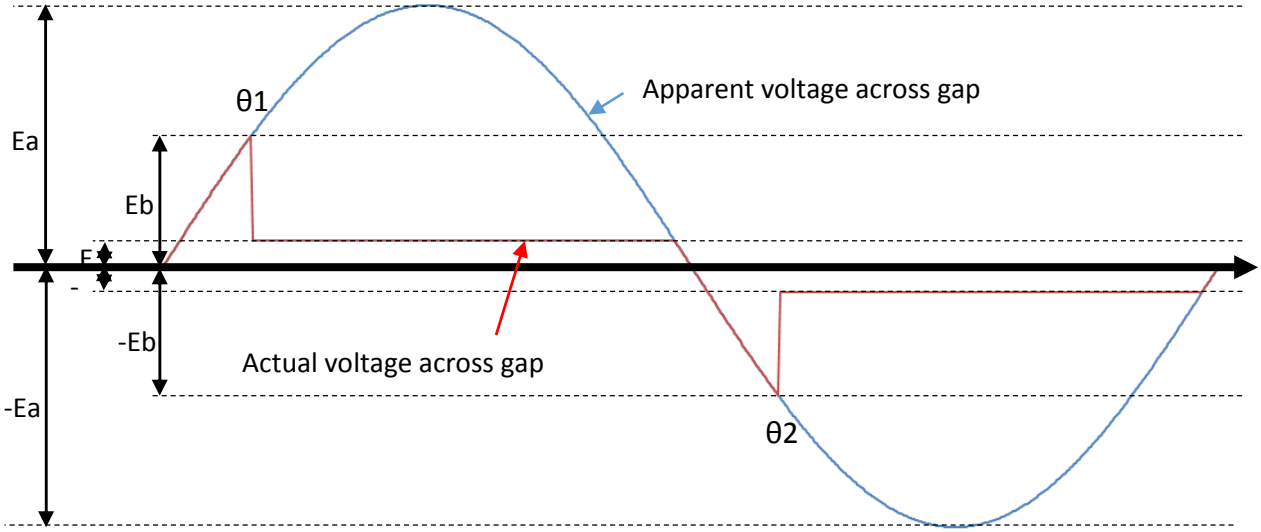

Figure 16: Voltage waveform across an idealized cavity which is undergoing a glow discharge

In contrast to the true glow discharge, the pseudo-glow discharge which was defined by [Bartnikas1] as being a voltage waveform discharge pattern containing numerous pulses with a magnitude too weak to be detected by conventional pulse detectors. Actually, when a discharge occurs, the voltage in the defect falls from the breakdown voltage (Eb) to the residual voltage (Er). Eb-Er defines the magnitude of the discharge. In the case of pseudo-glow discharge, Eb-Er tends to zero. Figure 17 shows a voltage waveform representing this concept from [Bartnikas1], typifying the pseudo-glow discharge.

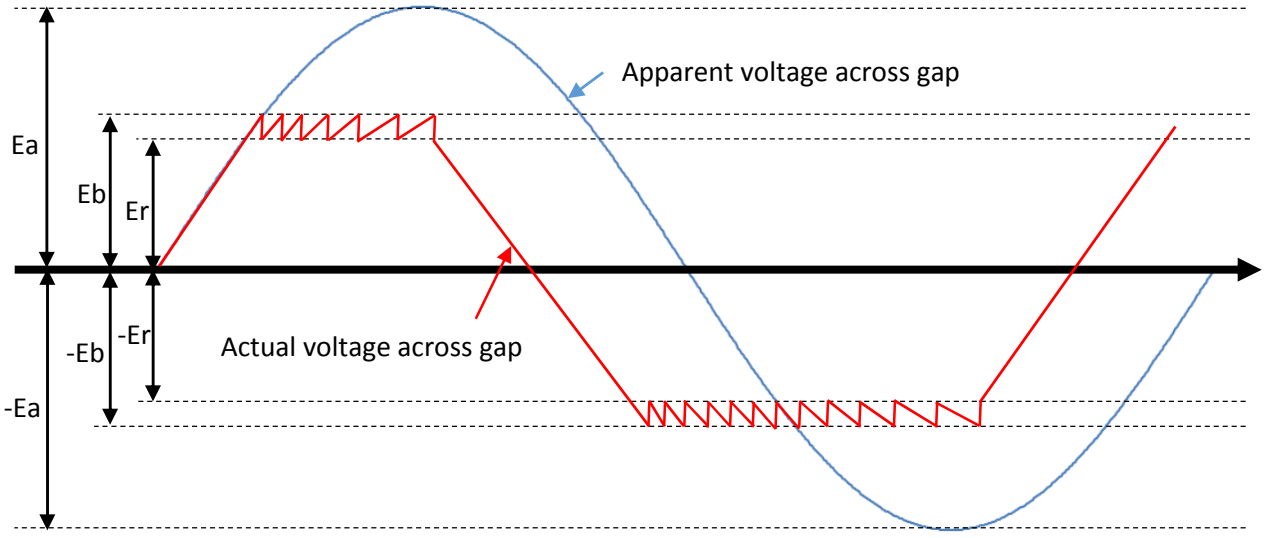

Figure 17: Voltage waveform typifying the pseudo-glow discharge

2.1.4 PASCHEN'S LAW

In 1889 the German physicist Louis Karl Heinrich Friedrich Paschen laid the foundations of gas breakdown voltage. Paschen's law is an empirical equation that gives the breakdown voltage of a gas as a function of the pressure times the distance (pd) between two electrodes. It is applicable in a homogeneous electric field.

The Paschen curve is obtained from the following equation:

$$V = \frac{Bpd}{\ln(pd) + C}$$

Equation 2: Paschen equation

p: pressure (Torr)

d: distance (cm)

B & C: values depending on the gas nature (e.g for air: B =365 V.Torr^{-1}.cm^{-1} C =1,18)

Once plotted, the equation gives the curve presented in Figure 18.

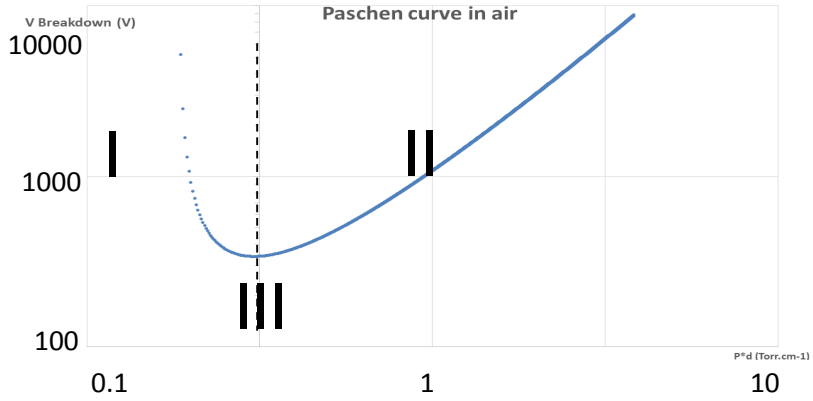

Figure 18: Paschen curve in air

Three different parts can be observed in the above figure:

I. The left side shows a very small *pressure* times *distance* product. This means that there are not enough molecules or atoms between the electrodes or that there is a small distance between the electrodes. Consequently, the probability for an electron to collide with molecules or atoms is very low. Therefore, the voltage required for breakdown tends towards infinity.

II. The right side shows a very high *pressure* times *distance* product. This means that there are a lot of molecules or atoms between the electrodes. Consequently, the mean free path is reduced so that electrons do not gain enough velocity to ionize other atoms or molecules. Here, the voltage required for breakdown tends towards infinity.

III. The Paschen minimum is the pressure times distance product at which the breakdown voltage is minimum. This particular value for a given gas indicates that a specific voltage exits under which no breakdown can occur.

In a homogeneous electric field, no electrical discharges can occur at a voltage below the Paschen minimum. Consequently, a safety zone where no partial discharges (PD) occur can be defined.

2.1.5 CONSEQUENCES OF PARTIAL DISCHARGES

Repetitive partial discharges in a system can lead to severe degradations of insulation. The flow of electrons in the cavity may induce extreme chemical transformations, such as the splitting of molecular bindings under the effect of electrons and ions bombardments. These transformations may create a highly conductive path which allows high current to flow and thus temperature to rise. Finally the insulation is seriously damaged and a complete breakdown or an arc may occur between two electrodes which are not anymore protected by the insulation. Figure 19 shows the degradation of insulation due to high voltage stress

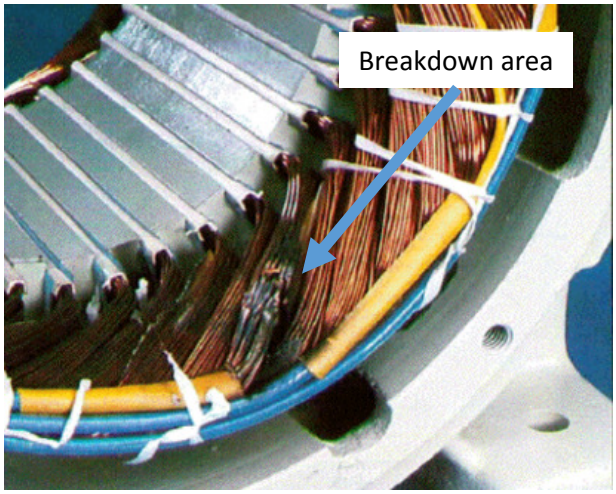

Figure 19: Damage on a stator after dielectric breakdown

2.2 PHYSICAL DESCRIPTION OF THE PARTIAL DISCHARGES PHENOMENON

Partial discharges occur only in a gaseous medium that, due to lower permittivity than the surrounding material, creates a reinforcement of the electric field. Figure 20 shows a physical description of the partial discharge process in a gas-filled cavity.

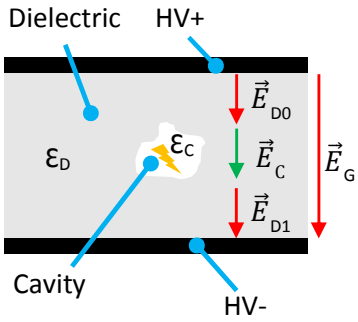

Figure 20: Electric field distribution around a gas field cavity

The voltage difference between the high voltage electrode and the ground generates an electric field E_G through the dielectric. Since this dielectric is not ideal, due to the presence of the cavity, and since the permittivity of the gas inside the cavity is lower than the permittivity of the dielectric, an electric field reinforcement is observed in the cavity.

The cavity is filled with gas which, as it is the case for all gas, has a permittivity ε_c close to that of the void ε_0.

$$\varepsilon_c = \varepsilon_0 = 8.854187 \text{ x } 10^{-12} \text{ F}.m^{-1}$$

However the permittivity of the dielectric, which is a solid, is higher than that for gas or void.

$$\varepsilon_C < \varepsilon_D$$

It is known that the permittivity of a medium can influence the electric field in which it is located, as shown the following formula:

$$\frac{D}{\varepsilon} = \text{E}$$

E: Electric field

D: Electric displacement field

ε: Permittivity

This equation means that the larger the permittivity, the lower the electric field.

Considering the previous conditions, it can be concluded that:

➡ $\varepsilon c < \varepsilon D$ ➡ $\frac{D}{\varepsilon D} < \frac{D}{\varepsilon C}$ $\vec{E}_D < \vec{E}_C$ With: $\vec{E}_D = \vec{E}_{D0} + \vec{E}_{D1}$

Consequently, since a voltage larger than the breakdown voltage is applied to the electrodes, an electrical discharge will first occur in the cavity. When electrons arrive at the edge of the cavity, they create a secondary electron generation, as described in the Townsend theory, which maintains the discharge in the cavity. The discharge occurs in the cavity first as a combined result of field enhancement and lower breakdown stress.

2.3 PARTIAL DISCHARGES UNDER AC VOLTAGE

In 1944, Austen and Hackett [Austen] proposed an equivalent circuit for the discharge process in voids. This was later used to explain the discharge sequence by Mason. Figure 21 is the schematic of this equivalent circuit.

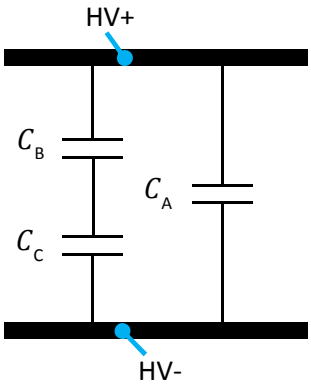

Figure 21: abc model

C_C: Capacitance representing a gas-filled cavity in a solid dielectric

C_B: Capacitance representing the solid dielectric in series with Cc

C_A: Capacitance representing the remaining dielectric

If a sinusoidal voltage of an amplitude V_a is applied to this circuit, and assuming that V_b is the breakdown voltage of the gas-filled cavity, when the apparent voltage across C_c reaches V_b, this leads to a breakdown in the cavity and C_c can be considered as a short circuit. The actual voltage across C_c then follows the apparent voltage until it again reaches the breakdown voltage of the gas in the cavity. The higher the magnitude of the AC source, the higher the number of occurring partial discharges. Figure 15 shows this process.

A simulation of this concept value shows a higher number of discharges (Figure 22*)*. A sinusoidal voltage is applied to the abc model (Figure 21) and switches (SW1 and SW2) simulates a discharge each time the voltage reach the inception voltage.

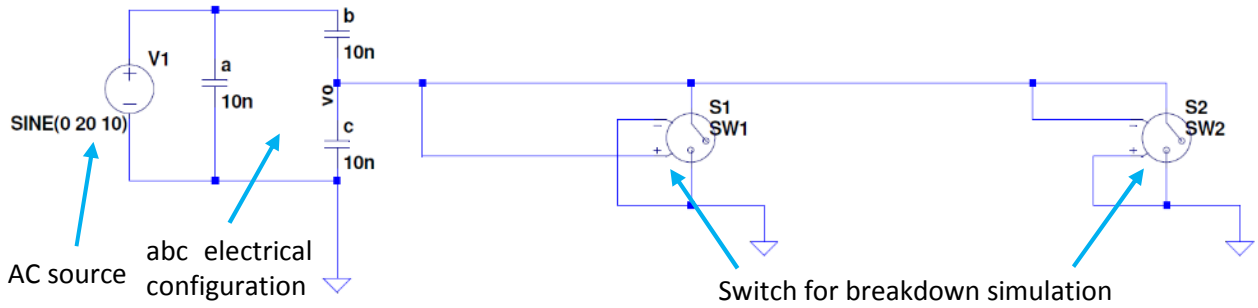

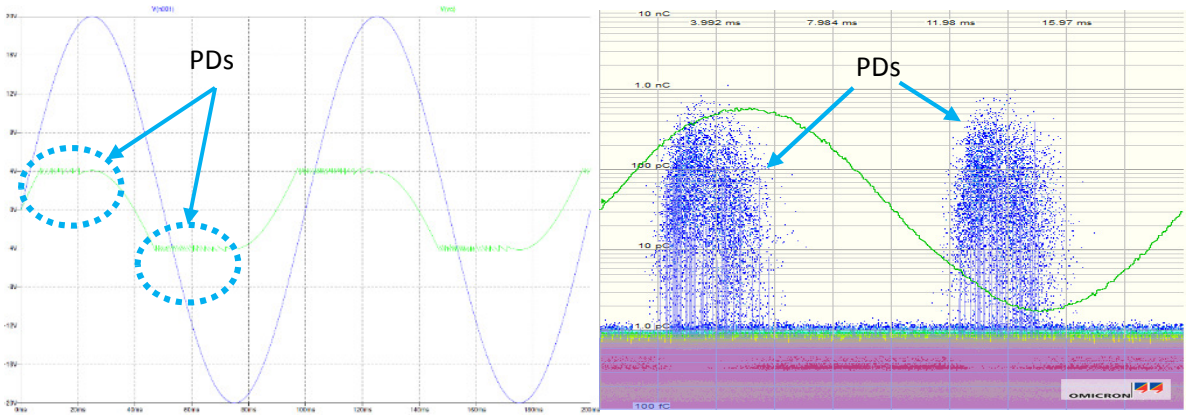

Figure 22: Simulation of the abc mode. Left: Simulation. Right: Measurements of a twisted pair of enamelled wire submitted to sinusoidal voltage.

The position of the discharges in the simulation is coherent with the theoretical (Figure 15) and empirical (Figure 22-right) data when studying partial discharges.

2.4 PARTIAL DISCHARGES UNDER PULSE-LIKE VOLTAGE

Although the behavior of electrical insulation subject to AC voltage stress is well documented, there have been relatively few studies on impulse voltage conditions. [Densley1] summarized the main foundations of this topic. As for AC voltage, partial discharges can occur in a gas-filled cavity surrounded by a solid or liquid dielectric material fed by impulse voltage. Therefore, the equivalent electric model with capacitors is also used to explain the discharge phenomenon under such voltage waveform.

Partial discharges occur when the electric field in the defect is high enough that an initial free electron can gain enough velocity to ionize atoms or molecules and end up creating an avalanche. However, initial free electron is not always available. The initiatory electron can be generated by natural irradiation. For alternating voltage below the MHz and direct voltage, there is sufficient time for natural irradiation to produce favorably positioned electrons. However for short-duration impulse voltages, an initiatory electron might not be produced during the time in which the voltage across the cavity is above the ionization potential. Consequently, no discharge occurs. The time measured from the moment the voltage across the cavity exceeds the ionization potential, up to the appearance of the initiatory electron, is known as the statistical time lag (STL). If the duration of an impulse is below the STL, no electrical discharges occur. And, if this duration slightly exceeds the STL, very high voltage is needed to create discharges. The longer the pulse duration, the smaller the voltage needed to create discharges. As shown in Figure 23.

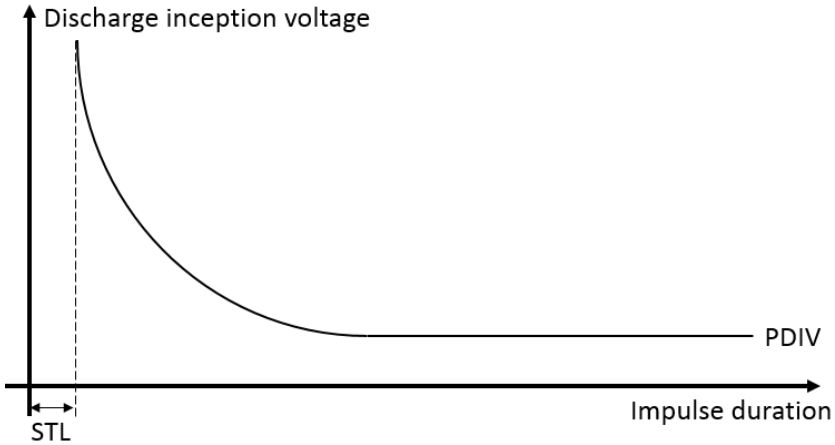

Figure 23: Discharge inception voltage as a function of impulse duration

This particularity explains why the partial discharge inception voltage (PDIV) is higher with impulse voltage conditions than for AC or DC voltage conditions.

The factor between PDIV under pulse voltage and PDIV under AC or DC voltage depends on the stress at the cathode surface, the type of cathode material, the temperature, and whether the surface is rough or smooth.

The discharge sequence during impulse voltage conditions may be divided in two groups: unipolar pulses and bipolar pulses.

2.4.1 UNIPOLAR PULSES

The voltage shape has a significant impact on the occurrence of the discharges. When performing measurements using unipolar pulses, it seems that the discharge inception voltage is higher than when tests are performed under AC voltage. This can be illustrated by applying a series of unipolar pulses to the theoretical abc model (Figure 21). The results are shown in Figure 24.

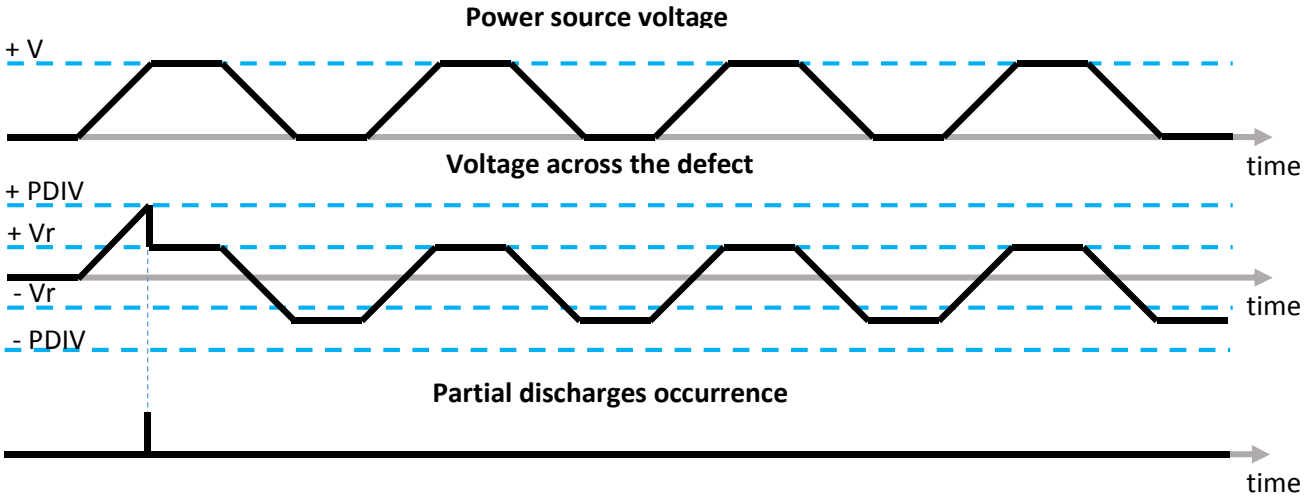

Figure 24: Unipolar pulses applied to the theoretical abc model at PDIV

Figure 24 shows that, at PDIV, one partial discharge occurs at the beginning of the test but afterward no more discharge occurs. It is therefore difficult to detect them.

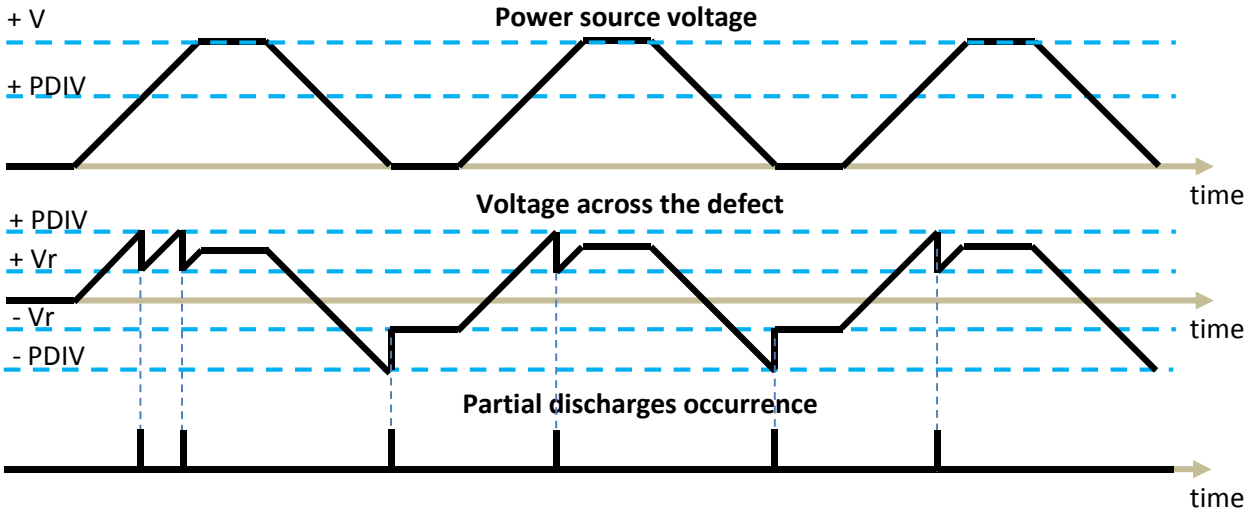

Figure 25: Unipolar pulses applied to the theoretical abc model at a voltage above PDIV

By increasing the voltage well above the inception level, partial discharges occur periodically, and are therefore easier to detect.

2.4.2 BIPOLAR PULSES

When performing measurements under bipolar pulses, it may be supposed that partial discharges occur at the same repetition than the tests done under AC voltage. This is illustrated by applying a series of bipolar pulses to the theoretical abc model (Figure 21). The results are shown in Figure 26.

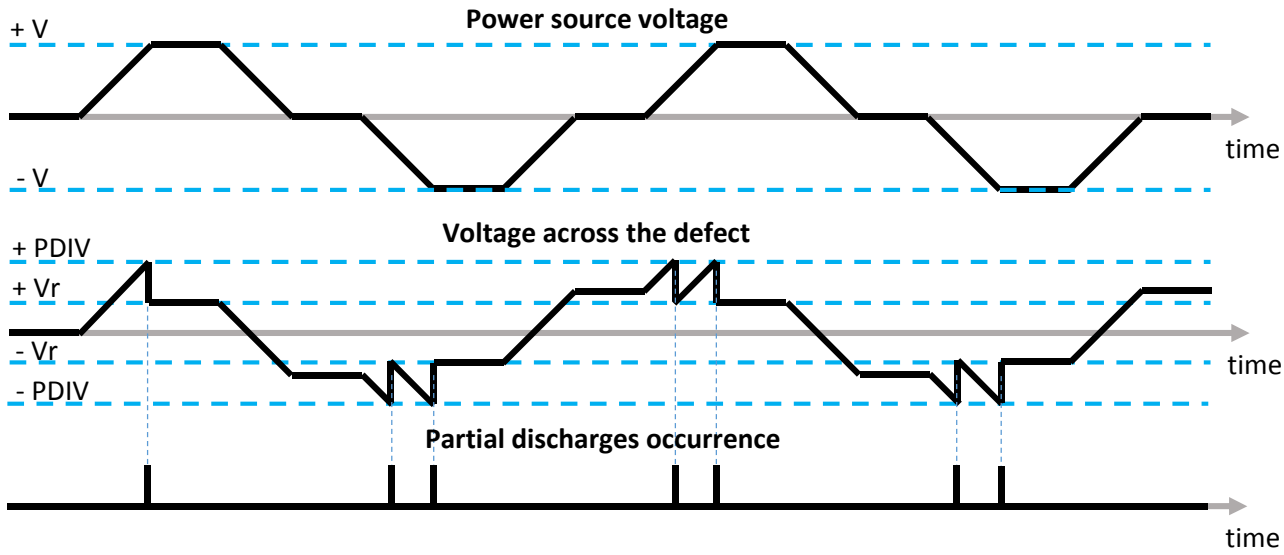

Figure 26: Bipolar pulses applied to the theoretical abc model at PDIV

Figure 26 shows that, when using bipolar voltage, partial discharges occur periodically at the inception. It is not needed, as under unipolar pulses, to increase the voltage above the inception level to get this result. This explains why, under bipolar pulses, partial discharges are detected at a voltage (Vpeak) lower than when test are performed under unipolar voltage.

2.5 PARTIAL DISCHARGES UNDER DC VOLTAGE

In their work to gather data on the topic of partial discharges, Bartnikas and Mc Mahon highlighted some conclusions drawn by [Densley2] about partial discharges under direct voltage conditions. The following general points were outlined:

- The discharge inception voltage under direct voltage conditions is difficult to specify because the discharge repetition rate is zero at the theoretical inception value. In practice, inception voltage is taken as either: (1) a certain number of discharges exceeding a particular magnitude per time unit, for example one discharge per minute, as in [ASTM1]; or (2) when the sum of the product of the number of discharges counted in each channel per time unit, and the minimum discharge magnitude that can be counted in that time, exceeds a certain limit; or (3) The direct current flowing through the insulation exceeds a specified limit.
- It is not possible to define a discharge extinction voltage, as discharges can occur a relatively long time after the applied voltage across the insulation has dropped to zero.
- The direct voltage discharge repetition rate is usually several orders of magnitude less than for alternating voltage.
- If the direct voltage is below the discharge inception value, superimposing direct voltage on alternating voltage does not change the AC discharge inception voltage. However, the number of AC discharges is sometimes reduced by the presence of direct voltage. If the

direct voltage is above the discharge inception value, a small alternating voltage will increase discharge frequency significantly.

Because of the low repetition rate, partial discharges under DC voltage conditions are very difficult to detect, and since a low repetition rate means a less risks for the system, this work mainly focuses on AC and pulsed voltage.

2.6 DISCHARGES ANALYSIS THROUGH ENVIRONMENTAL MODIFICATIONS

Information on the nature of partial discharges can be found by modifying the environmental conditions around the sample being tested. These modifications include:

- Changing the medium – immerging a sample into insulating liquid helps to distinguish surface from internal discharges.
- Varying the pressure – allows making the distinction between external and internal discharges. The inception level is modified by the pressure in which the discharges occur.
- Increasing the temperature – may close fissures, and temperature cycles may cause interstices. Increasing temperature may also increase a material's permittivity and thus decrease PDIV.
- Increasing humidity – can modify the partial discharge inception and extinction voltage.

Each of these environmental modifications only give an indication. More results have to be obtained and analyzed to get a better picture of the discharges.

2.7 DETECTION METHODS

Quantitative partial discharge detection requires accurate measurements because of the magnitude of the discharges, which extend from a few pico-coulombs to a few hundred pico-coulombs. Different methods exist to detect partial discharges. They are listed below:

- PD can be detected using the electric charges movement or consequences resulting from this movement. This method is called **electrical detection**.
- Electric charges movement produces electromagnetic waves that can be detected by an antenna. This is called **RF detection**.
- During their existence, PDs produce some new chemical elements (Ozone, NO_X) that cause damage to the material. This phenomenon may be used for **chemical detection**.
- PD also emits sounds which allow **acoustic detection**.
- One last method for detection uses the light emitted by the discharges, which extends from infrared to UV light. This method is called **optical detection**.

Chemical and acoustic detections are not used frequently because of the complicated test elaboration. However chemical detection has been sometimes used by means of ozone sensors. These are paper tabs which color changes when ozone is detected. Since partial discharges emit ozone, it is a good indicator to know if discharges occur in an object or not. Therefore, this thesis focus only on electrical, chemical, and optical detection. Each method described below requires a calibration stage before any test.

2.7.1 STANDARD ELECTRICAL DETECTION

To detect PD, this method uses the charge displacement (measurement of the current flowing into a conductor). The partial discharges current detector scheme is shown in Figure 27.

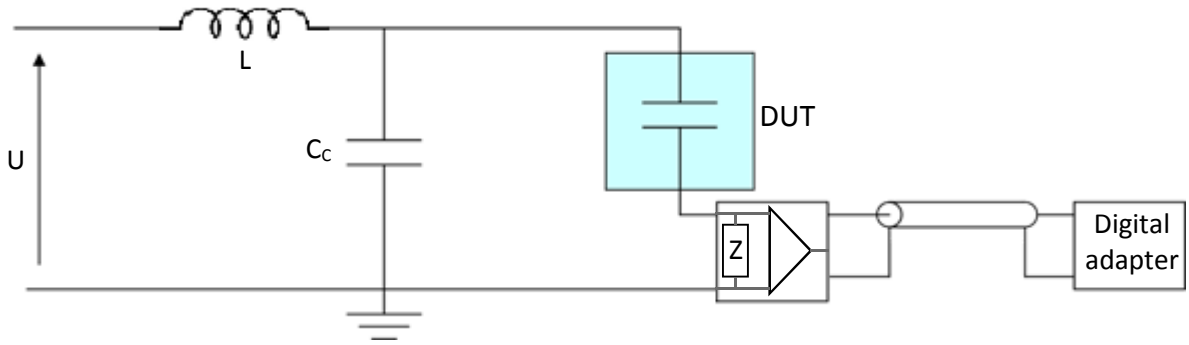

Figure 27: Setup for electrical PD detection

U is the voltage source. L is an inductance avoiding that high frequencies from the DUT reach the voltage source. C_c is a coupling capacitor. Z is an impedance through which the discharges current flows. The resulting voltage is used for partial discharges detection.

Since partial discharges are high frequency events, and since L is an inductance, the current created by the partial discharges (in AC) flows in the loop C_C, DUT, and Z. The small current variation is detected by Z (which is, most of the time, a RLC circuit), then amplified, digitalized and sent through an optical fiber (for galvanic insulation) to a computer with the appropriate software. This detection method leads to the example (Figure 28). In some applications Z, is in series with C_C. It has no influence on the result except the sign of the current measured by Z.

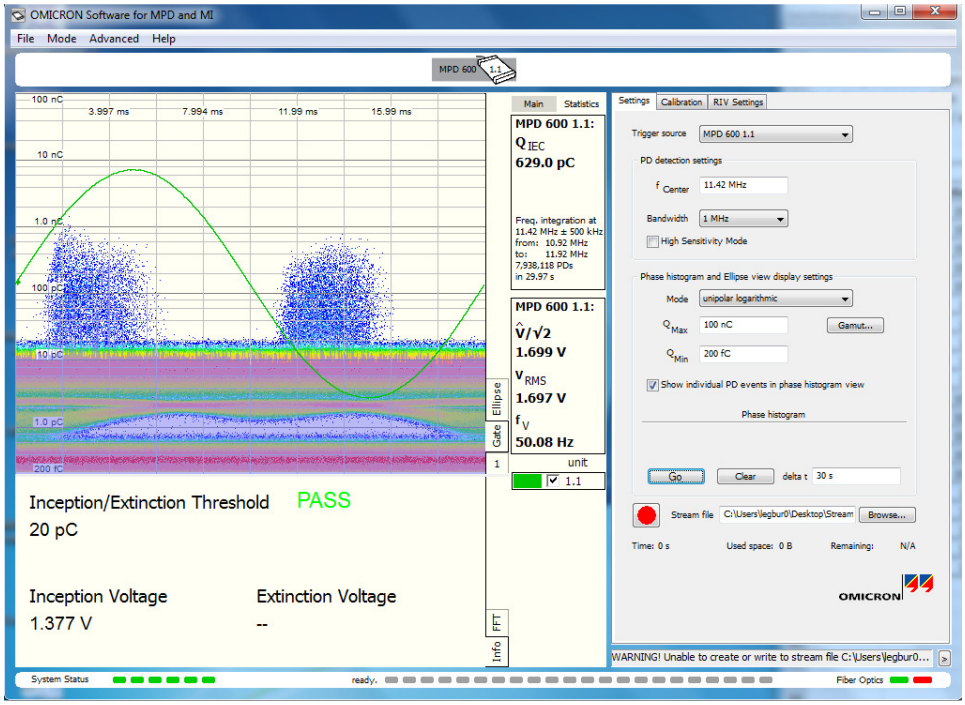

Figure 28: Example of results after electrical PD detection

The main advantage of this detection is the accuracy of the measurements. With such a method, it is possible to determine the quantity of apparent charges generated by each electrical discharge.

2.7.2 RADIO-FREQUENCY (RF) DETECTION

Partial discharges may also be detected by detecting electromagnetic wave emission. This method obviously uses an antenna, and is mainly based on wave shape recognition and analysis. The easiest method is to connect an oscilloscope or a spectrum analyzer to the antenna and to analyze curves. More elaborate devices use complex algorithms to recognize partial discharges. Figure 29 shows an example of such a detection system.

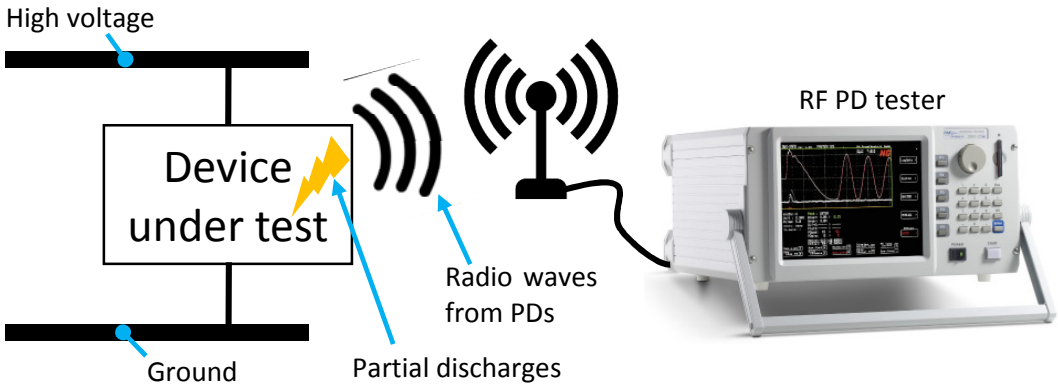

Figure 29: Setup for PD RF detection

2.7.3 OPTICAL DETECTION

Optical detection is the most useful method to localize PD with precision, at least when the discharges are external and located in an area reachable by an optical sensor. The discharge process is well described by the Townsend theory. During the ionic bombardment process, photons are emitted in a certain frequency band. This photon emission allows to localize partial discharges accurately. An example is shown Figure 30.

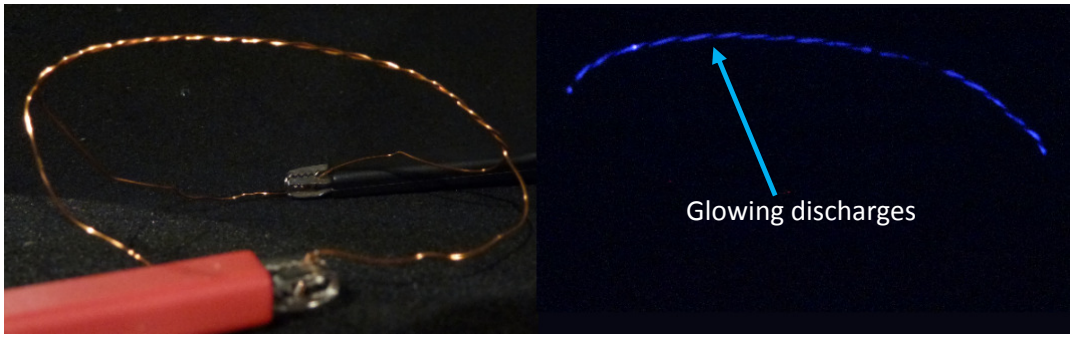

Figure 30: PD light emission on a twisted pair of enamelled wire sample

A very faint light and a luminous point can clearly been seen on the left side of the right picture in Figure 30.

2.8 ANALYSIS METHODS

Simply looking at some characteristics separately does not necessarily lead to the correct interpretation. Some characteristics must be considered together. Two main tools are used for analyzing partial discharges:

2.8.1 OSCILLOGRAM

Analyzing partial discharges occurrence as a function of phase position with respect to the voltage source is an effective way to obtain data regarding discharge type and origin. There are two ways to display this: classical depiction (on the right in Figure 31) and the Lissajous depiction (on the left in Figure 31).

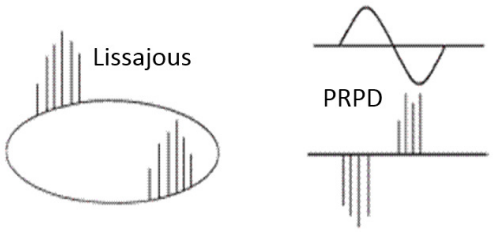

Figure 31: Lissajous and phase resolved pattern

The classical depiction enables highlighting a relevant pattern and comparing it with known patterns. Figure 32 shows oscillograms which depict different type of discharge (Surface, void, corona) according to the company Omicron. The following pictures are merely examples and are not intended to constitute any sort of “absolute” truth.

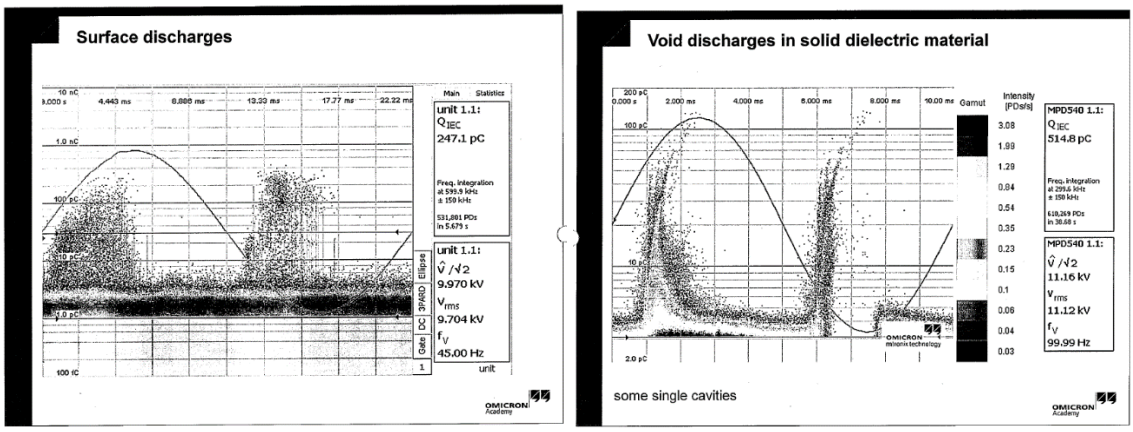

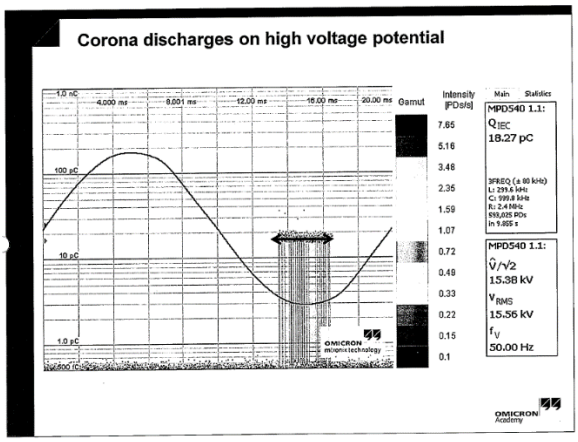

Figure 32: Different types of partial discharges after an electrical detection

The second method, the lissajous method, makes it possible to bring out the symmetry between positive and negative alternance. Figure 33 shows some measured shape of discharges displayed with the lissajous method.

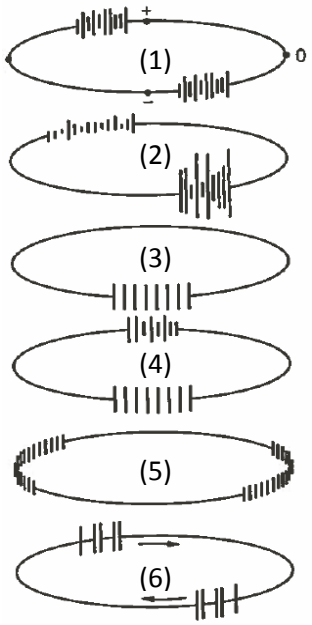

Figure 33: Several discharges measured with lissajous method [Kreuger1]

(1) Cavity completely surrounded by a dielectric: The discharges at both polarities are equal or do not differ more than a factor 3.
(2) Cavity or surface discharge, at one side bounded by an electrode: the discharges at both polarities differ more than a factor 3.
(3) Negative corona in gas: discharges are of equal magnitude and occur at one polarity only. At higher voltage, positive corona may appear at the other side of the ellipse.
(4) Corona in oil: Typical corona pattern at one side, indistinct corona pattern at the other side of the ellipse.
(5) Contact noise: indistinct noise pattern at the zero point where the capacitive current is maximal.
(6) Floating part: imperfect contact of an electrode floating in the electric field causes regularly repeating discharge groups, sometimes rotating along the ellipse.

2.8.2 X-Y DIAGRAM

This analysis method shows the discharge magnitude (logarithmic scale) as a function of test voltage (linear scale). Kreuger [Kreuger] pursued some investigations using this diagram. He outlined particular shapes for different types of discharge as shown in Figure 34.

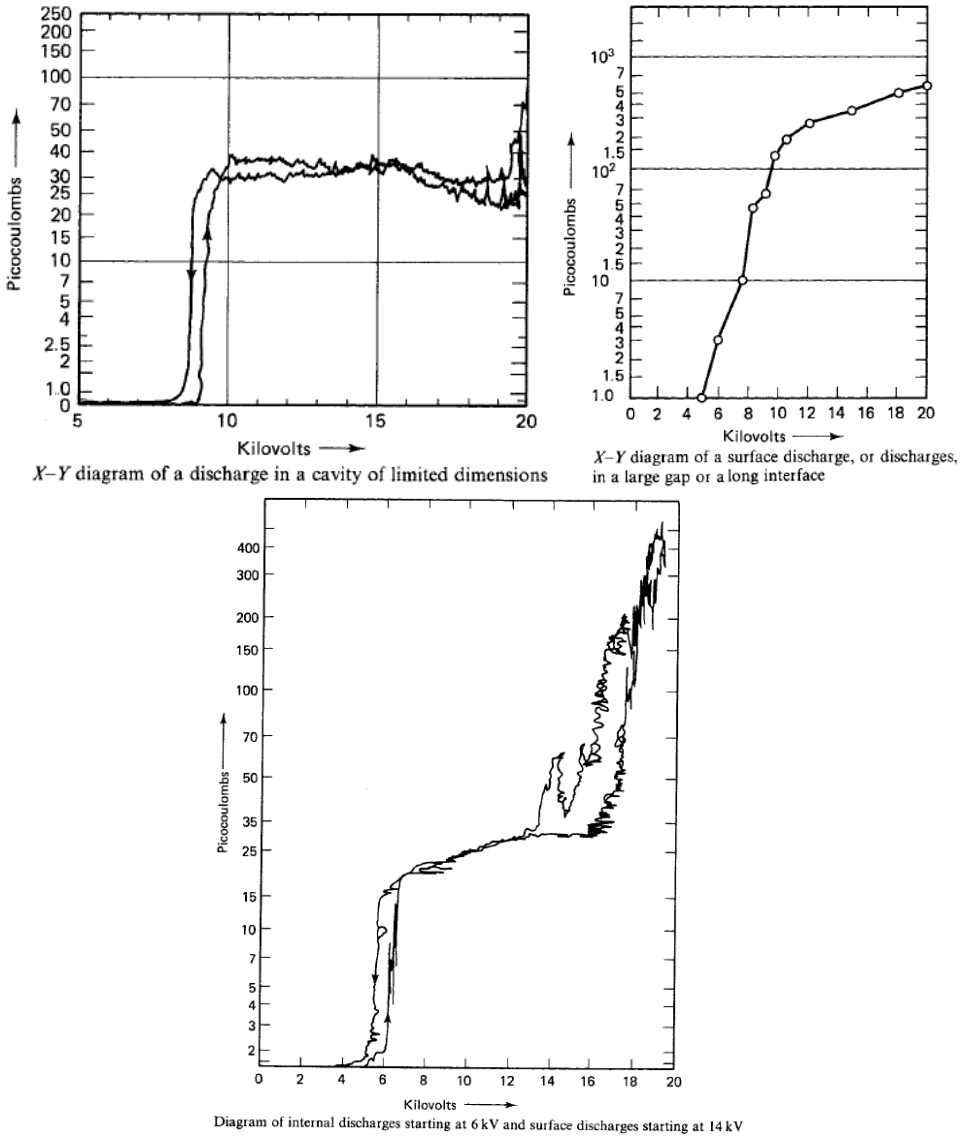

X–Y diagram of a discharge in a cavity of limited dimensions

X–Y diagram of a surface discharge, or discharges, in a large gap or a long interface

Diagram of internal discharges starting at 6 kV and surface discharges starting at 14 kV

Figure 34: XY analysis method [Kreuger]

Internal discharges show a squarely-shaped diagram, while surface discharges show an ever-increasing diagram. Thanks to such diagrams, it is possible to determine what kind of partial discharges are measured.

2.8.3 TIME EFFECT

A sample subject to partial discharges during a certain duration of time can provide data on the type of discharges and what is happening to the insulation. The following X-Y diagram, Figure 35 from [Kreuger2], shows an extinction voltage that is not the same after waiting 30 minutes or waiting 24 hours.

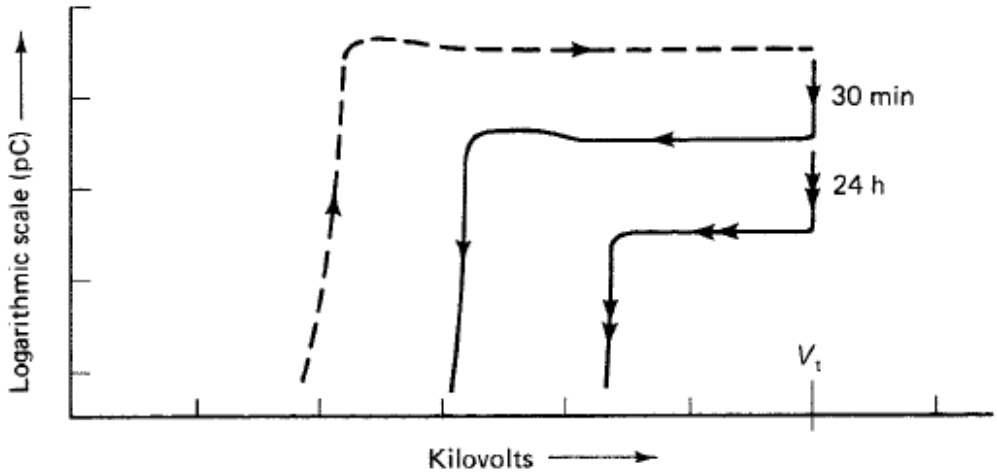

Square X–Y diagram, improving by prolonged exposure to test voltage V_t

Figure 35: XY analysis method with time parameter

This behavior has been found in elastomeric insulation, where fissures occur in the direction of the electric field. It can also occur in round cavities in thermoplastics where inhibitors or plasticizers are present.

2.9 CONCLUSION

This second chapter brings the basic knowledge required to understand the partial discharges phenomenon. Partial discharges must be studied with several tools, described in the previous sections, but the combination of these tools is as much important to conclude on the nature of an observed discharge. To get proper results, it is imperative to master these basic knowledges before any partial measurements.

3 AN ORIGINAL METHOD FOR DETECTING PARTIAL DISCHARGES IN THE AERONAUTICAL FIELD

Complex setup is generally required when deploying most types of partial discharges detecting device:

- The electrical method is an off-line method using a coupling capacitor, impedance, an amplifier, and sometimes a few meters of optical cable for galvanic insulation.
- The radio-frequency method uses a precisely calibrated antenna along with some accurate filters and amplifiers.
- The optical method may refer to accurate measurement using light sensors, a few meters of optical cable, and a spectrometer to analyze the data or, it may refer to a simple camera sensing any light emission (from IR to UV).

Each method focuses on particular objectives such as measuring the quantity of charge in the discharge which requires elaborated setup to be obtained.

The objective of the method presented in this study is actually simpler, since it seeks only to detect discharges (no measuring charge, no localization etc…). The method described in this thesis has been developed to detect partial discharges on-line at a lower cost in the environment of an airplane.

3.1 METHOD DESCRIPTION

Figure 36 describes the basic setup used to detect partial discharges using the proposed method. It is based on a coupler sensitive to the dV/dt related to the discharge. When a discharge occurs, its current flows in the loop between the device under test and the power source. When it reaches the sensor, this one detects the variations of the discharges' current which are sent to the oscilloscope through a high pass filter. The filter removes any "low frequency" generated by the device under test or by the power source.

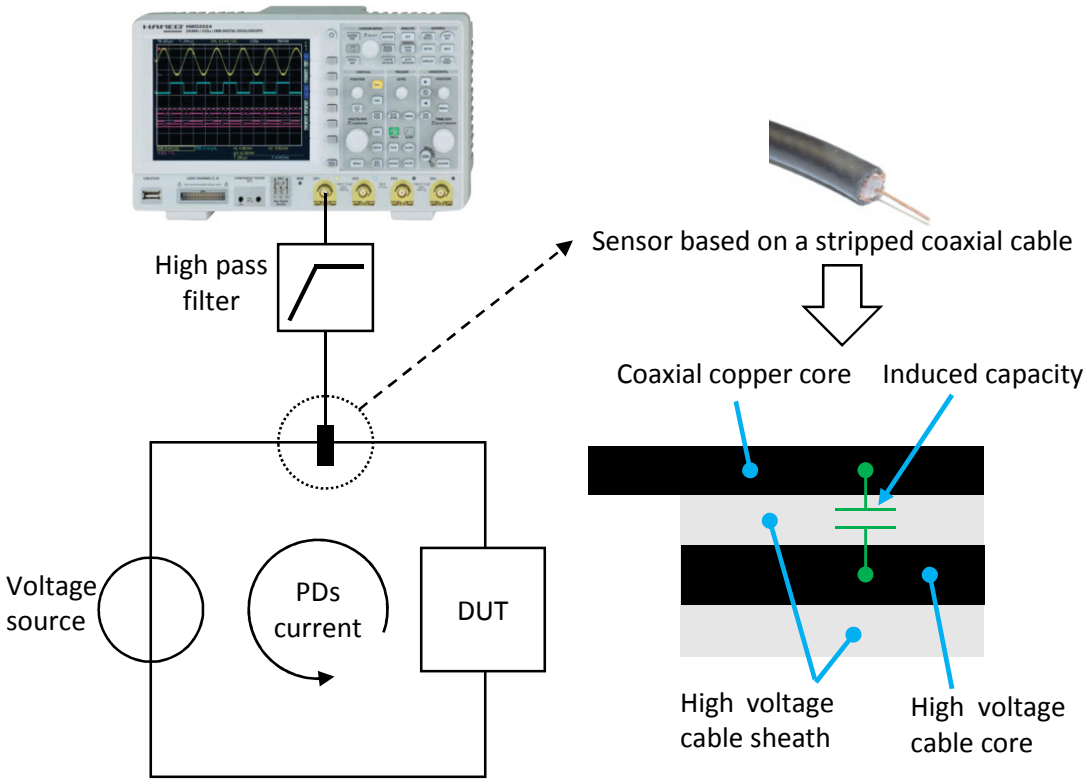

Figure 36: Setup of the partial discharge detection method

The main advantages of the sensing method are its low cost and the small size of the sensor. It allows building an inexpensive setup rapidly, and to reach small places where larger sensors would not fit. It allows to make the distinction between partial discharges signals and switching noise.

3.2 PHYSICAL CHARACTERISTICS OF THE SENSING SECTION

Figure 37 shows an electronic representation of the capacitive aspect from the sensing method. Each component or parameter which may have an influence on partial discharges measurement is represented.

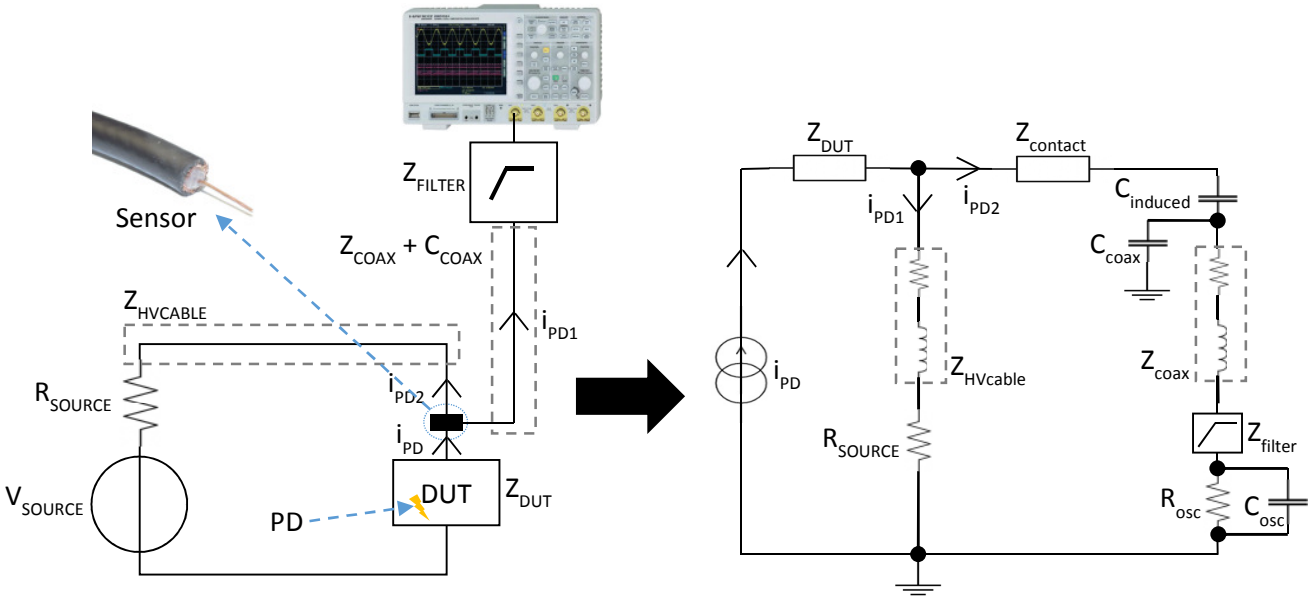

Figure 37: Possible electronic representation of the partial discharge sensing method

i_{PD} is the current generated by partial discharges in the DUT. This value depends on the magnitude of the discharges. It is generally used to calculate the apparent charge, but not the real charge. Z_{system} is the impedance created by the studied system, for example, the components in the converter through which the discharges' current flows to reach the sensor. R_{AC} is the internal resistance of the power source. $Z_{contact}$ is an impedance created by imperfect contact between the coaxial core and the high voltage cable sheath. This value may depend on environmental parameters. $C_{induced}$ is the induced capacitor. Its value depends on several factors described below. Z_{filter} is the filter's impedance. R_{osc} and C_{osc} are respectively the oscilloscope's internal input resistor and capacitor. $Z_{HVcable}$ and Z_{coax} are impedances respectively dependent on the length of the high voltage cable and the coaxial cable.

This representation of the discharges circuit shows that the sensing method uses the common mode current to bring the discharges' current from the DUT to the oscilloscope.

3.3 ANTENNA FEATURES

Considering that every unshielded metallic wire acts as an antenna, the sensor proposed in this thesis is thus able to detect electromagnetic waves at a particular frequency (resonance frequency) depending on its shape and dimensions. This section determines whether the sensor acts as an antenna able to detect frequencies at which partial discharges occur.

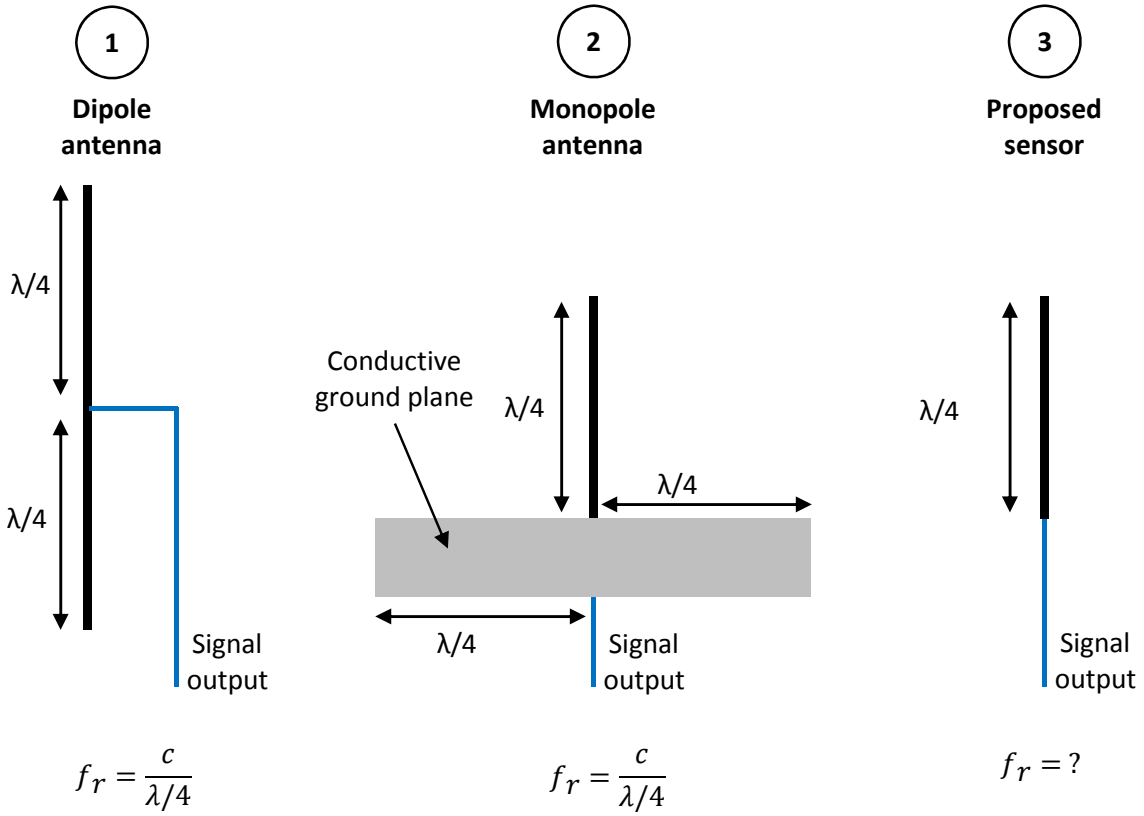

Figure 38: Representation of different type of antenna and their resonance frequency

Figure 38 represents three types of antenna: dipole, monopole and full wave. Their resonance frequencies is calculated as shown at the bottom of the figure.

The sensor presented in this thesis does not have the characteristics of an usual antenna as ① and ②. Its resonance frequency cannot be simply calculated as the other cases.

$$\frac{c}{\lambda/4}$$

Equation 3: Antenna length calculation

λ: Length of the copper core (m)
c : Speed of light in the vacuum (m/s)
f: Frequency that can be received (Hz)

Consequently, to prove that our sensor is a poor antenna at low frequencies (<1GHz), measurements have been made using a network analyzer. S11 measurement has been performed and are described in Figure 39.

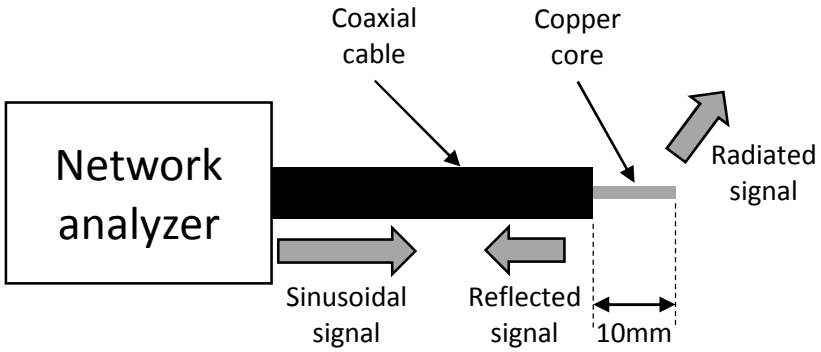

Figure 39: Representation of the S11 measurement on the coaxial cable

S11 measurement allows to determine the resonance frequency of an antenna. The network analyzer send a series of sinusoidal signals to the tested object (in our case, the coaxial cable), and measures the magnitude of the reflected signal. The magnitude of the sinusoidal signal being the sum of the reflected signal and the radiated signal. A range of several frequencies is sent and the result is given as a graph as a function of the frequency. Figure 40 shows an example with an antenna which has been built to get a 250MHz resonance frequency.

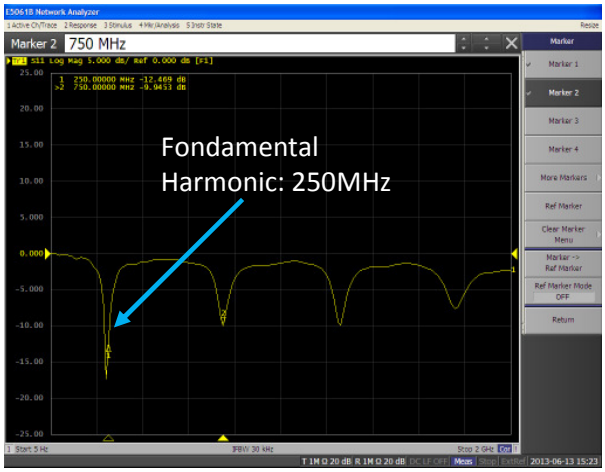

Figure 40: S11 measurement on a 250 MHz antenna

Figure 40 shows that the fundamental harmonic (first harmonic) is at 250MHz. The other harmonics are odd harmonics. Figure 41 shows the S11 measurement of the coaxial cable with a copper core of 10 mm length.

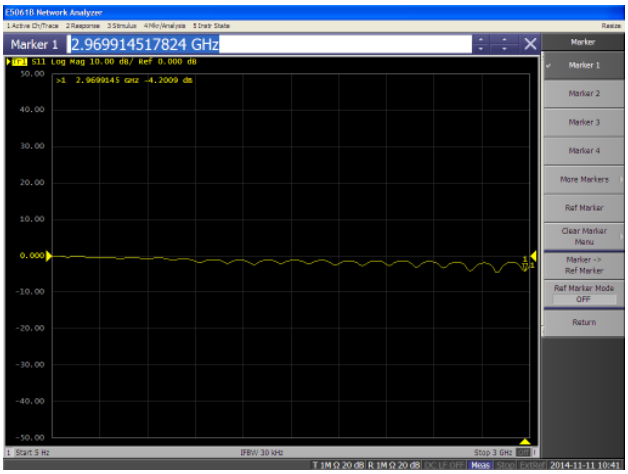

Figure 41: S11 measurement on the sensor

Figure 41 shows that no pulses are visible. This means that the coaxial cable is a very poor antenna, at least up to 3 GHz. Consequently the proposed sensor should not be able to detect the electromagnetic waves emitted by partial discharges since they are situated below 1 GHz. This is the reason why it will be called “sensor” and not “antenna” in the following chapters.

3.4 METHODS COMPARISON

Table 1 shows a comparison of the existing partial discharges sensing methods with the method proposed in this thesis.

	Standard electrical method	Optical	Acoustical	Chemical	Proposed method
PDs localization	No (Require analysis afterward)	If the discharges are external	Using triangulation PDs can be localized	Depending on the setup	Not (Require analysis afterward)
PDs Quantification	Yes	Yes	Yes	No	No
Setup	This method requires a complex and bulky setup to be assembled	When using just a camera, the setup is simple but an elaborated setup using light sensors and optical fibers could be complex and bulky	Elaborated setup (Microphone, amplifier etc.) are required	When using ozone sensing paper the setup is simple but more complex chemical investigations require knowledges in chemistry and appropriate chemical products	Simple (Stripped coaxial cable, filtering, oscilloscope)
PDs distinction under pulse-like voltage	No	If the discharges are external and are emitting enough light to be detected.	If the discharges emits enough noise	If the discharges induce chemical transformations that can be detected	Yes
Cost	Expensive (Coupling capacitor, amplifiers, calibrated impedance, calibrator, software etc.)	An inexpensive camera may be enough to perform optical detection but an elaborated setup using light sensors and optical fibers is expensive	Relatively expensive depending on the quality of the detection (Microphone, audio amplifier, analyzing software)	Relatively expensive depending on the setup	Inexpensive (Stripped coaxial cable, filtering, oscilloscope)

Table 1: Comparison of the existing methods with the proposed method

Considering that the objective of the study presented in this thesis is to develop a sensing method to detect partial discharges on-line in an aeronautical converter, the preponderant characteristic of the method must be the ability to distinguish partial discharges over the switching noise of the converter. The proposed method has this characteristic. Moreover the setup is simple and inexpensive. Partial discharges cannot be directly localized or quantified but this is not necessary to fulfill the requirements. Consequently the proposed method is the most appropriate one.

4 EXPERIMENTAL STUDY

4.1 CONSTITUENTS INVESTIGATION: USING SAMPLES TO VALIDATE THE SENSING METHOD

Investigating constituents is the very first step on the road to ensure the design of partial discharges-free converters by taking into account the specificity of the different stresses applied on the electric components (and of course on their insulating constituents) and of the process for realizing them. This part describes the tests realized on samples made with insulating constituents used in aerospace power electronics converters. Partial discharges measurements are performed using the new detection while comparing results (when possible) to those obtained using the standard electrical method. Materials used as insulation in these systems are first listed and then tested in different conditions.

4.1.1 CONSTITUENTS SUMMARY

Samples have been created following the description in chapter 2.1.2. The goal is to get samples representative of all types of defects that can exist in power electronics systems. Several types of dielectric materials are used as insulation, and are described below.
A non-exhaustive list of materials used in aeronautical power electronics systems is established. The materials are applied carefully on each sample to create the appropriate defects. Some of the insulating materials, such as enameled wire, were already applied. For these materials, the defects were created by modifying their geometry (e.g. twisting them together to create external defects).
Coils and transformers use copper wires insulated with a thin layer of polyurethane (PU). This material is tested, using the standard [ASTM2], by twisting two enameled wires around each other as shown in Figure 42. It creates external or surface discharges.

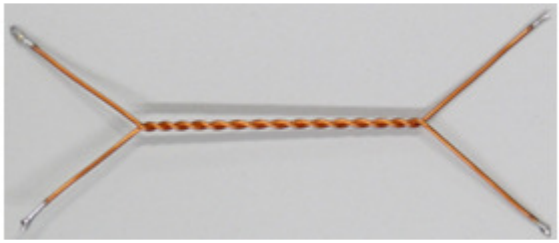

Figure 42: Twisted pair of enameled wire

The insulation of some cables used in aerospace are made with Fluorinated Ethylene Propylene (FEP). This material is subject to high voltage and laid down on a ground plane. This configuration may ignite partial discharges between the insulation and the plane (external defect). This cable is thus attached to a copper plate, as shown in Figure 43, and the high voltage is applied between them.

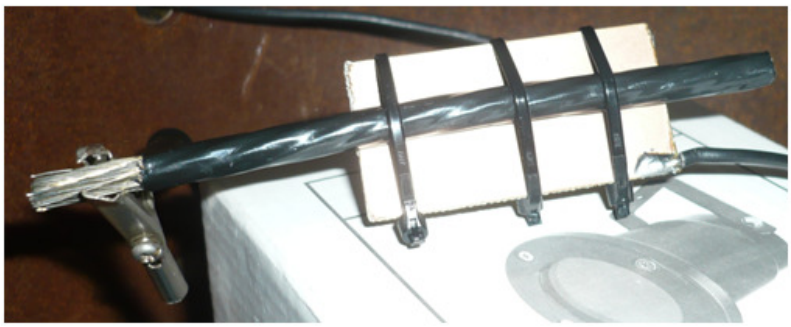

Figure 43: High voltage cable on a copper plane

A type of material, called Humiseal®1B31, is used to protect PCBs against harsh environmental variations. This coating is applied on a bare copper plane, with a sharp needle hanging above it. When the high voltage is applied to the needle, a corona defect is created (Figure 44).

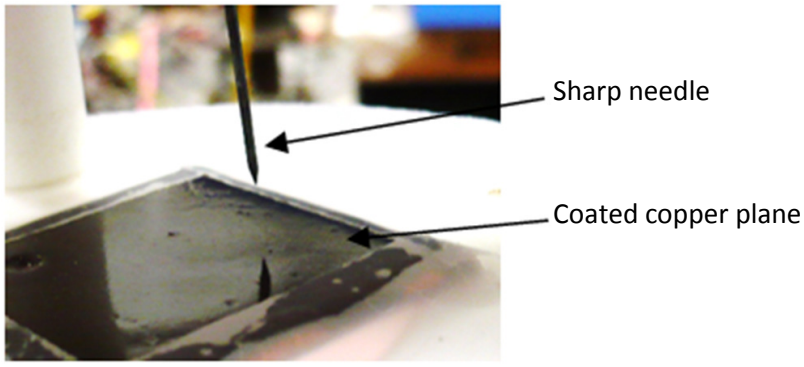

Figure 44: Sharp needle on a coated copper plane to create corona defect

In aircrafts environment, heavy HV components (such as transformers) must be insulated and fixed correctly so that they can withstand vibrations and avoid any electrical damages. This is often achieved by potting the component using the material applied in Figure 44.

Lastly, to study internal defects, polyetheretherketone (PEEK) is used to form a vented sample, thanks to the staking of different layers, (Figure 45) and electrodes are brought on each side.

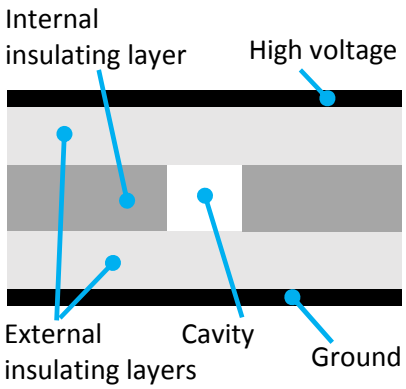

Figure 45: Vented sample for the simulation of an internal defect

The object is immersed into Fluorinert liquid [FC72] to be sure that discharges occur only internally. PEEK is used in aerospace to reinforce structures based on carbon fiber. In that case, the material is not subject to high voltage. Nevertheless we chose to include it in order to cover all possible types of defects that can exist, since it is not the degradation of the material which has to be studied but

the ability of our methods to detect PD. Table 2 summarizes the materials used.

	Short name	Location on PE system	Type of defect
Polyuerthane	PU	Coil - transformers	External
Fluorinated ethylene propylene	FEP	HV cable	External
Coating 1B31	1B31	On PCB	Corona
Potting (Harz + Härter)	POT	Transformers	Corona
Polyetheretherketone	PEEK	Carbon fiber based structures	Internal

Table 2: List of materials used to investigate constituents

4.1.2 MEASUREMENT RESULTS

The first part of this chapter details the results obtained under AC and pulse-like voltage. DC voltage is a peculiar case that will be treated afterwards. Relative humidity and ambient room temperature are recorded before and after each test.

4.1.2.1 Measurement setup

Measurements in this chapter are based on the setup shown in Figure 46. Three partial discharges sensing method are compared. First of all, the stripped coaxial sensor which is the core of this investigation. Secondly, a Rogowski coil (Bandwidth: 0 - 80MHz) which gives a voltage representative of the alternating current flowing into a circuit. And finally, the standard electrical sensing method (ICM Systems from Power Diagnostics).

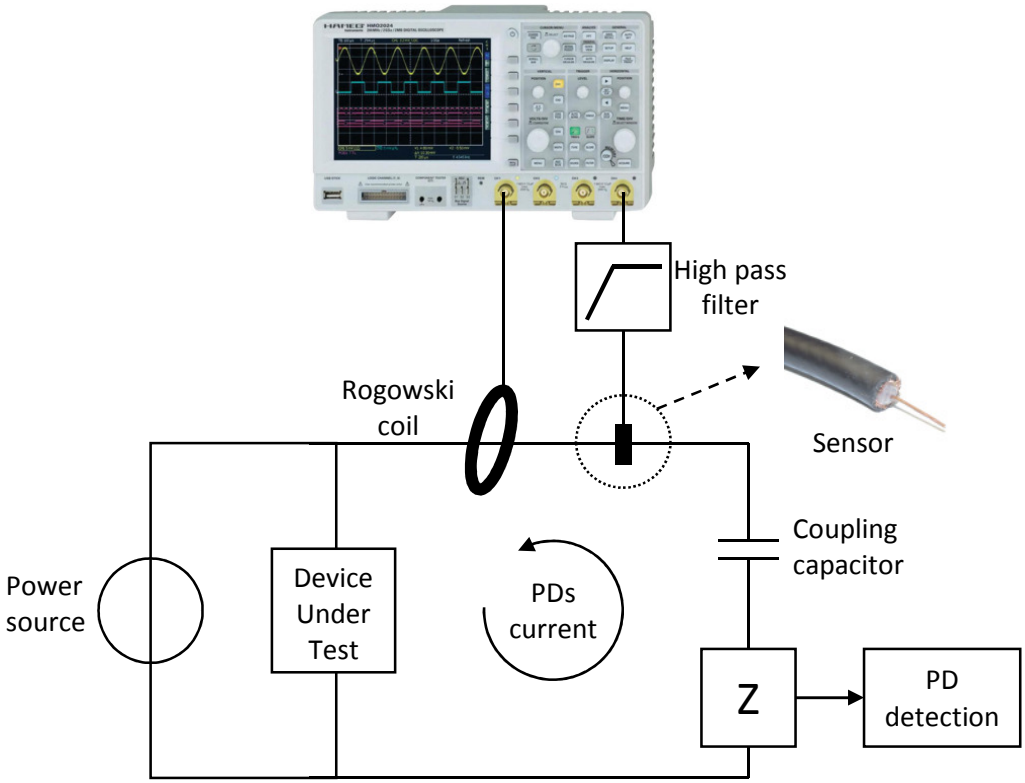

Figure 46: Measurement setup for constituent investigation

4.1.2.2 Check-up of the defect types

Before providing any results, checking the nature of each defect is important. For example, the twisted pair of enameled wire is supposed to present external discharges. This must be checked. The same reasoning applies to internal and corona discharges. It is essential that our samples represent all potential types of defects to ensure that our detection method can detect every type of partial discharges. Starting with the external type of defect, PU and FEP materials (Table 2) are first investigated.

a) External defect

The easiest way to check that partial discharges occur on the outside of the object is to insert it into an insulating liquid (FC72). When the twisted pair of enameled wire (Figure 42) or the cable-to-plane (Figure 43) are immerged into this liquid no discharges are measurable, whereas they are in ambient air. This implies that the discharges for this sample occur externally.

External discharges can also be investigated using optical detection since photons from ionization are not trapped into the material. Analyzing the video composite signal from a camera that is immersed in a black chamber with a sample emitting partial discharges can help for localization. A composite video signal is comprised of a series of signals that represent one line of the current image displayed. These signals are separated by a low level that is used as synchronization (Figure 47).

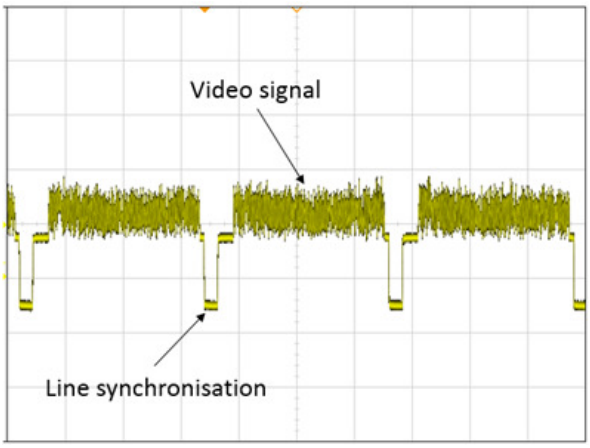

Figure 47: Typical shape of a composite video signal

The setup shown in Figure 48 is used and the video signal is recorded with and without partial discharges.

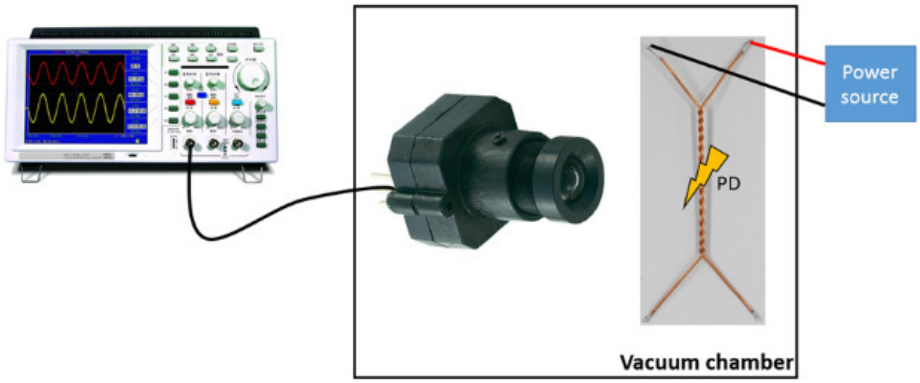

Figure 48: Setup for optical detection on a twisted pair of enameled wire

Figure 47 shows the signal when no PDs occur. It can be seen that the video signal is constant, and at a relatively low level, due to the darkness of the vacuum chamber.
Figure 49 shows the video signal when partial discharges occur. The visual persistency of the scope is used in order to display the complete image in one display. The line sychronisation seems imperfect due to another sychronisation called “image synchronisation”. This does not change the line display, it simply means that several images are superimposed.

We can observe an increase of the signal level in the middle of the image. This means that photons are emmited by the samples and, consequently, that partial discharges are occuring.

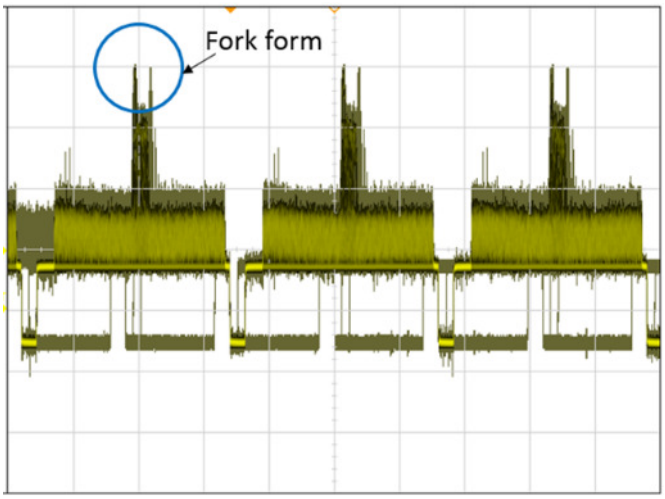

Figure 49: Composite video signal measurements by the camera when external partial discharges occur

We can point out the particular shape of the signal at the highest level, fork like. Knowing the type of defect of our sample, this can be easily explained. The defect being extern, we know that PD have to occur at the periphery of the twisted sample as shown in Figure 50.

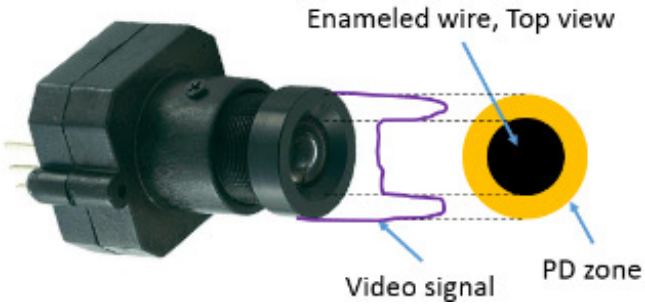

Figure 50: Representation of external partial discharges observed from the side of the sample

The camera automatically receives more photons from the sides of the sample than from its center. That is indeed what is measured. This is further evidence that partial discharges on this sample occur externally. Moreover, at a low level of intensity, the camera is still able to detect the discharges, whereas the human eye cannot. This method is used in components investigation in order to help localizing external or corona discharges.

b) Internal defect

The second type of defect that must be checked is the internal one. It is quite hard to obtain, as it requires very thin material to ignite partial discharges. The only way to check that partial discharges occur internally is, to immerge the sample into insulating liquid. Using this method on the vented sample (Figure 45) with PEEK material, we measure an inception level (PDIV) of about 2kV with and without insulating liquid. This means that partial discharges are necessarily occurring inside the sample.

c) Corona defect

Lastly, corona defects must be checked. The simplest way to confirm that PD occur in a corona defect is to analyze the symmetry of the discharges signal. “Corona discharges” are known to provoke dissymmetry on partial discharges occurrences.

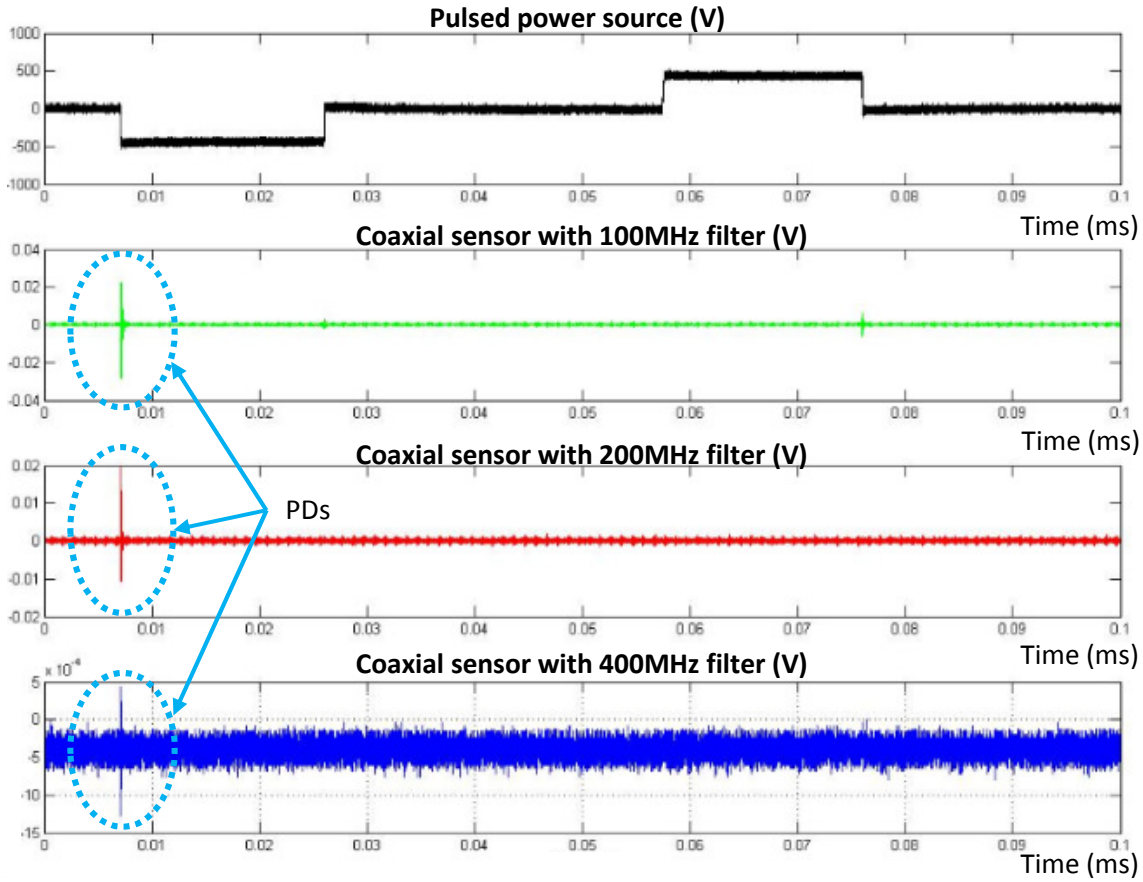

Figure 51: Corona discharges in a sample subject to pulse-like voltage. Power source (black curve), Coaxial sensor + 100MHz filter (Green curve), Coaxial sensor + 200MHz filter (red curve), Coaxial sensor + 400MHz filter (blue curve)

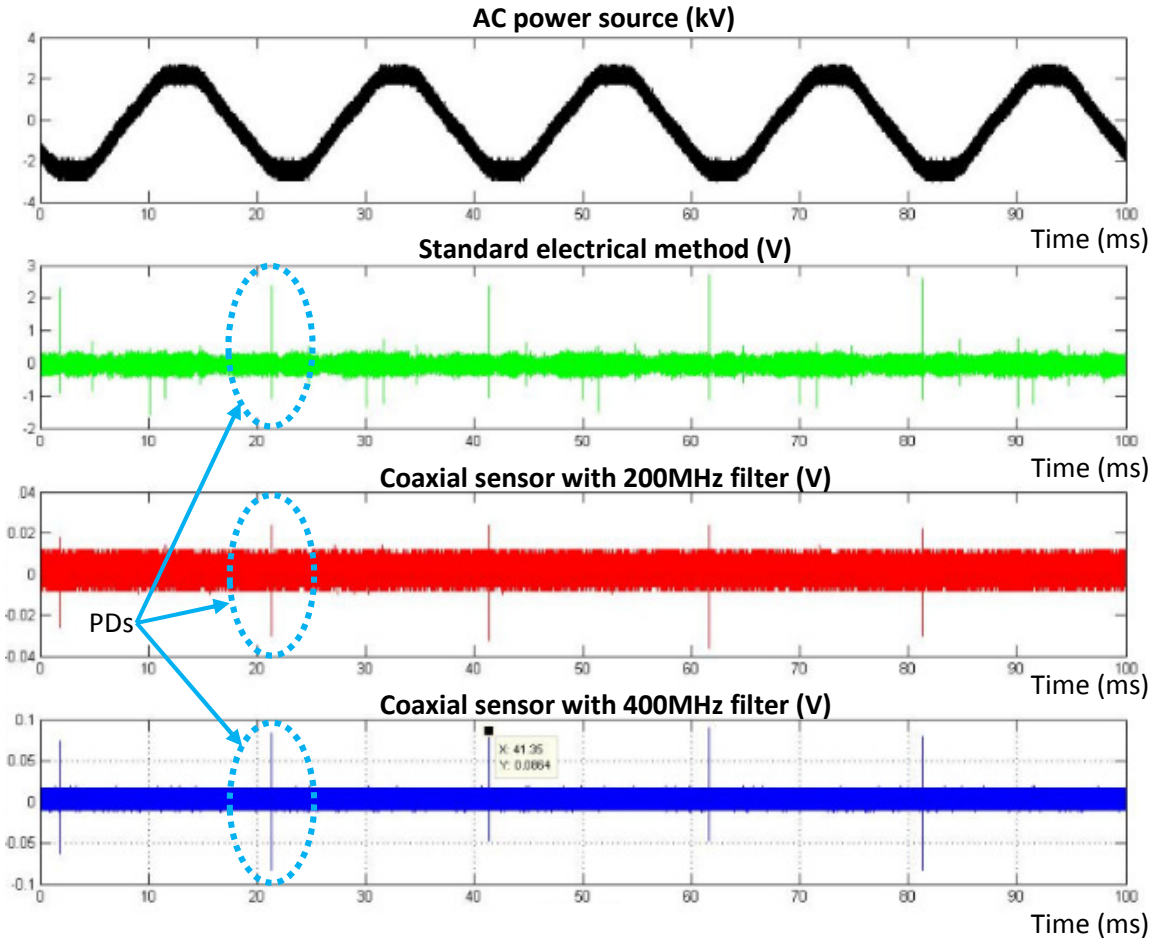

Figure 52: Corona discharges in a sample subject to AC voltage. Power source (black curve), Power diagnostic detection device (Green curve), Coaxial sensor + 200MHz filter (red curve), Coaxial sensor + 400MHz filter (blue curve)

Figure 51 and Figure 52 show partial discharges measurements performed on a point to plane sample (Figure 44). It can be observed that pulses occur mainly on one polarity of the pulse-like signal and the AC signal. This dissymmetry is characteristic of the corona defect.

All samples were tested successfully as described previously to be sure that all types of defects are represented in the study.

4.1.2.3 Filter influence

As described earlier, this work investigates a new method using filters. This section describes the influence of filtering on partial discharges detection for samples subjected to AC and pulse-like voltage.

a) AC voltage

Table 3 shows the results of the tests on a twisted pair of enameled wire submitted to AC voltage. The upper line shows results at atmospheric pressure, and the lower line at 100 mbar.

Sample PU under AC voltage	Voltage at which partial discharges are observed						
	ICM	**Rogowski**	**Sensor without filter**	**50MHz**	**100MHz**	**200MHz**	**400MHz**
1000 mbar	900	900	900	900	900	900	-
100 mbar	620	620	620	620	820	820	-

Table 3: PDIV comparison of a twisted pair of enameled wire subject to AC voltage with different high pass filters (None - 50MHz - 100MHz - 200MHz - 400MHz). ICM is the partial discharge sensing device using the standard electrical method to detect partial discharges.

The ICM is the standard partial discharges detection method (c.f. 2.7.1).

At atmospheric pressure, only the 400MHz filter did not detect any discharges. This outlines a degradation of the detection when using a high pass filter with a higher cutoff frequency. At low pressure (100 mbar), this degradation occur at a lower voltage. The voltage, at which partial discharges are observed, is increased by using a filter above 50MHz. It can be noticed that, without filtering, the proposed sensing method is able to detected partial discharges at the same inception voltage as the ICM. Tests performed on all samples gave equivalent results.

Figure 53 shows the measurement of corona defect sample submitted to AC voltage. Having a look on the magnitude of the pulses, the ICM appears to have the biggest one (1.72V), followed by the Rogowski coil (190mV) and by the coaxial sensor (20mV).

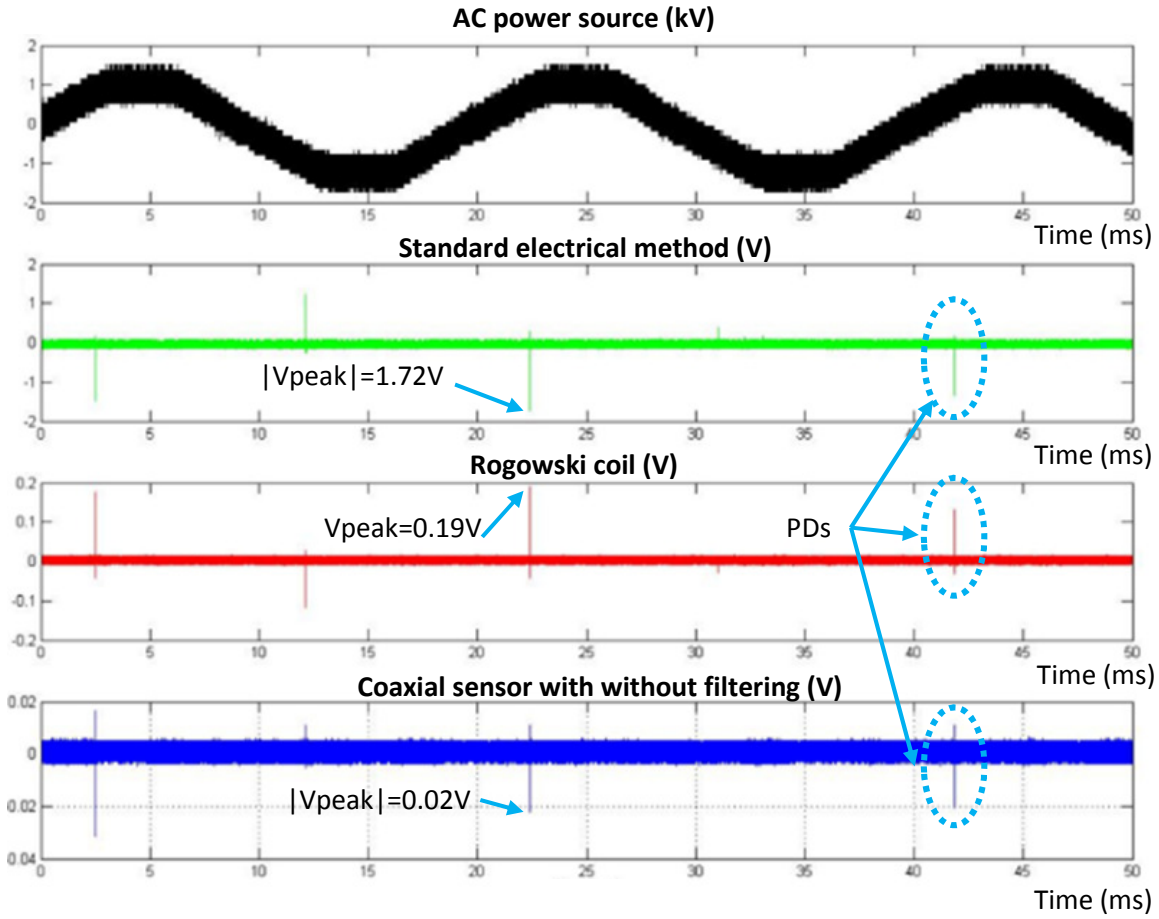

Figure 53: PDs magnitude comparison on a corona defect sample

The standard electrical method (ICM system) appears to be the most suitable method for detecting partial discharges under AC voltage, and actually it is since it uses a direct sensing of the current whearas the two other methods use indirect method to detect the current. However, considering the proposed method, since only the sinusoidal voltage has to be filtered, it is better to use the sensor without filter to detect partial discharges off-line under AC voltage.

b) Pulse-like voltage

Table 4 shows the results from the measurements performed on a twisted pair of enameled wire submitted to pulse-like voltage.

Sample PU under pulse-like voltage	Voltage at which partial discharges are observed					
	Rogowski	**Sensor without filter**	**50MHz**	**100MHz**	**200MHz**	**400MHz**
1000 mbar	PD drowned in switching noise	PD drowned in switching noise	PD drowned in switching noise	PD drowned in switching noise	850	850
100 mbar	PD drowned in switching noise	PD drowned in switching noise	PD drowned in switching noise	PD drowned in switching noise	450	450

Table 4: PDIV comparison of a twisted pair of enameled wire subject to pulse-like voltage with different high pass filters (None - 50MHz - 100MHz - 200MHz - 400MHz)

Table 4 shows the main issue when trying to detect partial discharges under pulse-like voltage: switching noise. The noise created by the sharp edges (dV/dt) of the signal make any partial discharges detection difficult.
That is where the coaxial sensing method and its filter are the most useful. As it can be seen in Table 4, the 200MHz and 400 MHz high pass filters are able to bring the partial discharges signal out of the switching noise, making it possible to define a PDIV.
In this case, filtering is necessary. For that reason, four different high pass filters are compared. Their cut-off frequencies are 50MHz, 100MHz, 200MHz and 400MHz. The most efficient filter for noise suppression must be determined. Figure 54, Figure 55, and Figure 56 represent the results of measuring a twisted pair of enameled wire and show many pulses. Among these results, it is worth distinguishing those related to the switching from those related to partial discharges. Since switching noise has a linear behavior with increasing voltage, the concept of linear behavior is used assuming that the magnitude of the switching pulses follows proportionally the magnitude of the voltage source, contrary to partial discharges signals. Hence, for voltage values varying from zero to PDIV, only the pulses associated with switching are detected. For voltages equal to or greater than PDIV, partial discharges pulses are added to switching noise. These pulses present a non-linear behavior with the voltage and can therefore be considered as partial discharges.

Moreover, Figure 54 and Figure 56 show that when PDs occur, the Rogowski coil, the coaxial cable without filtering, and the coaxial cable with the 50MHz filter and the 100MHz filter detect three or four pulses. These pulses are a combination of partial discharges signal and switching noise. For voltage below PDIV (Figure 55), no pulses are measured with the 200MHz filter and the 400MHz. When partial discharges occur, only two pulses are measured during each rising front of the power signal with the 200MHz filter (Figure 56). Furthermore, it is important to note that whatever the voltage magnitude is (above or below PDIV), no pulses are measured with the 400MHz filter. Applying this detection methodology on the various samples yields the same results.

From these measurements, the 200MHz filter appears to offer the best trade-off for partial discharges detection and noise reduction under pulse-like voltage. The Rogowski coil, the 50MHz and 100MHz filter do not suppress switching noise, whereas the 400MHz filter suppresses everything, including PD signals for the samples under study.

Finally it is worth saying that since the 400MHz filter can detect PD under pulse voltage but not under AC, it seems that the characteristic of the PD is changing.

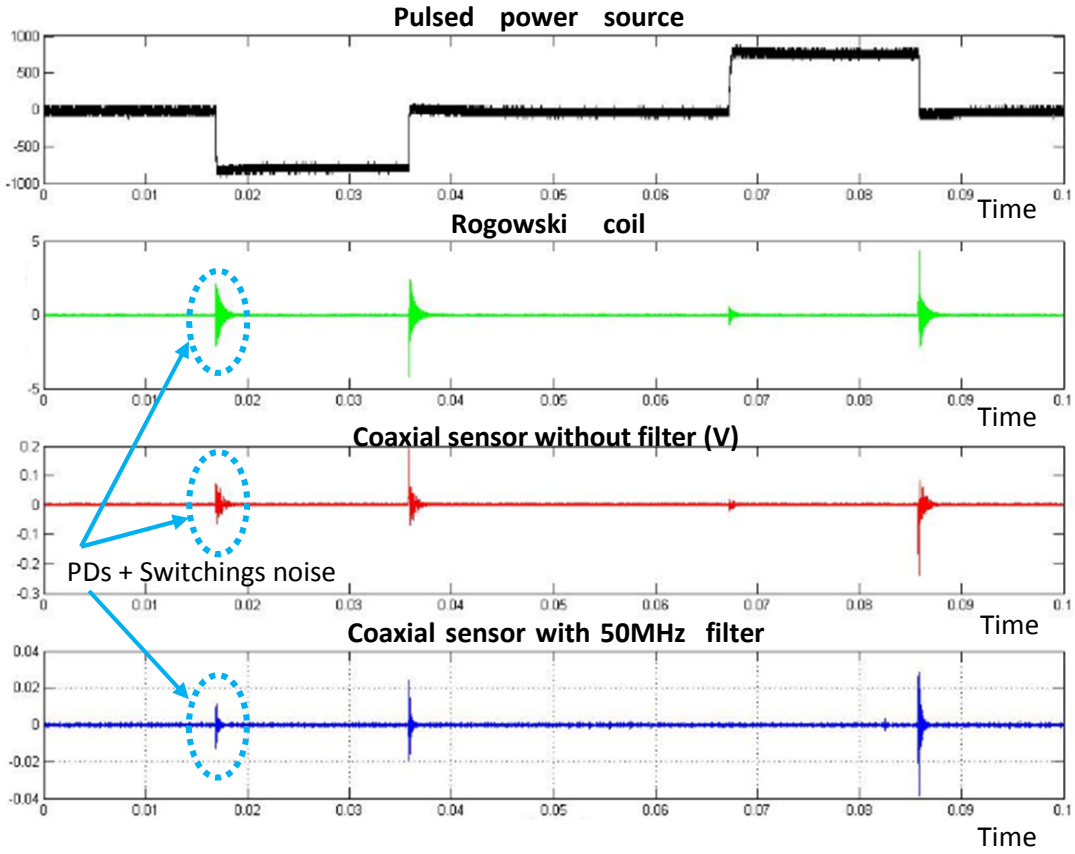

Figure 54: Partial discharges and switchings noise occurring simultaneously

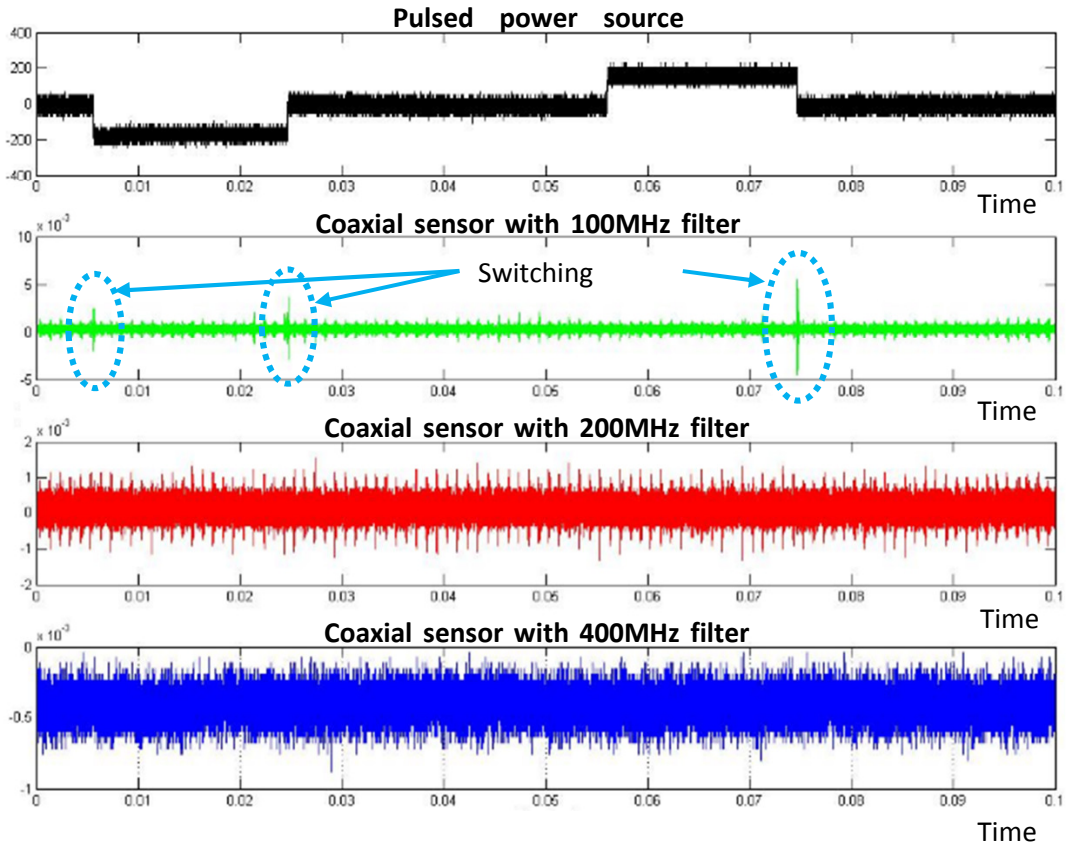

Figure 55: Before PDs occur, only switching noise is visible

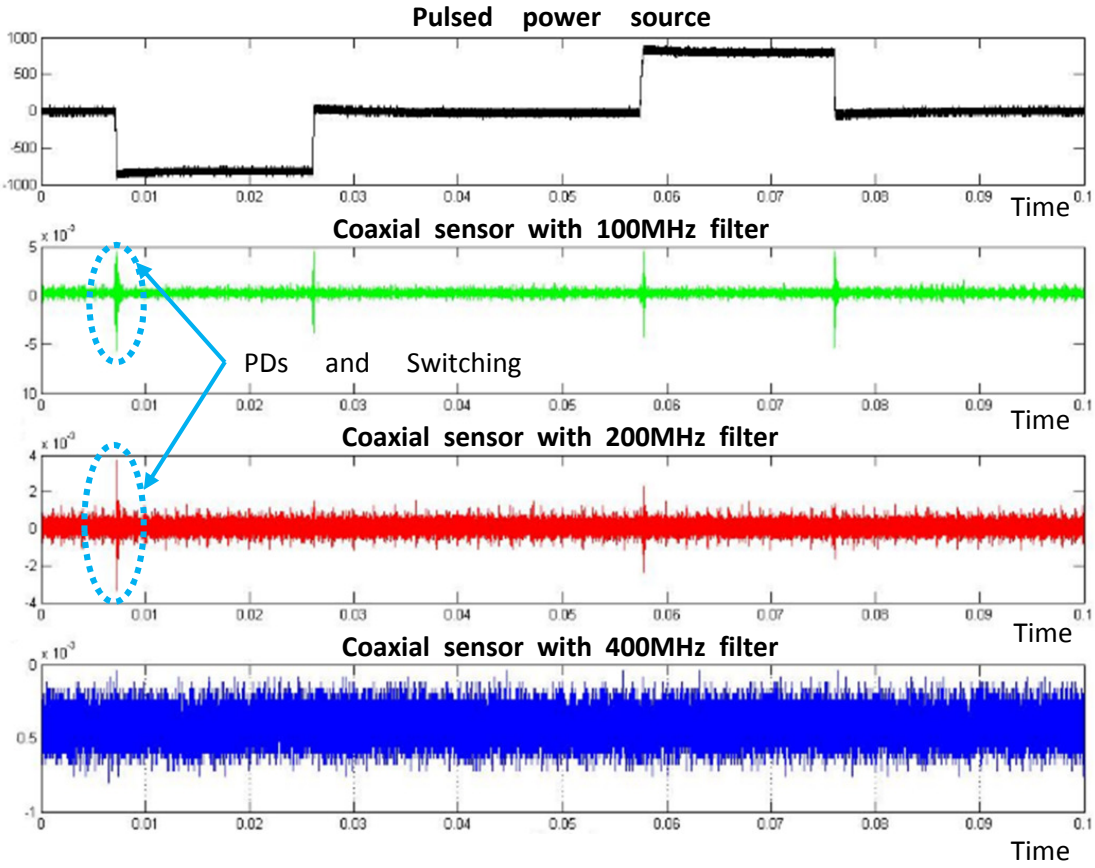

Figure 56: PDs and switching noises occurring simultaneously

During his investigation of this method on converters from the company Renault, Thibaut Billard [Billard] found out that the most appropriate filter for PD detection was the 400MHz. The results presented in this work indicates that the 200MHz is the most suitable. It means that it is not possible to define a unique filter which could cover all type of discharges. By changing the nature of the discharges, its frequency components may also vary and thus may require a different filter for partial discharges detection.

4.1.2.4 Particular phenomenon

While performing measurements on the twisted pair of enameled wire under pulse-like voltage, a peculiar behavior regarding discharges has been observed.
At ambient pressure, the voltage magnitude is increased, partial discharges are observed at about 750Vpeak, and a slight glow appears on the sample (Figure 57).

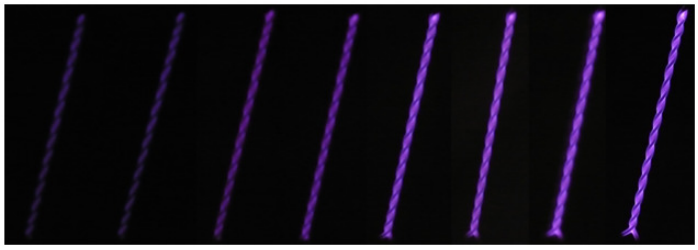

Figure 57: Twisted pair of enameled wire glowing under pulse-like voltage. The glow intensity increases with increasing voltage

At low pressure, as expected, partial discharges start at a lower voltage, about 440Vpeak. As the voltage is still increased, the magnitude of the partial discharges pulses decreases until they disappear. A glowing is still apparent on the sample, and even when the discharges were no longer electrically measurable on the scope the brightness of this glow remained strong.
It means that ionization is still occurring on the sample, but none of the electrical detection method used in this study is able to measure the discharges. Figure 58 gives a graphical summary of our observations.

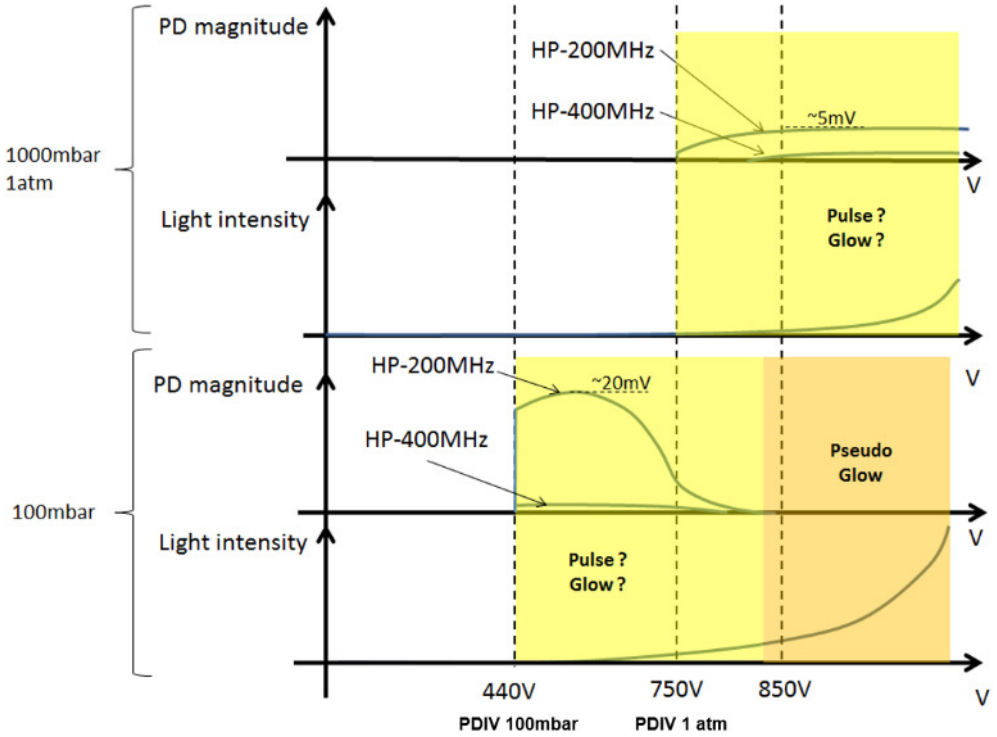

Figure 58: partial discharges measurement on a twisted pair of enameled wire subject to pulse-like voltage

The yellow area of the graph shows pulses and glowing (detectable by the human eye). The discharges occurring here could be of Townsend type (Pulse type) or Glow type, both showing pulses according to [Bartnikas1]. The orange area of the graph has a strong glow, but no discharges are electrically detected. This is referred as Pseudo-Glow discharges by [*Bartnikas1*]. A description of

Pulse type, Glow, and Pseudo Glow discharges has already been made respectively in Figure 15, Figure 16 and Figure 17.

Bartnikas explained that the discharge may emit light but only two pulses per period (Glow discharge) or no pulses at all (Pseudo-Glow) can be measured.
In the case of Pseudo-Glow discharges, the conditions are met so that the inception voltage and the résidual voltage are very close: Eb – Er tends to zero (Figure 17).

$$q = C * V \textbf{ with } V = Eb - Er \textbf{ and } (Eb - Er) \to 0$$

$$\textbf{Thus } q \to 0$$

$$\textbf{Since } i = \frac{q}{t} \textbf{ Thus } i \to 0$$

q: Quantity of charge in the discharge
C: Capacity of the defect
V: Voltage drop across the defect during the discharge
Eb: Breakdown voltage
Er: Residual voltage
i: Discharge current
t: Time

According to the above equations, since Eb-Er tends to zero, the discharges current tends also to zero. Therefore, the discharges magnitudes are weaker during pseudo-glow discharges. This is the reason why it is not possible to measure them.

Consequently we can assume that under pulse-like voltage, and in external defects at low pressure (100mbar), Pseudo-Glow discharges can be ignited. Furthermore, the samples subjected to this type of discharge breakdown after ten minutes. Pseudo-Glow discharges are very harmful for insulation.

This type of discharge was not detected in internal and corona defects. If they mainly (or only) appear in external defects, then optical detection with the camera (Fig. 13) might be the one way to detect pseudo-glow discharges. However, considering a complex system as a converter, it would not be possible to monitor every side of the system with one or some cameras. Consequently, this reveals a limitation of the PD sensing method which is not able to detect pseudo-glow discharges because of their pulseless nature.

4.1.2.5 DC voltage

Partial discharges measurements under DC voltage is a special case, since the time between two discharges can be very long (from a few minutes to several weeks, depending mainly on the type of insulating material).
Under alternative voltage (AC or pulsed), the discharge mechanism depends strongly on the permittivity of the dielectric material, as explained in section 2.5 In the case of DC voltage, the resistivity plays a more significant role.

This means that the defect, represented by a capacity, charges slowly through the "resistance" of the dielectric, which can reach the giga-ohm level. After a sufficient period of time, the voltage at the terminal of the defect reaches inception voltage and one discharge occurs. Then the process repeats.

Concretely, it means that pulses are measured randomly over time, and with a very low repetition rate. That is why partial discharges measurements under DC voltage is quite complex.

Nevertheless some tests have been performed on our samples using the same setup as in Figure 46.

In the first test the sample is supplied with a voltage that is 10% above PDIV under AC, and then let it sit during 15 minutes while the oscilloscope is observed. This test is repeated several times on all the samples. The oscilloscope showed a noise level, and very rarely one pulse (one peak every 3 tests). But it is very hard to determine the difference between partial discharges and external noise.

Therefore we decided to slowly change the value of the DC voltage over a 100 second period in the following protocole:
*800V → Decrease to zero → Decrease to -800V → Increase to zero → Increase to 800V (*Figure 59*).*

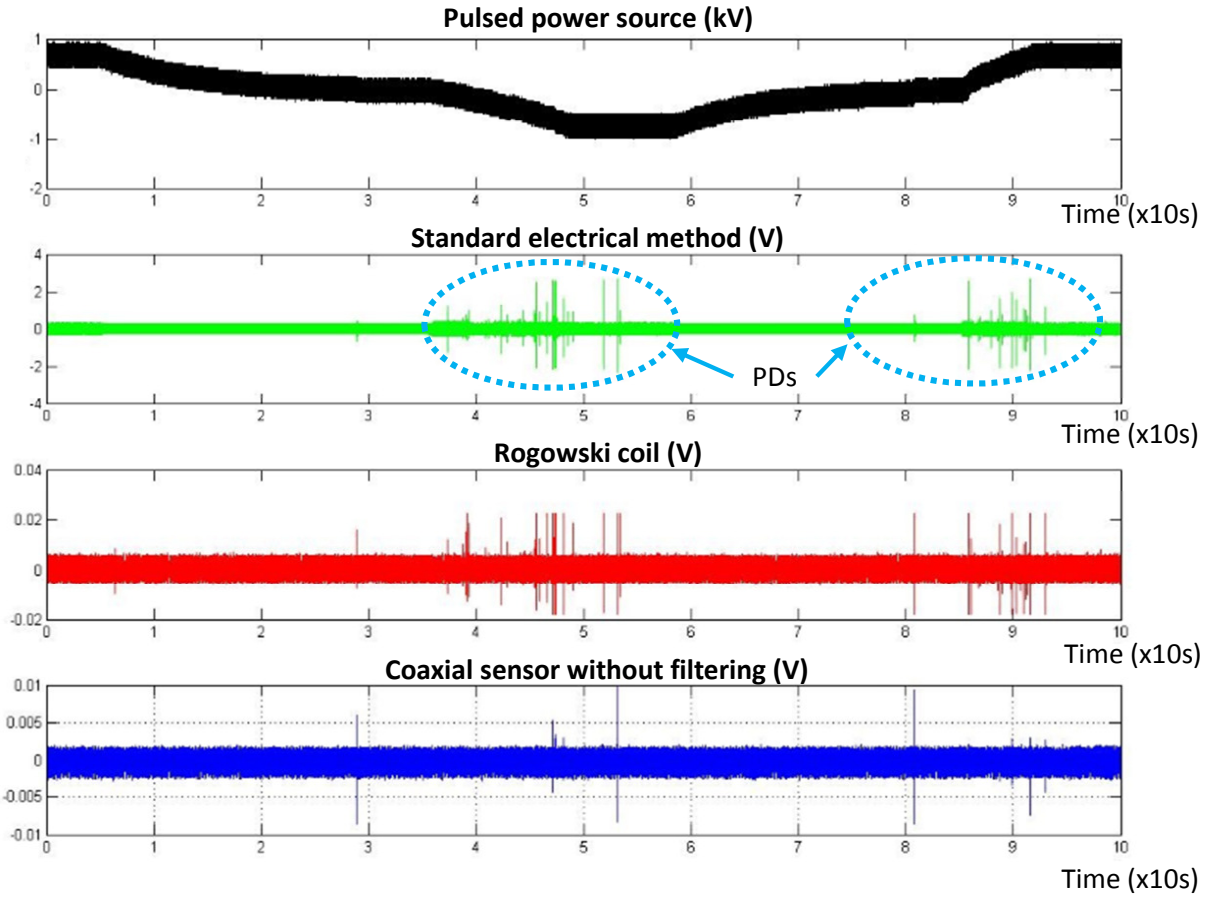

Figure 59: PD measurement under DC voltage on a twisted pair of enameled wire. Power diagnostic (green), Rogowski coil (red), coaxial cable without filtering (blue)

Figure 59 shows the results of these measurements. First of all, the pulses occurring near 30 and 80 seconds are not partial discharges. They are due to the discharge of the coupling capacitor before each polarity reversal. Then two groups of pulses can be seen around 45 and 90 seconds. These are probably partial discharges due to the change in polarity.
During the first 35 seconds, charges were accumulated into the sample defect. These charges created an electric field that reinforced the global electric field when polarity changes. This allowed discharges to be ignited. But, of course, the measured pulses are not partial discharges due to the DC voltage, since they need a polarity reversal to be created.

In conclusion, it is reasonable to say that, since the partial discharges repetition rate under DC voltage is very low, and since the only way to detect partial discharges is to reverse polarity (which does not currently happened in aeronautics converters), it is safe to assume that partial discharges under DC voltage are not harmful for PE systems. It is more important to focus our efforts on AC and pulse voltages where recurrent discharges with high magnitudes can occur.

4.1.3 CONCLUSION ON CONSTITUENT INVESTIGATION

The main conclusion of this chapter concerns the method's efficiency. A simple and stripped coaxial cable is able to detect partial discharges under AC conditions and, by adding filtering, discharges events can be dissociated from switching noise under pulse-like voltage. Among the different possibilities, the 200MHz filter proved to be the most efficient in our situations. The different types of defects (external, internal, and corona) that can exist in a real environment were tested, each of them showing that partial discharges can be detected using this method.

The efficiency of partial discharges detection under DC was not demonstrated, since electrical discharges are difficult to trigger. However, it was demonstrated that the dangerousness and the probability for these DC discharges to occur are very low.

4.2 COMPONENTS INVESTIGATION: INDIVIDUAL COMPONENTS

This chapter describes the measurements performed on components presents in a converter:

- High voltage connectors (AC input, PWM output)
- Input EMC filter
- ATRU (Auto Transformer Rectifier Unit)
- Power board (IGBT drivers)
- High-voltage cable

In this part of the study a large number of components have been tested. This section describes only the most significant results.

4.2.1 TEST VOLTAGES

The overall tests use voltages described in standards [ABD] and a second standard for DC voltage in aeronautics. The first being considered for tests under AC voltage, and the second for tests under PWM voltage (since the DC bus supplies the IGBTs that generate the pulsed voltage). Standards define two voltage levels during operation: rated and transient as shown in Table 5 and Table 6 for AC and DC voltages defined by the converter manufacturers.

AC voltage	**Single phase**		**Phase to phase** (Single phase x √3)	
	Normal condition	**Transient condition**	**Nominal condition**	**Transient condition**
Nominal rms voltage	230	-	398	-
Maximum rms voltage	260	360	450	623
Maximum peak voltage (Maximum RMS voltage x √2)	367	509	636	881
Maximum peak voltage + 10%	403	560	700	970

Table 5: Definition of the AC voltage according to manufacturer standard

DC Voltage	DC voltage – differential mode		DC Voltage – common mode	
	Normal condition	Transient condition	Normal condition	Transient condition
Nominal DC value	540	-	???	-
Maximum DC value	650	900	600	900
Maximum DC value + 10 %	715	990	660	990

Table 6: Definition of the DC voltage according to manufacturer standard

The tests described in this chapter use the worst case for each standard, namely, the maximum transient level + 10% (see blue and green cells in Table 5 and Table 6). A 10% safety factor has been added as a safety factor in order to prevent any inaccuracies from the voltage sources or voltage probes. Table 7 summarizes the voltages used in the tests.

Voltage type	Phase to ground (Vpeak)	Phase to phase (Vpeak)
AC	560	970
Pulse	990	990

Table 7: Test voltage description

Our investigations consider the following test protocol: The voltage is increased until detecting partial discharges or reaching the maximal specified level. If partial discharges are detected, the test is stopped and the results are noted (PDIV, test conditions, partial discharges magnitude, etc.). If no partial discharges are observed, the voltage is increased up to 2kVpeak, which is nearly twice the maximum voltage in the table. This voltage increase is intended to determine a safety margin regarding the maximum voltage that can occur in a real system.

4.2.2 COMPONENT INVESTIGATION

4.2.2.1 Results analysis

The values in the results tables are the ratio between the inception voltage measured during the test and either the maximum nominal voltage under AC condition (636Vpeak) or the maximum transient voltage (881Vpeak) as defined in Table 5.

These values intends to be easier to read since a value lower than 1 means that the discharges inception voltage is lower than, either, the maximum nominal voltage or the maximum transient voltage, depending on the column which is looked. Each time a value is lower than one the cell is colored in red and each time a breakdown occurred and no partial discharges were measurable, the cell is colored in orange.

When partial discharges occur at a voltage higher than the maximum nominal voltage or the maximum transient voltage, it is possible to directly read the additional voltage percentage required to ignite partial discharges. i.e. In Table 8 on Phase A to Phase B test, at 100mbar, partial discharges occured at a voltage 72% higher than the maximum nominal volatge which supplies these phases during normal operation and at a voltage 24% higher than the maximum transient voltage which may occur between these phases.

Each table of this document is written using this method. It allows a rapid analysis of the weakest point in this components investigation.

4.2.2.2 Setups and power sources

Figure 60 describes the main functions of the studied converter.

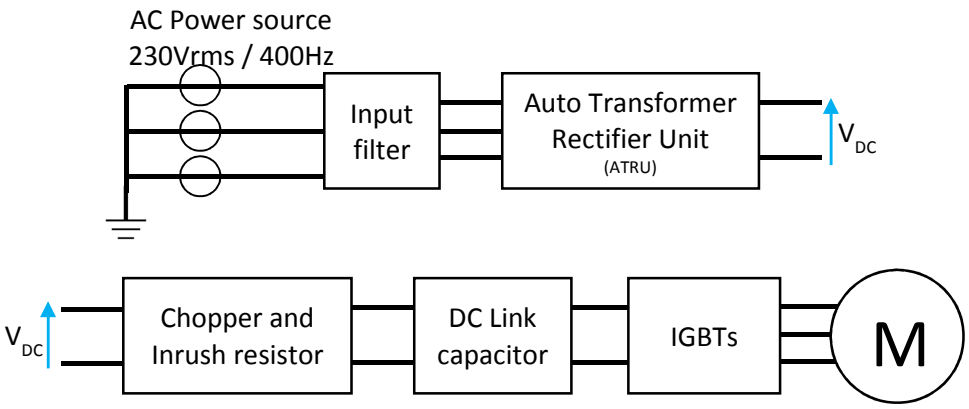

Figure 60: Voltage distribution in the ADGB

The chain is supplied by an AC power source 230Vrms 400Hz. At the input of the chain, a filter suppresses the electromagnetic interferences and protects against lightning. Then, an Auto Transformer Rectifier Unit (ATRU), which is an AC/DC converter, rectifies the voltage and filter high frequency harmonics. DC voltage is sent to the DC link capacitor through the inrush resistors. Finally

the IGBTs mounted in a three-phase bridge topology, controlled by the drivers, generates the PWM voltage which drives the motor.

Measurements are based on the setup described in Figure 61. The coaxial cable method and the Rogowski coil are used with filtering. The 200MHz filter is mainly used, considering its performance in our preliminary investigations (c.f. 4.1).

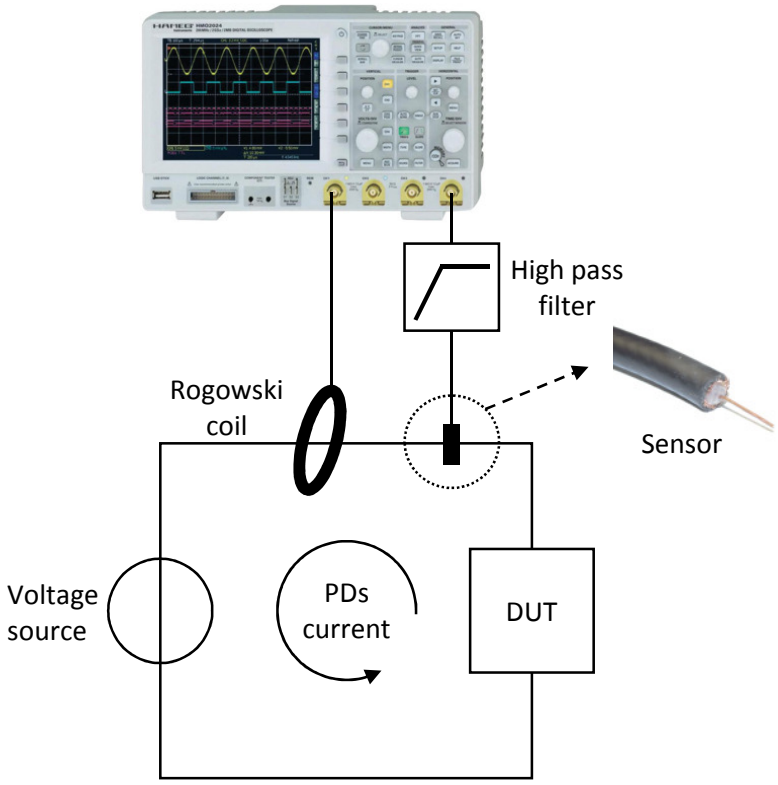

Figure 61: Components test setup

Two types of power sources are used: an AC source and a PWM-like source (Figure 62 and Figure 63). Only two phases are connected to the tested object.

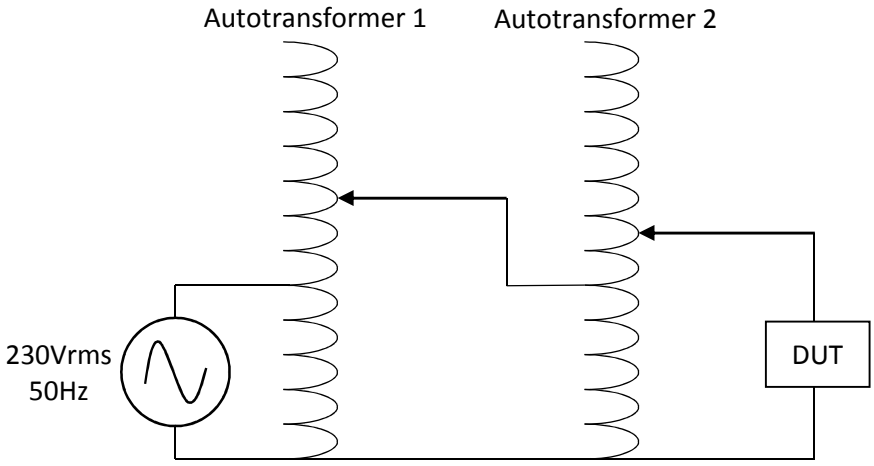

Figure 62: Electrical representation of the AC source

Using the configuration described in Figure 62, the DUT can received a voltage up to 4kV.

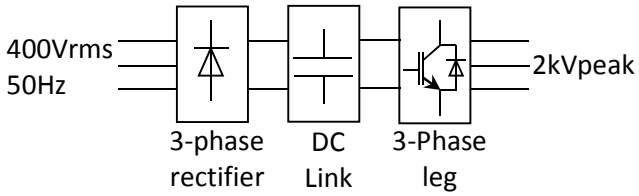

Figure 63: Electrical representation of the pulse-like source

The pulse-like source uses a three-phase topology to generate periodic bipolar pulses. The output voltage can reach 2kVpeak with a maximum current of 1A. The output frequency is about 12kHz.

4.2.2.3 High voltage connectors and cables

The first test is to determine if partial discharges can occur in the high-voltage connectors of the studied system. It is important to note that the connectors are already assembled to their cable when they are tested. Therefore, tests on connectors are divided into three steps:

- Female alone
- Male alone
- Male and female connected

The test setup is shown in Figure 64.

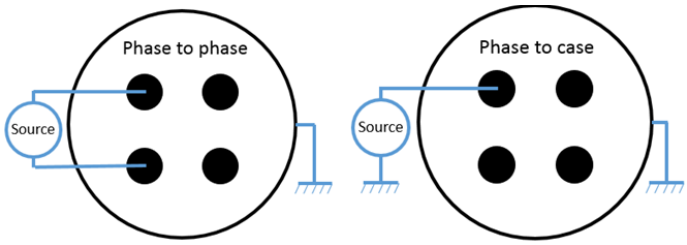

Figure 64: Connector test setups

Input connector:

In actual operations, the input connectors are subject to AC voltage. Therefore, as described in Table 7, they are tested with 560Vpeak phase-to-case and 970Vpeak phase-to-phase. Table 8 summarizes the results on the female connector.

Female connector	Ratio PDIV / Maximum nominal voltage		Ratio PDIV / Maximum transient voltage	
	1000 mbar	100 mbar	1000 mbar	100 mbar
Ph A to ph B	no PD	1.72	no PD	1.24
Ph B to ph C	no PD	2.04	no PD	1.47
Ph A to ph C	no PD	2.04	no PD	1.47
Ph A to case	no PD	3.26	no PD	2.35
Ph B to case	no PD	3.53	no PD	2.55
Ph C to case	no PD	3.53	no PD	2.55

Table 8: Measurement results on the female input connector

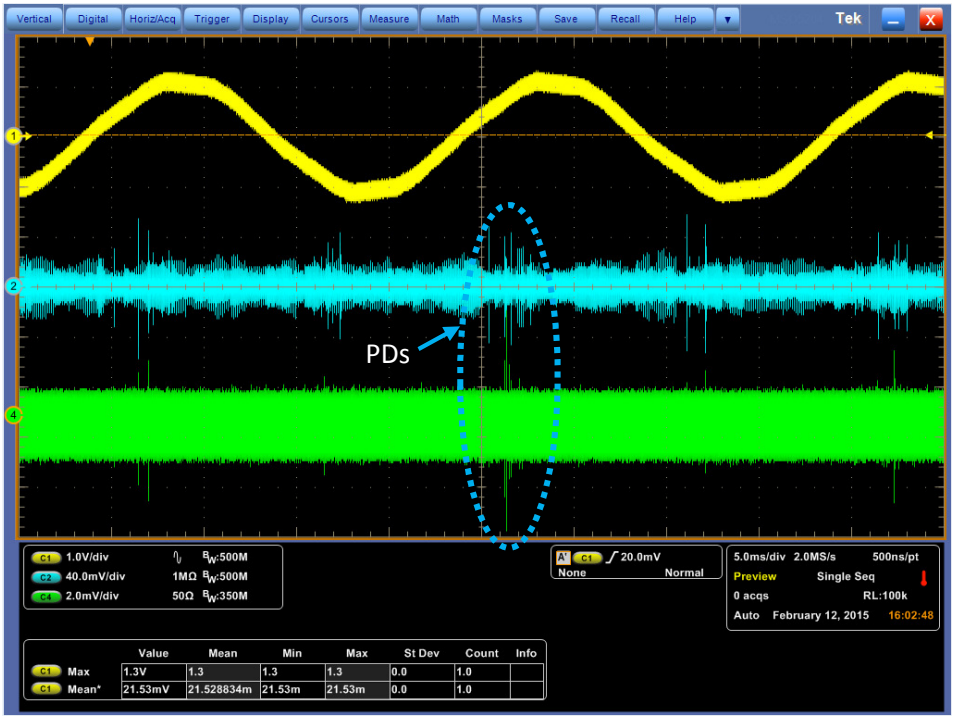

Figure 65: Partial discharges measured on the female part of the connector subject to AC voltage (phase-to-phase test). Channel 1: Power source (kV). Channel 2: Rogowski coil without filter. Channel 4: Coaxial cable without filter.

Table 9 shows the results of the male part of the connector.

Male connector	Ratio PDIV / Maximum nominal voltage		Ratio PDIV / Maximum transient voltage	
	1000 mbar	100 mbar	1000 mbar	100 mbar
Ph A to ph B	no PD	2.04	no PD	1.47
Ph B to ph C	no PD	2.19	no PD	1.58
Ph A to ph C	2.82	2.35	2.04	1.7
Ph A to case	no PD	4.07	no PD	2.94
Ph B to case	no PD	4.61	no PD	3.33
Ph C to case	no PD	-	no PD	-

Table 9: Measurement results on the male input connector

Remark: During the phase A to phase C test, and at low pressure (orange cells), the voltage source is distorted. This means that a strong current is flowing at the maximum of the voltage. The only plausible conclusion is that a electrical breakdown occurs before any partial discharges.

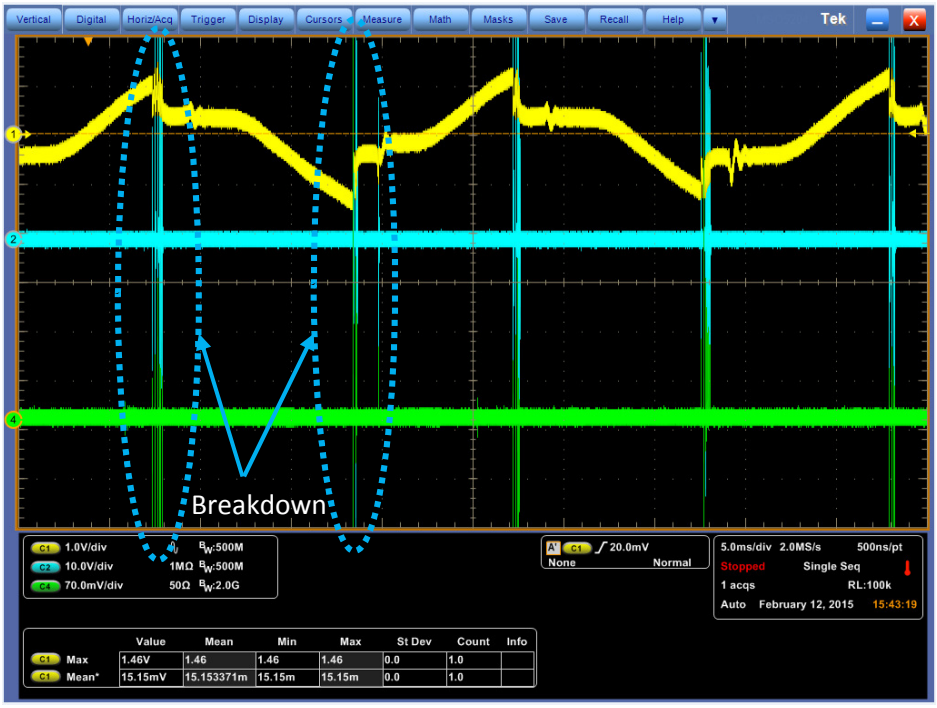

Figure 66: Voltage waveform during a breakdown event on the male part of the connector subject to AC voltage (phase-to-phase test). Channel 1: Power source (kV). Channel 2: Rogowski coil without filter. Channel 4: Coaxial cable without filter

The Table 10 shows the results of the male and the female connectors connected together.

Male + Female connectors	Ratio PDIV / Maximum nominal voltage		Ratio PDIV / Maximum transient voltage	
	1000 mbar	100 mbar	1000 mbar	100 mbar
Ph A to ph B	no PD	2.04	no PD	1.47
Ph B to ph C	no PD	1.88	no PD	1.36
Ph A to ph C	no PD	1.88	no PD	1.36
Ph A to case	no PD	2.98	no PD	2.16
Ph B to case	no PD	3.53	no PD	2.55
Ph C to case	no PD	3.53	no PD	2.55

Table 10: Measurement results on the male and female connectors connected together

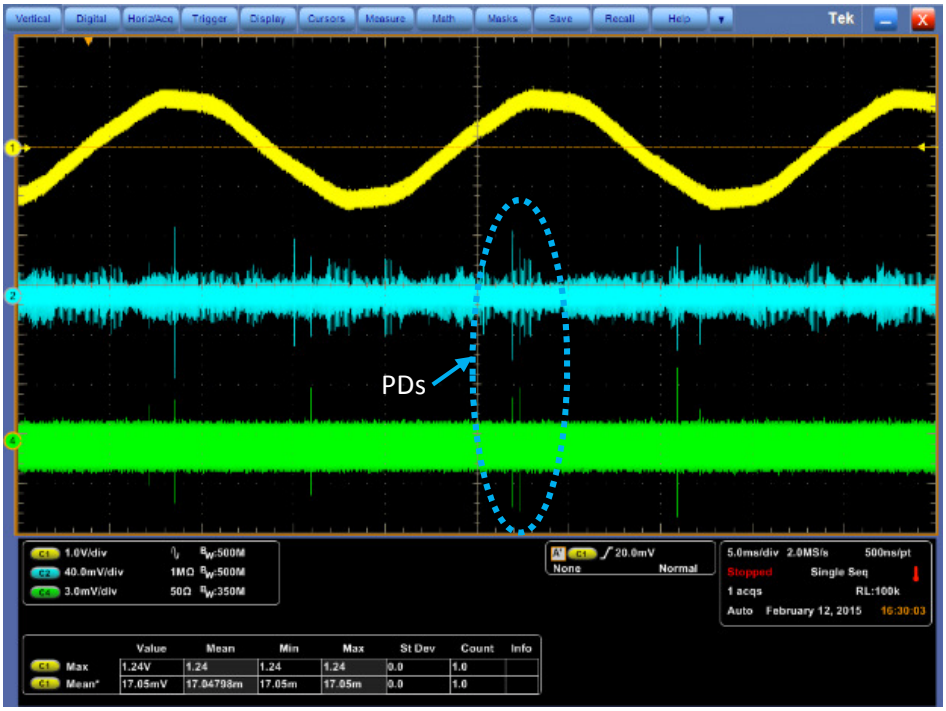

Figure 67: Partial discharges on the male and female part of the connector, connected together and subject to AC voltage (phase-to-phase test). Channel 1: Power source (kV). Channel 2: Rogowski coil without filter. Channel 4: Coaxial cable without filter

Measurements on the high-voltage input connectors did not show any partial discharge under nominal voltage or under transient voltage. To ignite partial discharges, the voltage must be increased to at least 24% higher than the transient voltage (Table 8). We can assume that this will never happen in the system in operation, neither at atmospheric nor at low pressure.

Output connector:

The output connectors are subject to PWM voltage. Therefore, following Table 7, they are tested under 990Vpeak phase-to-phase and phase-to-case. Table 11 sumarizes the results of the female part of the high voltage output connector.

Female connector	Ratio PDIV / Maximum nominal voltage		Ratio PDIV / Maximum transient voltage	
	1000 mbar	100mbar	1000 mbar	100mbar
Ph A to ph B	no PD	3,16	no PD	2,11
Ph B to ph C	no PD	no PD	no PD	no PD
Ph A to ph C	no PD	no PD	no PD	no PD
Ph A to case	no PD	no PD	no PD	no PD
Ph B to case	no PD	no PD	no PD	no PD
Ph C to case	no PD	no PD	no PD	no PD

Table 11: Measurement results on the female connector

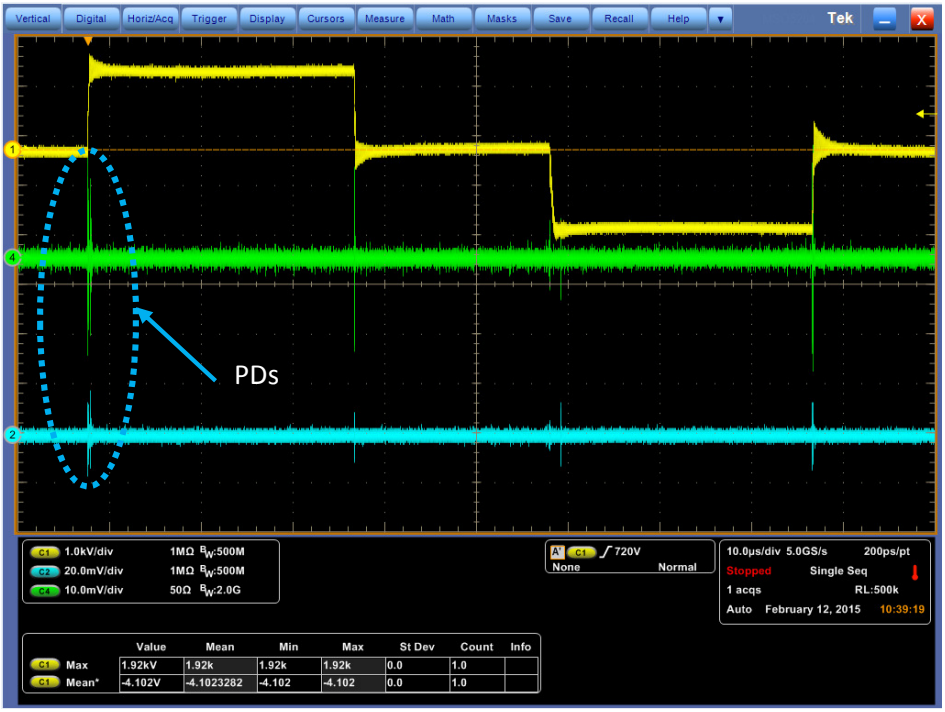

Figure 68: Voltage waveform during PD on the female part of the connector subject to pulse-like voltage (Phase-to-phase test). Channel 1: Power source (kV). Channel 2: Rogowski coil + 200MHz filter. Channel 4: Coaxial cable + 200MHz filter.

Table 12 shows the results of the male part of the high voltage output connector.

Male connector	Ratio PDIV / Maximum nominal voltage		Ratio PDIV / Maximum transient voltage	
	1000 mbar	100 mbar	1000 mbar	100 mbar
Ph A to ph B	no PD	1.36	no PD	0.91
Ph B to ph C	no PD	1.36	no PD	0.91
Ph A to ph C	no PD	1.46	no PD	0.97
Ph A to case	no PD	1.26	no PD	0.91
Ph B to case	no PD	1.26	no PD	0.91
Ph C to case	no PD	1.33	no PD	0.96

Table 12: Measurement results on the male connector

Partial discharges occur at voltages that may be reached during the life of the connector, though only in abnormal transient conditions with a very low repetition rate (according to manufacturer standard, less than 100 times in the system life-time).

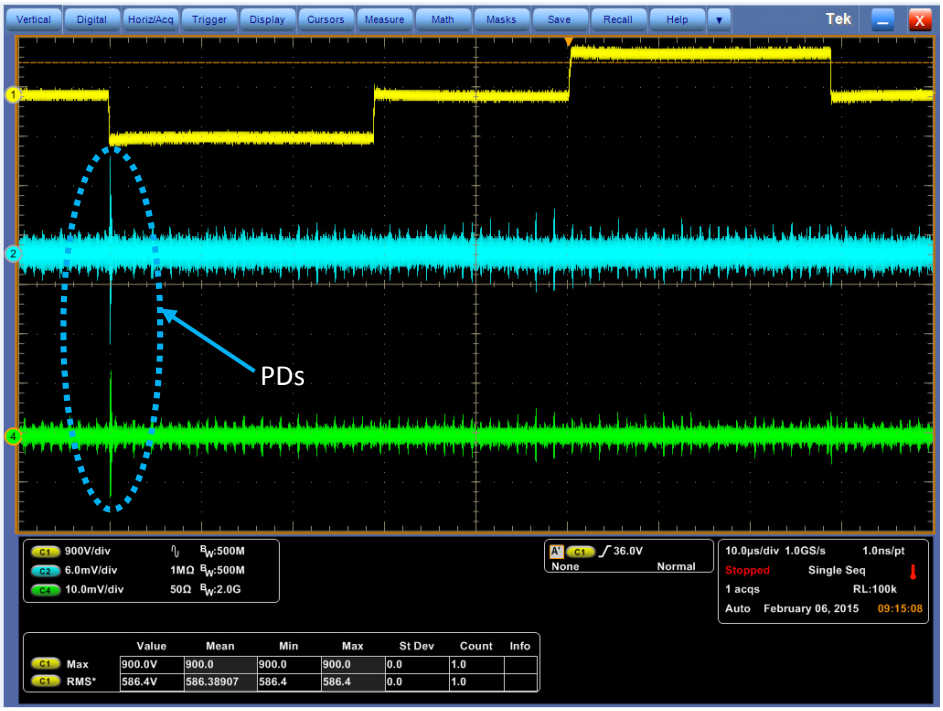

Figure 69: Voltage waveform during PD on the male part of the connector subject to pulse-like voltage (phase-to-case test). Channel 1: Power source (kV). Channel 2: Rogowski coil + 200MHz filter. Channel 4: Coaxial cable + 200MHz filter

The pattern is asymmetric (partial discharges during negative polarity's reversal but none on positive polarity's reversal) which lets assume that a corona effect occur.

Table 13 shows the results of the male and female connectors connected together.

Male + Female connectors	Ratio PDIV / Maximum nominal voltage		Ratio PDIV / Maximum transient voltage	
	1000 mbar	100 mbar	1000 mbar	100 mbar
Ph A to ph B	no PD	1.38	no PD	0.92
Ph B to ph C	no PD	1.53	no PD	1.02
Ph A to ph C	no PD	1.53	no PD	1.02
Ph A to case	no PD	1.26	no PD	0.91
Ph B to case	no PD	1.27	no PD	0.92
Ph C to case	no PD	1.26	no PD	0.91

Table 13: Measurement results on the male and female connectors connected together

Partial discharges occur at voltages that can be reached during the life of the connector (mainly between phase-to-case tests), though only in abnormal transient conditions with a very low repetition rate over service life.

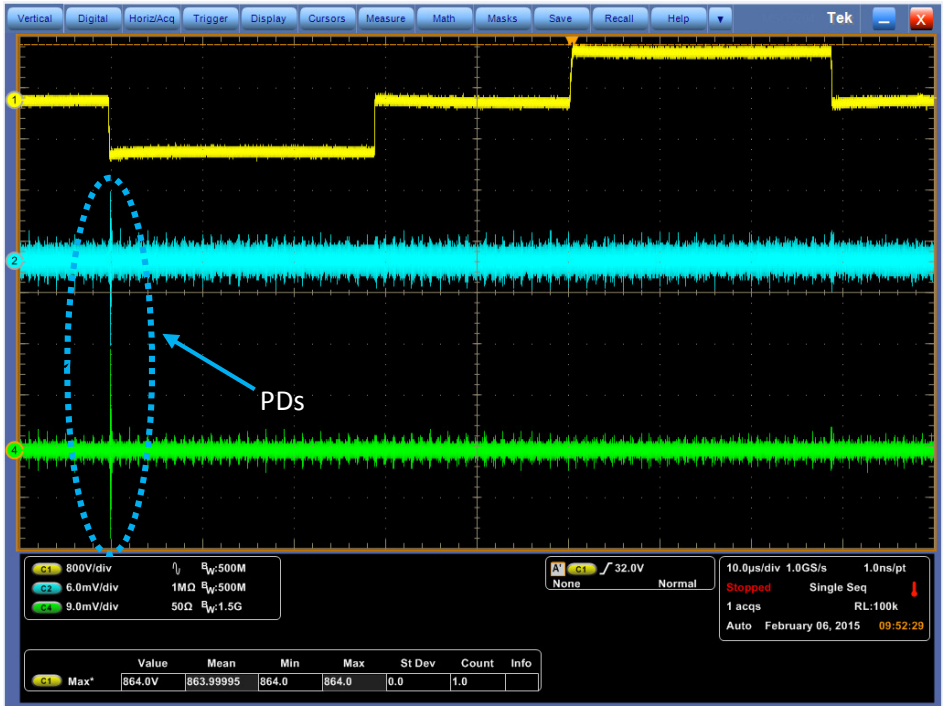

Figure 70: Voltage waveform during PD on the male and female part of the connectors connected together and subject to PWM voltage (phase-to-phase test). Channel 1: Power source (kV). Channel 2: Rogowski coil + 200MHz filter. Channel 4: Coaxial cable + 200MHz filter

There again, and not surprisingly, the pattern is still asymmetric (Partial discharge is observed during the negative polarity's change but not during the positive polarity's one) which let assume that a corona effect is occurring.

As a conclusion on the output connectors, we highlighted a defect either in the connector or in the cable connected to it. Since only male tests and male/female tests showed partial discharges, we can conclude that partial discharges occur in the male connector. Partial discharges are able to occur at transient voltages as defined in HVDC standard (8% below 900Vpeak). See Table 7. It means that partial discharges may occur in a system in operation, however, since transient does not occur very often, we can assume that the impact of these discharges will be negligible.

4.2.2.4 Input filter

In a system in operation, the input filter is directly connected to the AC source through the high voltage input connector. It is a passive filter as shown in Figure 71.

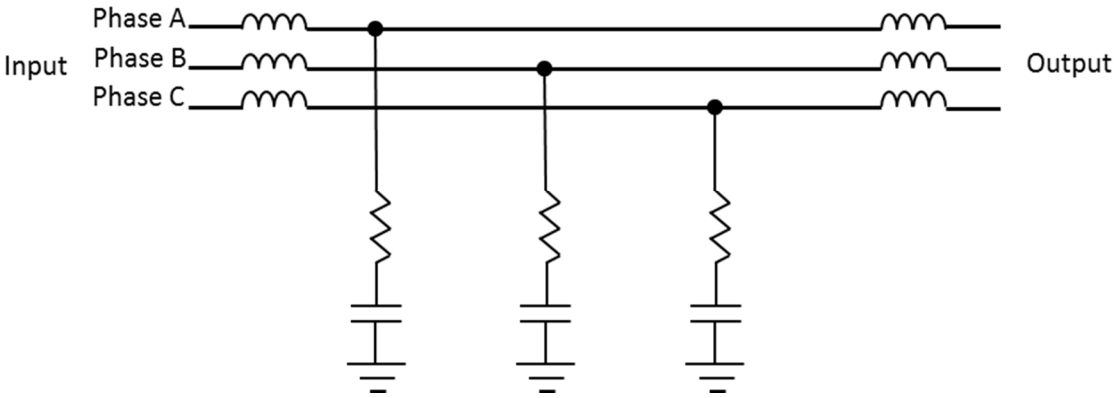

Figure 71: Electrical representation of the input filter

Figure 72 shows the setups used to test the input filter.

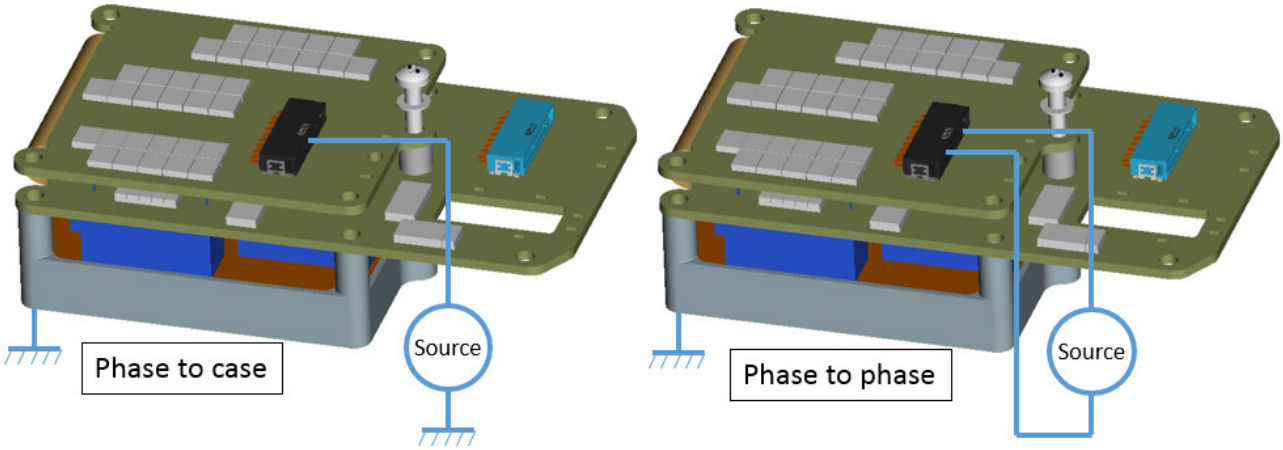

Figure 72: Input filter test setups

Following Table 7, the input filter is tested with 560Vpeak phase-to-case and 970Vpeak phase-to-phase.

Table 14 summarized the results of the input filter.

Input filter	Ratio PDIV / Maximum nominal voltage		Ratio PDIV / Maximum transient voltage	
	1000 mbar	100mbar	1000 mbar	100mbar
Ph A to ph B	no PD	0,86	no PD	0,62
Ph B to ph C	no PD	0,89	no PD	0,64
Ph A to ph C	no PD	0,92	no PD	0,66
Ph A to case	no PD	1,6	no PD	1,15
Ph B to case	no PD	1,63	no PD	1,17
Ph C to case	no PD	no DP	no PD	no DP

Table 14: Measurement results on the input filter

Partial discharges occur at voltages which are able to be reached in the life of the filter (only between two phases) even in nominal voltage conditions.

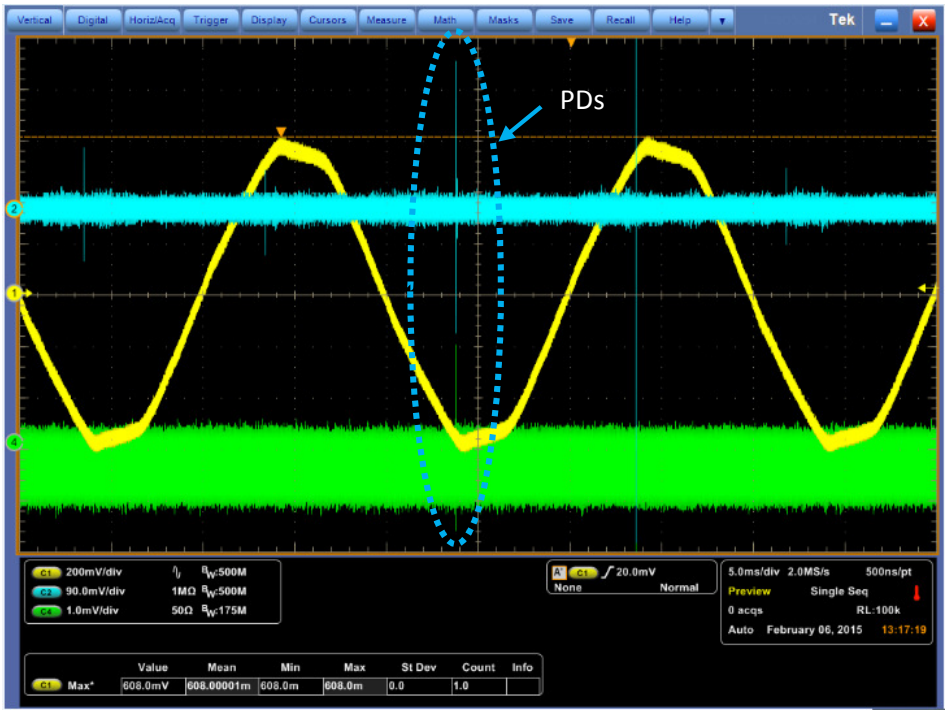

Figure 73: Voltage waveform during PD on the input filter subject to AC voltage (Phase-to-phase test). Channel 1: Power source (kV). Channel 2: Rogowski coil without filter. Channel 4: Coaxial cable without filter

Measurements were made to characterize these discharges. The results show a symmetry between positive and negative half-periods. It means that the discharges are not of corona type. Moreover the discharges are external, since the pressure has an influence on the inception voltage.

Considering the mechanical aspect of the component, our first assumption is that partial discharges occur between the two PCBs. Therefore, we decided to unfold the filter module, as shown in Figure 74, and to test it again. After testing, partial discharges still occur at the same level, which means that partial discharges actually occur on the other side of the PCB between the case and the PCB (probably between the potted coils).

In order to confirm this, we decided to examine the video signal coming from a video camera, watching inside the input filter (Between the PCB and the case, in the coils area), while it was inserted into a dark vacuum chamber.

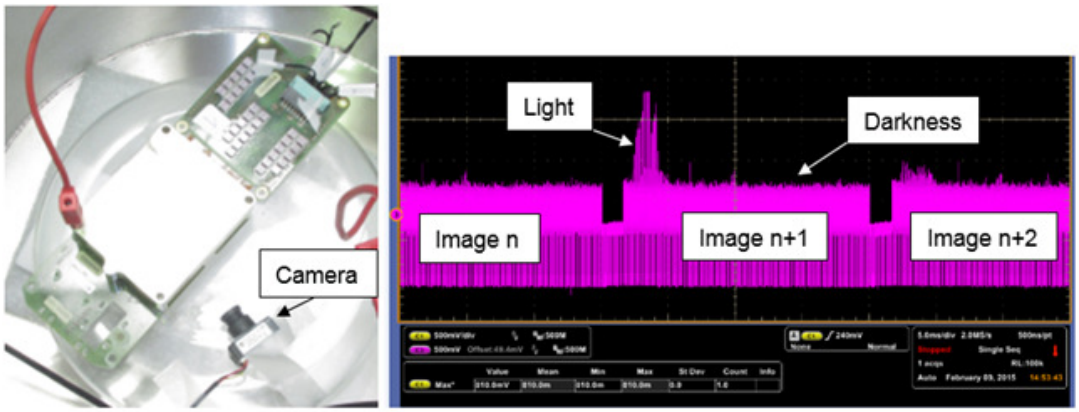

Figure 74: Optical PD detection inside the input filter (picture and results)

An emission of blinking light was measured at the inception level. This shows that ionization occurs in the filter module when partial discharges are detected.

The main conclusion on the input filter is that external discharges can occur between two phases over the potted region, at low pressure (100mbar) and at nominal voltage. During the final tests on a complete converter chain, it will be interesting to check whether these discharges are still present once the filter is mounted into the system (c.f. 7).

4.2.2.5 Auto-Transformer Rectifier Unit (ATRU)

The ATRU transformer is tested in two steps: First, all pins were connected together and tested with AC voltage against the case. Second, each individual phase is tested with pulse-like voltage against another phase.
This component is not actually supplied by pulse-like voltage during operation. However, it was not possible to test it phase-to-phase with AC voltage. The coils having a low impedance at 50Hz, the current is too large. Therefore, and although it is not representative of the system in operation, the three input phases are tested with pulse-like voltage. Under those conditions, the ATRU transformer is tested with 990Vpeak phase-to-case and phase-to-phase. After analyzing the results, we can conclude that partial discharge cannot occur in the ATRU transformer, even under transient voltage conditions.

The ATRU components possess two potted inductances which are subject to DC voltage in operation. However, for test convenience, we supply them with AC voltage (560Vpeak phase-to-case) in order to test the potting material. Moreover, for reasons similar to the ATRU transformer tests, it was not possible to test the coils themselves with AC voltage. Therefore, and although it is not representative of the system in operation, we decided to test this component with pulse-like voltage (990Vpeak phase-to-phase) in order to test inter-turn insulation. After analyzing the results, it has been concluded that partial discharges cannot occur in the ATRU inductances.

4.2.2.6 Insulated-Gate Bipolar Transistors power module (IGBT)

IGBT testing requires particular care because, in operation, they are supplied by DC voltage and their switching transients generate the pulsed waveform. A method to test IGBTs has been developed by [Lebey], superimposing DC and AC voltage. By this way, the voltage V_{test} received by the power module between the collector and the emitter verifies at all times the condition $V_{test} > 0$ so that the diode never conducts. The power component is maintained in a turned off state during the test by the control gate which is connected to the ground. This method requires the IGBTs to be removed from the PCB and tested separately.

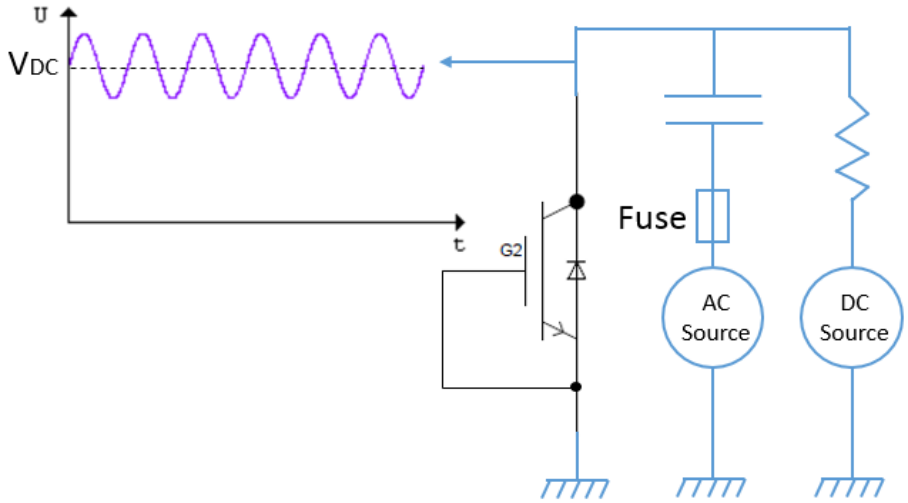

Figure 75: IGBT test setup

The voltages used for this test are: 500VDC for the DC signal, and 1000V peak-to-peak for the sinusoidal signal. This represents a minimum of 0V and a maximum of 1000V.
The first measurements did not show any partial discharges at either low or ambient pressure. After some time, the sensor detected some weak magnitude pulses synchronized with the AC source. These pulses actually occurred in the falling phase of the sinus, which is unconventional.
The pulses have very low magnitude (<1mV) and are not influenced by pressure.
To confirm the influence of voltage, DC voltage is increased and RMS voltage is reduced so that the maximum voltage still stayed at 1000Vpeak. Then DC voltage is decreased down to 500V and RMS voltage is increased up to 1000V peak-to-peak. As a conclusion, increasing DC voltage reduces the magnitude and repetition rate of the pulses. The dependency on the DC voltage type tends to prove that these pulses are partial discharges.
After some time, the pulses disappeared and never reappeared again. In this current case, we cannot establish the nature of the measured pulses. It is, however, important to highlight that a minimum voltage of 940V peak is required to ignite them. Consequently these pulses are not hazardous once used in an operating system.

4.2.2.7 High-voltage cable

The tested high-voltage cable is used in the converter to link the ATRU and the power board (DC voltage). It may also be found at the output of the system (pulse like voltage side). Therefore, the high-voltage cable is tested under pulse-like votage (990Vpeak phase-to-phase).

Partial discharges were measured during the tests. First remark concerns the influence of pressure: decreasing pressure ignites either partial discharges or electrical breakdown. This means that the discharges or breakdowns occur externally.

In operation, an insulating band between the cables and the grounded case is used to insulate the high voltage part from the ground of the PCB on which they lie. After measurements,this band has the expected effect, which is to increase PD inception voltage. Figure 76 is a picture of the test using the insulating band.

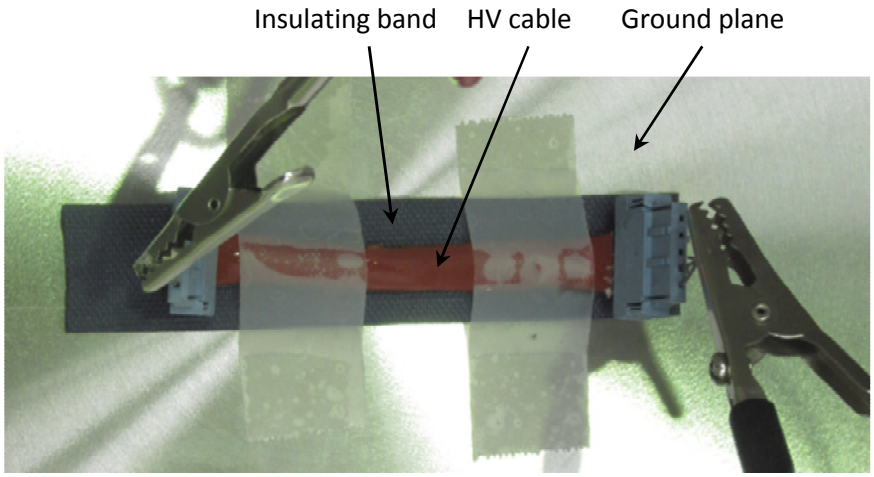

Figure 76: Picture of the HV cable test on the isolating band

The discharges pattern look like corona discharges, which implies that discharges occur at sharp edges or needles. The important thing to remember from these measurements is the very high voltage (1100Vpk) at which PDs or breakdown occur, which is well above the system's maximum transient voltage. PDs are highly unlikely to occur in a system operating with this component.

4.2.2.8 Power board

The output part of the power board is tested. In real operation, this part of the converter is subject to PWM voltage. Therefore, based on Table 7, the power board is tested with 990Vpeak phase-to-case and phase-to-phase as shown in Figure 77.

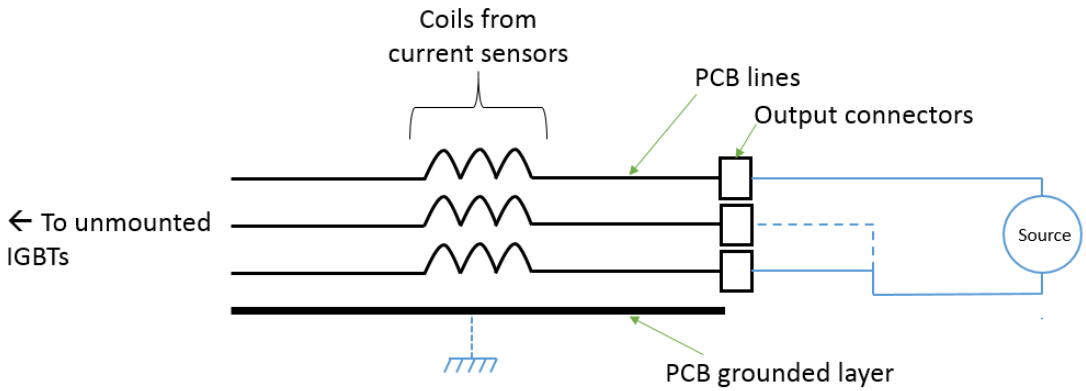

Figure 77: Test setup of the output PCB's lines of the power board

No partial discharges are measured on this component. Only electrical breakdown occurred between 1.2kV and 1.8kV on almost every test at low pressure. It means that some electrical discharges are ignited, which induce a strong current. Measurements are performed in two steps, first by connecting the ground to the PCB, and then without connecting it. The results show that the ratios (breakdown voltage / Maximum nominal voltage and breakdown voltage / Maximum transient voltage) are lower when the ground is connected. The only logical conclusion is that the electrical breakdown occurs between the phases and the ground. It is also important to notice that the ratios are very high in each test, which means that there is no chance that an electrical breakdown occur in real operation, even at low pressure and even if transients occur.

4.2.3 CONCLUSION ON COMPONENT INVESTIGATION

This investigation outlines the behavior of some components regarding partial discharges. Two weak points must be pointed out regarding the given components:
The first point concerns the output connectors, which show partial discharges at a voltage 9% lower than the maximum transient voltage described in the manufacturer standard.
This one shows that transients in normal conditions may occur less than 100 times in the device's lifetime. This clearly cannot be harmful for the system, as discharge degradation is a long-term matter.
The second weak point concerns the input filter, which shows that external partial discharges may occur between the potted coils and the PCBs. These discharges may be critical, as they appear at a voltage that is 14% lower than the standard rated voltage. This means that, at low pressure, partial discharges may occur very frequently (400Hz → Several occurrences every 2.5ms). This will be discussed by measuring the complete system under low pressure.
Other components in this investigation showed sometimes partial discharges or electrical breakdown, but at a voltage that cannot be reached by the converter. It is safe to say that the components from the converter in a pressurized area are partial discharge free, but if the system is faced with low pressure, care must be taken for specific components, such as the input filter and output connectors.

4.3 SYSTEM INVESTIGATION: CONVERTER UNDER OPERATION

This chapter describes partial discharge measurements performed on an entire aeronautics power chain (converter + cables + motor).

4.3.1 EXPERIMENTAL PROTOCOL

The investigation is divided in five steps:

- In a first step, the influence of filtering on the converter noise suppression is studied
- Second, the power chain (converter + motor + cables) is investigated “on-line” at atmospheric pressure.
- Third, the power chain, still under operation, is tested at low pressure (~115mbar).
- Then, some more specific tests are then detailed.
- Finally, the time effects of the duration of the voltage application and of the temperature are investigated.

In a general way, the converter is started at rated voltage (230Vrms / 325Vpeak). The sensors outputs are observed on the oscilloscope. Afterwards, the voltage is increased up to (312Vrms / 441Vpeak) which is the maximum voltage of the AC power source. This voltage is well above the rated voltage. During the voltage rise, if any pulse is detected, the voltage is not increased anymore and the data are recorded and analyzed. If nothing is measured up to the maximum voltage, the voltage is reduced to rated voltage and the protocol is repeated.

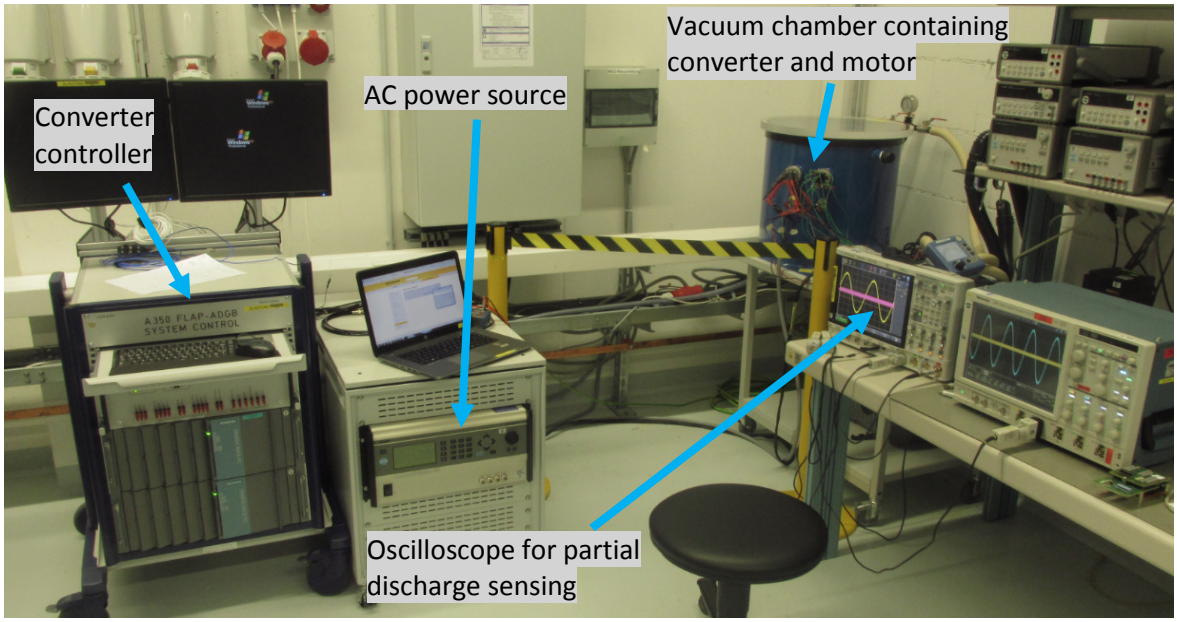

Figure 78: Picture of the test setup

Figure 78 shows the test setup mounted in the laboratory.

4.3.2 INFLUENCE OF FILTERING

a) PWM side

In order to study the influence of the filter cutoff frequency on partial discharges sensing, some tests have been done using four filters (50MHz, 100MHz, 200 MHz and 400 MHz) and without any filter. The first tests are achieved at the output of the converter (PWM voltage) and the seconds at the input of the converter (AC voltage). The setup Figure 79 is used. These measurements are achieved at atmospheric pressure.

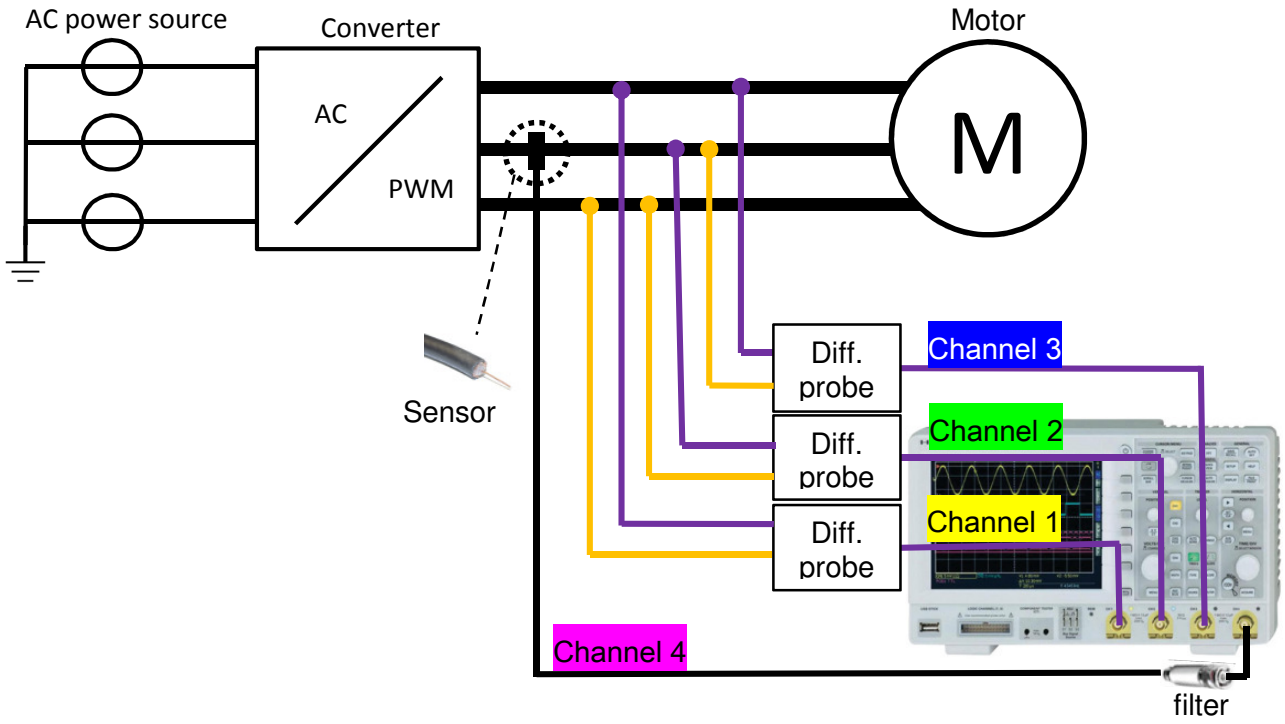

Figure 79: Setup for assessing the influence of filtering on PD detection at the output of the converter

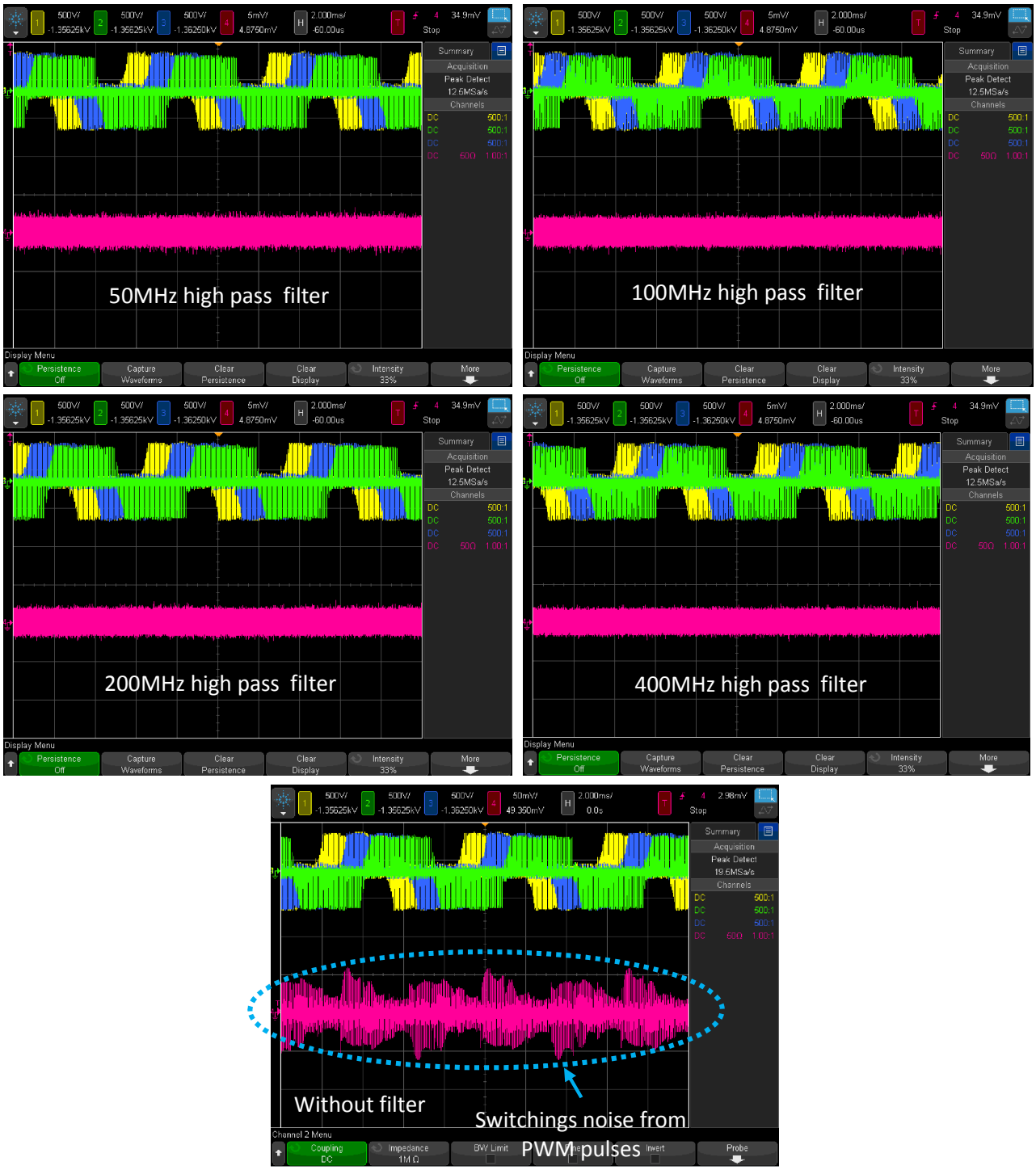

Figure 80: On-line measurement using various high pass filter at the output of the converter. Channel 1: Phase to phase voltage (A and C). Channel 2: Phase to phase voltage (B and C). Channel 3: Phase to phase voltage (A and B). Channel 4: Partial discharges detection on phase B using different filters

Considering the results in Figure 80, two remarks have to be made: first of all, the effect of the different filters (50MHz, 100MHz, 200MHz, 400MHz) on the switching noises from the PWM pulses is substantially the same, namely, the maximum magnitude of the noise level is below 3mV regardless of the used filter. In other words, any filter (among these four) would be efficient enough to make the distinction between partial discharges and switching noise from this converter. It is important to precise “this converter” because another converter with different pulses rise time (dv/dt) would require the use of filters with higher cut-off frequencies.

The common mode frequency spectra from a converter using equivalent IGBTs as we are using, and from the same converter using SiC MOSFET are given in Figure 81. SiC MOSFET having a shorter rise time than the IGBT, Figure 81 shows that, in the case of IGBT (our case), the signal generated by the converter is located in the 0-10 MHz frequency range. Beyond 10MHz the signal may be considered as “noise”. It is therefore not surprising that the 50MHz filter is able to remove the switching noise (Figure 80). It can also be remarked that the SiC MOSFET shows a higher level around 50MHz. Consequently a filter with a cut-off frequency higher than 50MHz will be necessary when using SiC MOSFET with a lower rise time.

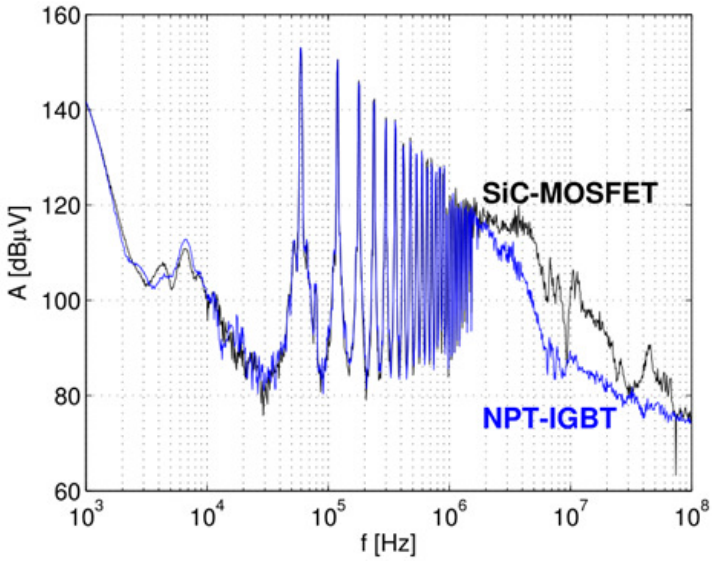

Figure 81: Common mode frequency spectrum of one converters with different IGBTs. [Liebig]

On the other hand, when looking at the maximum magnitude of the switching noise without filter (~60mV), it appears that it is higher than any of the partial discharges pulses measured during the constituents and components investigation phases (except the ATRU investigation).It means that if any discharge is measured with a magnitude lower than 60mV, this one could be drowned in the switching noise from the converter. Consequently, a filter is required to detect partial discharge on the output side of the converter.

b) AC side

The impact of the filtering at the input of the converter is studied. The test setup is given in Figure 82 and the results are presented in Figure 83.

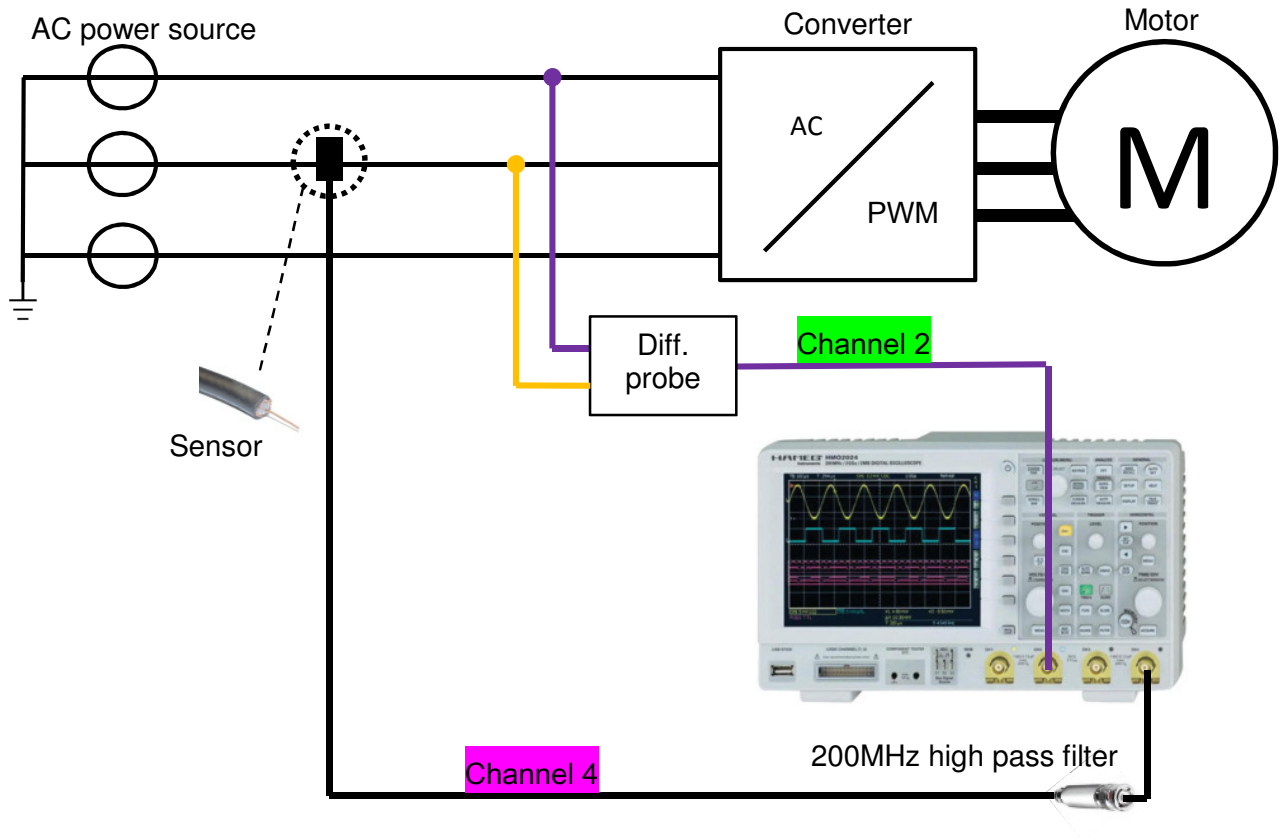

Figure 82: Setup for assessing the influence of filtering on PD detection at the input of the converter

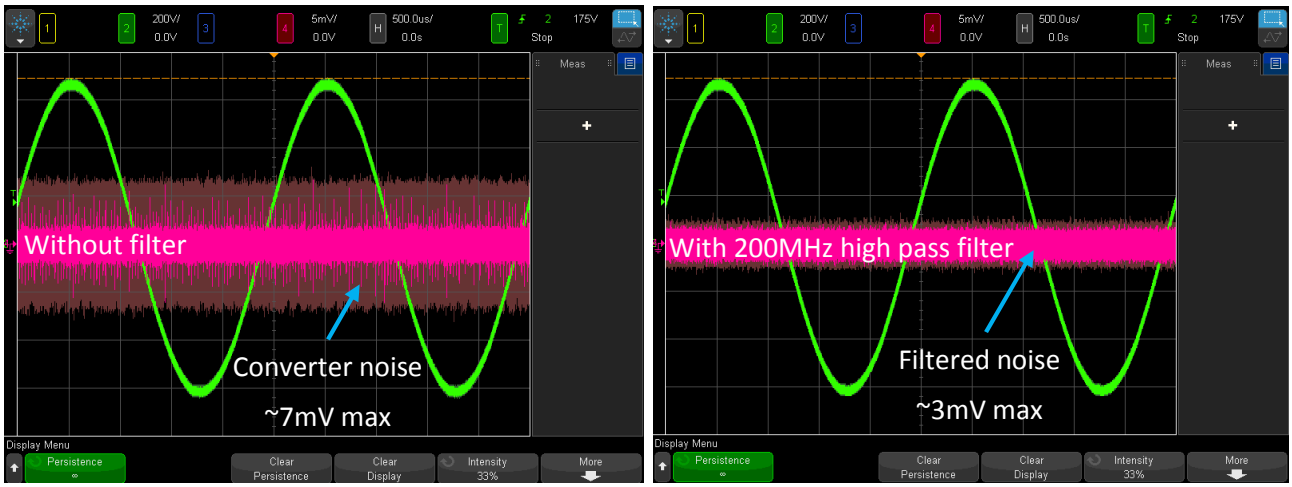

Figure 83: On-line measurement using the 200MHz high pass filter at the input of the converter. Channel 2: Phase to phase voltage (A and B). Channel 4: Partial discharges detection on phase B using a 200MHz filter

The results in Figure 83 outlines the impact of the 200MHz high pass filter on the suppression of the converter noise. We first note that, without filtering, the noise generated by the converter is low (~7mV) compared to the noise at the output of the converter (~60mV). It means that any discharges, occurring on the AC side, displaying a magnitude higher than 7mV could be detected by the sensor without filters. Once the filter is used, it reduces the noise level down to 3mV.

As a conclusion on the filtering influence at the input of the converter (AC voltage), the results show that it is better to use a filter in order to ensure that any partial discharge showing a magnitude higher than 3mV can be detected.
Concerning the filtering influence at the output of the converter, the use of a filter is mandatory to remove the noise from the switching. The question of the cut-off frequency of the filter depends on the IGBTs' speed of the converter. Faster IGBTs will require filters with higher cut-off frequency and vice versa. Trying several filter at the beginning of the investigation is a good methodology to follow.

4.3.3 TESTS ON THE ENTIRE POWER CHAIN AT 1000 MBAR

This section describes the tests performed on the complete power chain (converter + motor + cables) at ambient pressure.

Foremost the setup described in Figure 84 is used. Two differential probes are used to measure the voltage between phase A and B, and between phase B and C. Two sensors, placed on phase B and C with respectively a 200MHz and 400MHz high pass filter, appear as the best compromises for PD detection as demonstrated in the previous chapters.

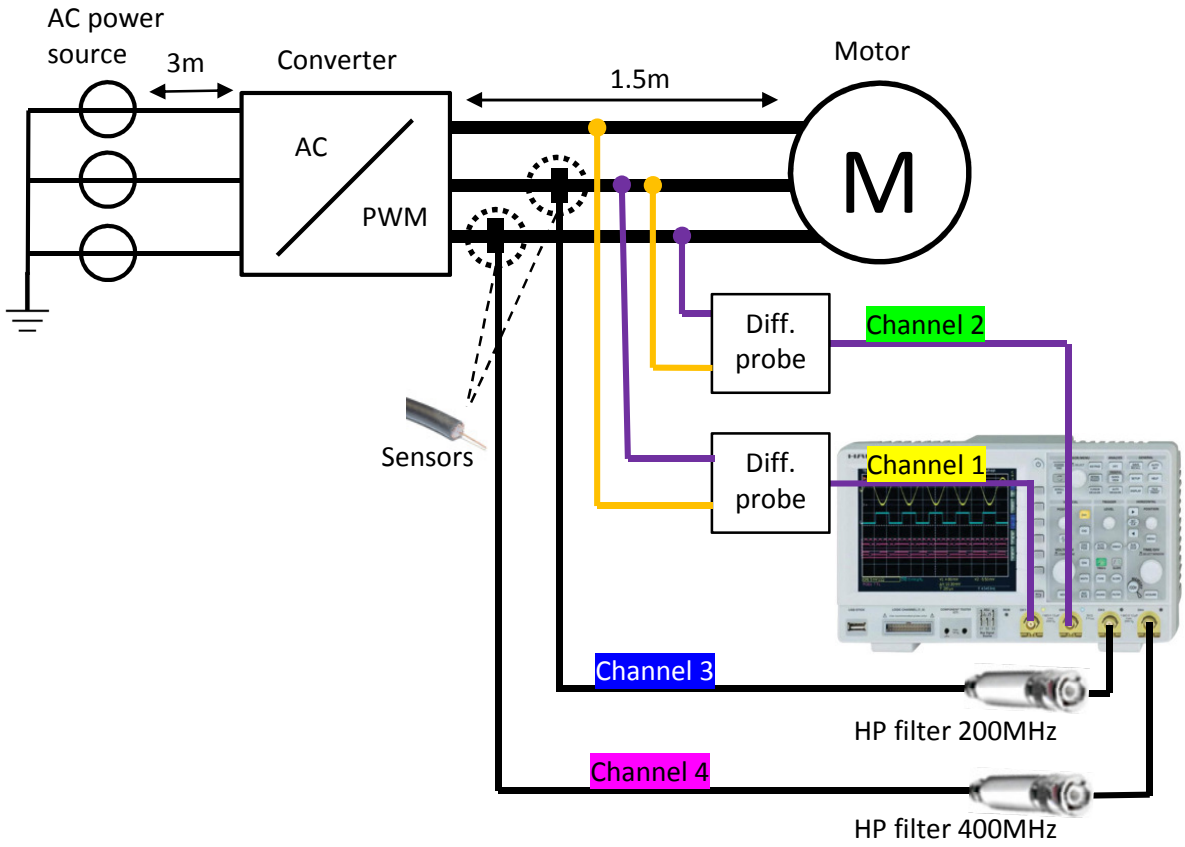

Figure 84: Initial test setup for PD detection on the power chain at 1000 mbar

The AC power source is a three-phase power source. Each phase can deliver a 400Hz and 312Vrms maximum sinusoidal voltage. The converter is a 3-phase 230Vrms AC/PWM converter with a maximum power of 20kVA. It has been deeply detailed in the previous section (components investigation). Finally, the motor is a 3-phase, brushless DC motor.

The results obtained during the measurements are shown in Figure 85. The experimental protocol previously described in chapter 4.3.1 has been applied. The oscilloscope has been set with a wide time base (50s/div) in order to easily observe and record any partial discharge event which would be dependent on the PWM voltage. Since the magnitude of the possible discharges is in the mV range a 5mV/div magnitude is displayed on the oscilloscope.

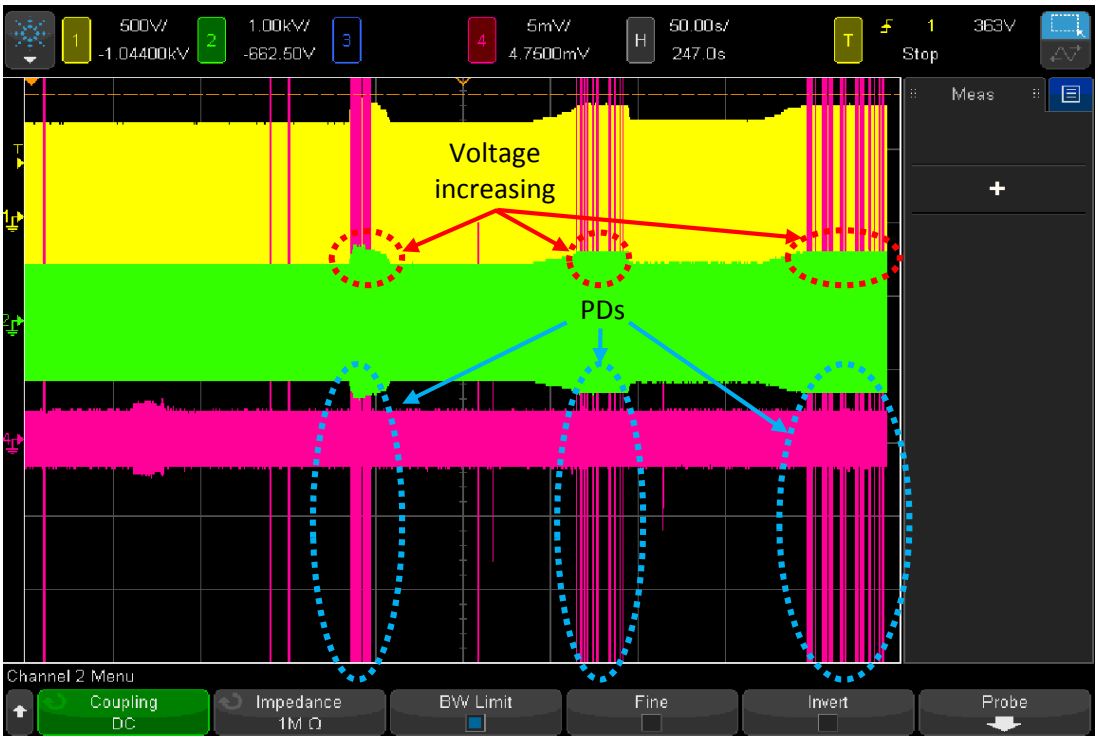

Figure 85: Measurements of "partial discharges ?" with a long time resolution (50s/div). Channel 1: Phase to phase voltage (A and B). Channel 2: Phase to phase voltage (B and C). Channel 4: Partial discharges detection on phase C using a 400MHz filter

At the beginning of the measurements, one pulse is measured. This one has a huge magnitude (at least > 25mV). This kind of pulse has been measured two times more in the next 150 seconds. It appears first to be a very rare phenomenon with a random aspect. At about 330s, the voltage is increased until the limit of the AC power source. During the rise of the voltage, a large number of pulses appear. Due to the time scale chosen, their number is unquantifiable. After 20 seconds, the voltage is decreased down to the nominal voltage and the pulses stopped. This operation is repeated two times.

Except the five pulses which occurred at rated voltage in the overall frame (500s), the measured pulses appear to be dependent on the voltage magnitude. We may thus conclude that it should be possible to define an inception voltage. During the investigation, these pulses appear to have a complex behaviour which is detailed in the chapter 4.3.6.

At that stage of the investigation, it is important to remember that some pulses have been measured on the power chain and that they are dependent on the voltage. To our knowledge, this is the very first time that such events are measured "on-line" in a real system.

The same measurements are performed using another time base (200ns/div) and voltage base (200mV/div). The interests of this measurement are first to get the maximum magnitude of the pulses and to find their position regarding the PWM voltage (Channel 1 and 2). Figure 86 presents an example of results.

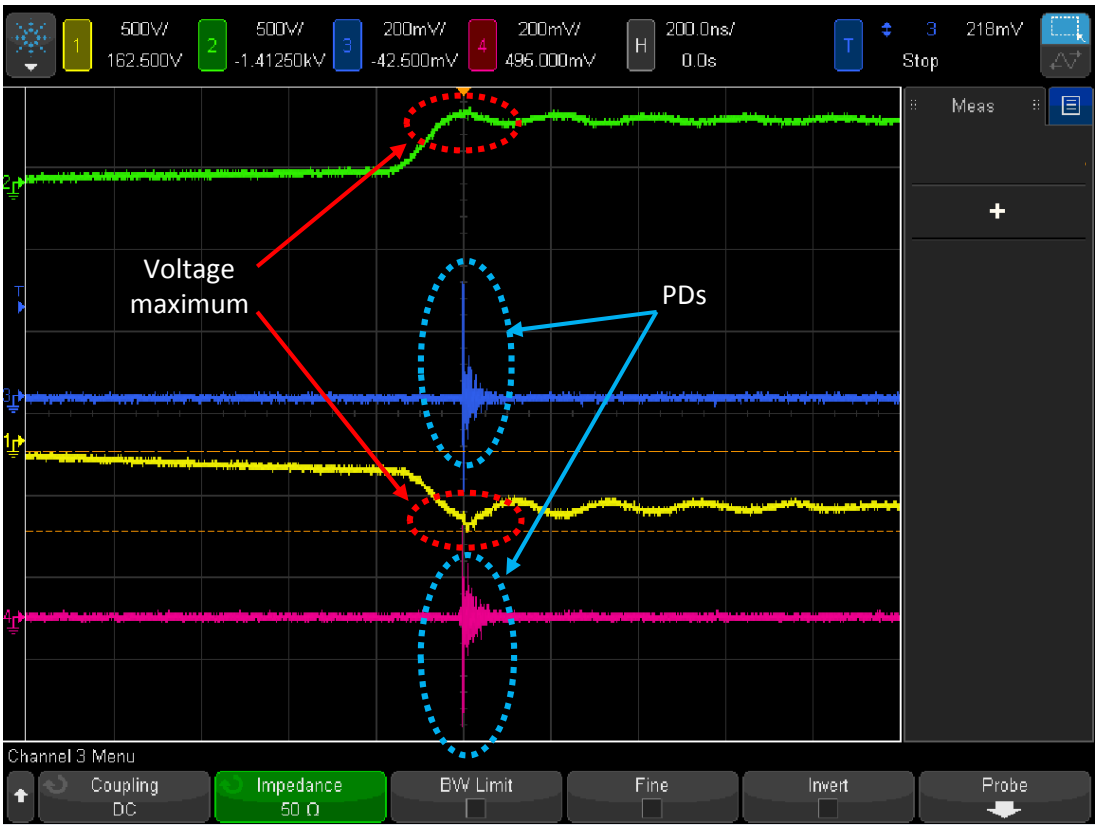

Figure 86: Measurements of partial discharges with a low time resolution (200ns/div). Channel 1: Phase to phase voltage (A and B). Channel 2: Phase to phase voltage (B and C). Channel 3: Partial discharges detection on phase B using a 200MHz filter. Channel 4: Partial discharges detection on phase C using a 400MHz filter

First of all, the magnitude of the pulse is very large. Most of the pulses measured are in the 200mV, 300mV range. The only measurement which showed such a magnitude has been observed on the ATRU (~600mV) during the components measurement phase (c.f. 4.2.2.5).
Then, looking at the position of the pulses regarding the PWM voltage, it can be observed that the pulses occur at its maximum value. This behaviour outlines, once more, the dependency of the pulses to the voltage magnitude.

During our measurements, another type of pulse has been measured. Figure 87 shows the results with a slightly different test setup, namely, channel 1 is the phase to phase (A-B) voltage, and channel 2, 3 and 4 are the sensors with respectively the 100MHz, 200MHz and 400MHz high pass filter.

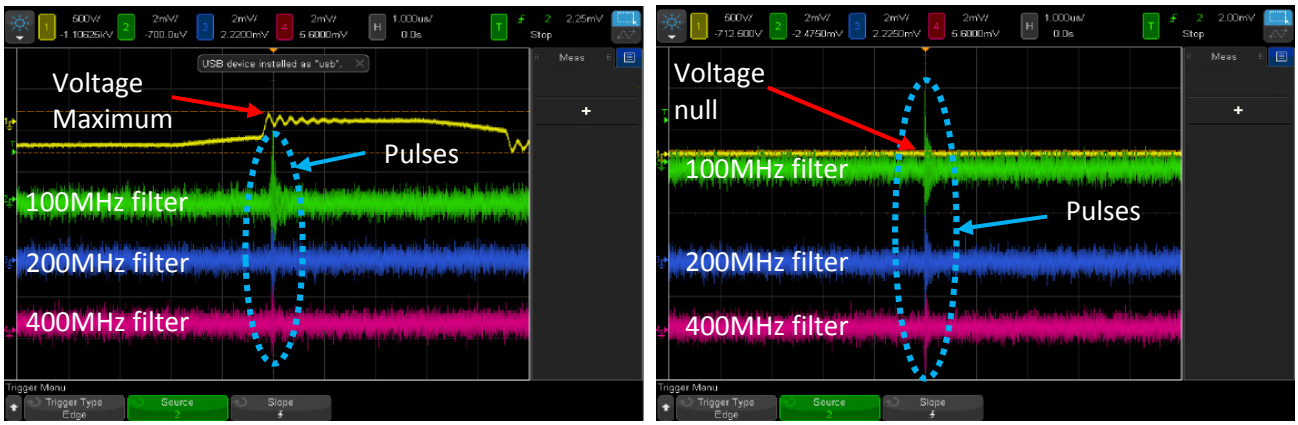

Figure 87: Measurement of pulses with different filters. Channel 1: Phase to phase voltage (A and B). Channel 2: Partial discharges detection on phase B using a 100MHz filter. Channel 3: Partial discharges detection on phase B using a 200MHz filter. Channel 4: Partial discharges detection on phase B using a 400MHz filter

The first remark concerns the magnitude of the pulses which are very low (< 3 mV). Second, the position of these pulses regarding the voltage is random. On the left picture of Figure 87 the pulses seems to occur around the maximum value of the voltage, whereas on the right picture, the pulses occur although the voltage is null. Moreover these pulses have not been observed anymore afterward.

The most obvious explanation is that they are not partial discharge. Probably they are due to any external disturbances. Indeed, it may happen that during partial discharges measurements, the sensors detect pulses which are not partial discharges. This may occur when an electrical machine is turned on in the same room. To avoid confounding these pulses with actual partial discharges, it is important to work in a “clean” area, electro-magnetically speaking, and to look after the repeatability of the pulses since partial discharges are supposed to be repeatable.

As a first conclusion, the pulses measured are dependent on voltage and they occur when the voltage is maximum. These behaviors let us assume that these pulses are partial discharges. Although it is not possible to define the inception voltage because of a complex behavior (c.f. 4.3.6), these pulses are probably partial discharges.

4.3.4 TESTS ON THE ENTIRE POWER CHAIN AT 115MBAR

The previous tests are repeated but this time the pressure is 115mbar. The test setup in Figure 84 is used with a vacuum chamber. At first, only the motor in placed inside the vacuum chamber, then the complete setup (motor + cables + converter), and finally only the converter. The objective is to measure the effect of the pressure on the different part of the power chain. Regarding the voltage increase and peak detection the same protocol is applied as before (c.f. 4.3.1).

a) Motor in the low pressure environment (115mbar)

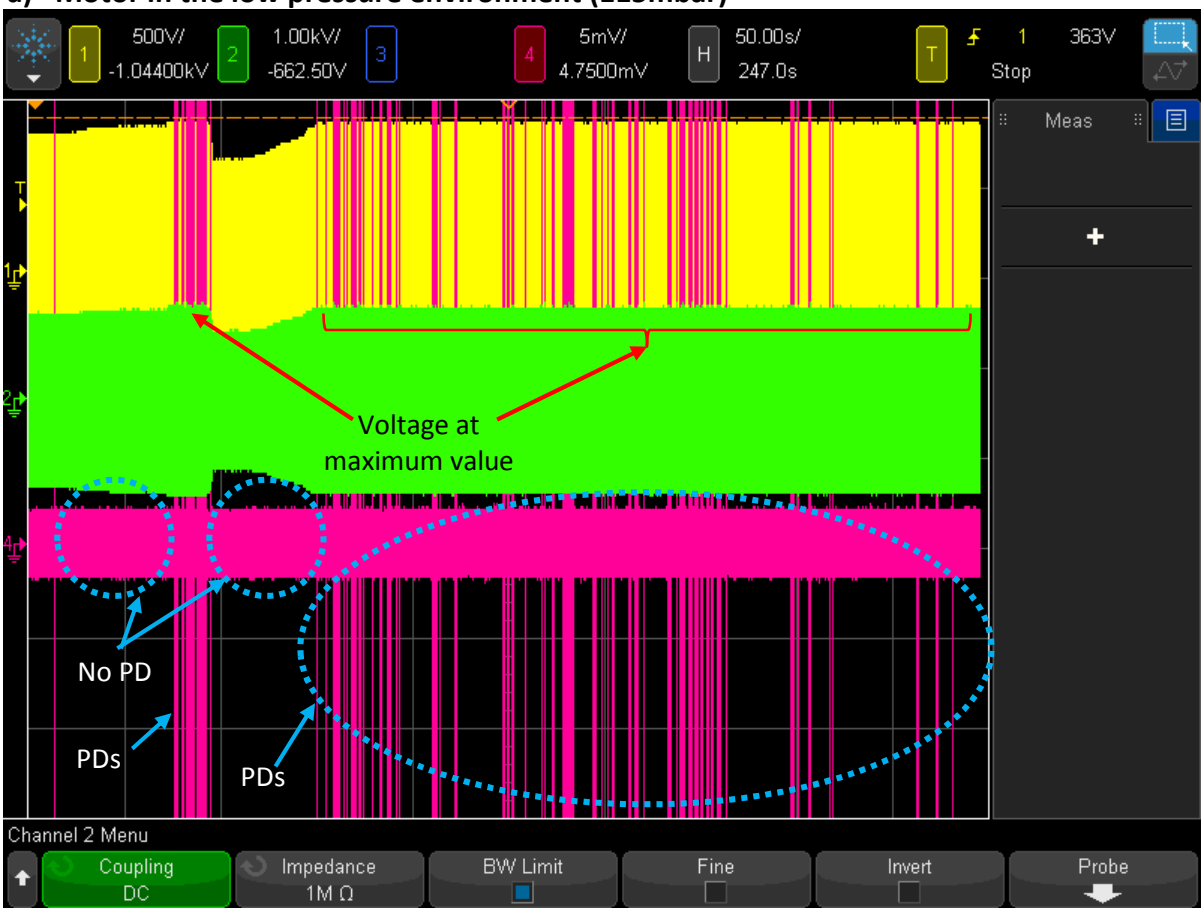

Figure 88: Measurement of partial discharges when motor is at low pressure (115mbar). Channel 1: Phase to phase voltage (A and B). Channel 2: Phase to phase voltage (B and C). Channel 4: Partial discharges detection on phase C using a 400MHz filter

The measurements when the motor is in a low pressure environment show the same large pulses as the ones observed during the tests at ambient pressure. They occur at the maximum value of the PWM voltage (Channel 1 and 2). Only one pulse occurs, in a total period of 100s, when the voltage is below the maximum. No more pulses with low magnitude have been observed. The same behavior as the one observed at atmospheric pressure occurs, namely, the detected pulses are dependent on the voltage magnitude and their magnitudes are still very large (< 200mV). The discharges do not seem to be influenced by the pressure.

b) Converter + Motor in the low pressure environment (115mbar)

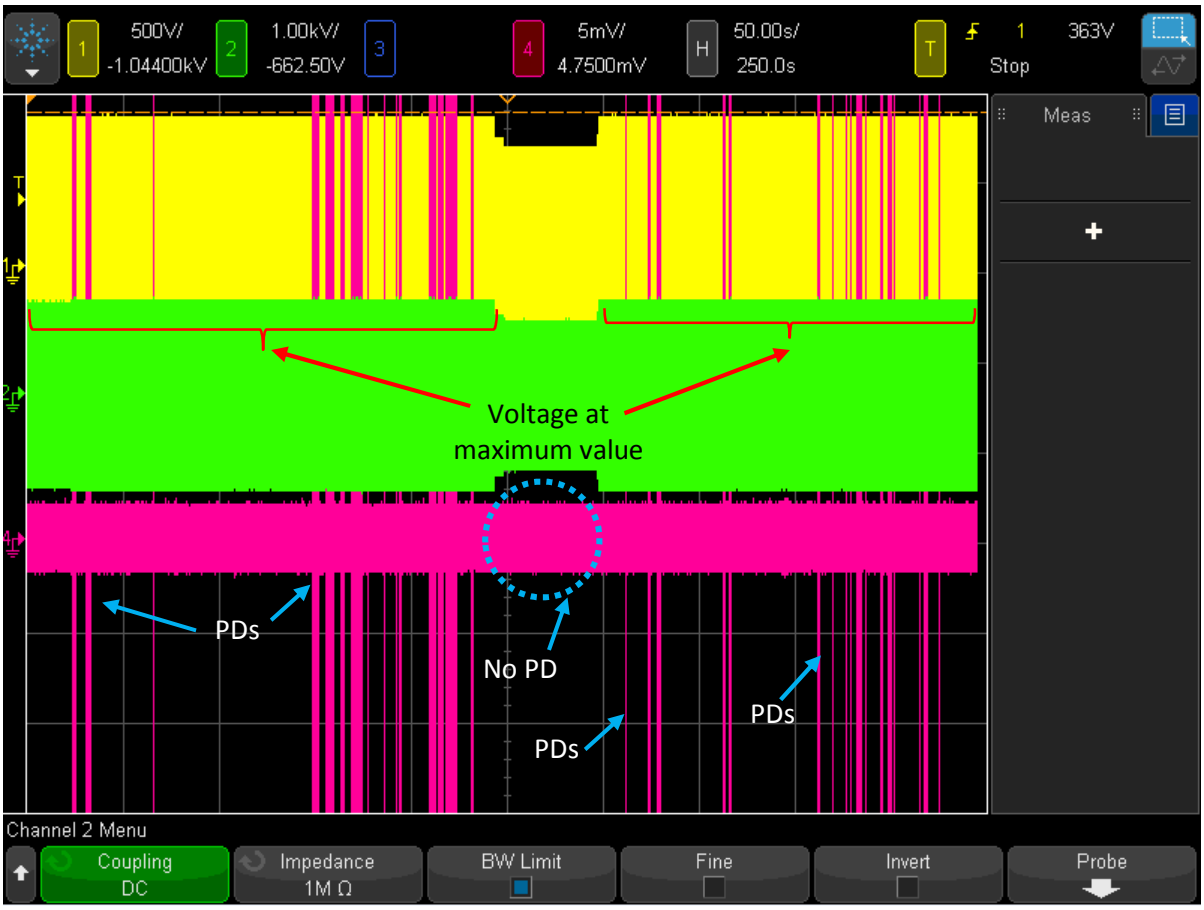

Figure 89: Measurement of partial discharges when converter and motor are at low pressure (115mbar). Channel 1: Phase to phase voltage (A and B). Channel 2: Phase to phase voltage (B and C). Channel 4: Partial discharges detection on phase C using a 400MHz filter

The converter and the motor are both placed into the vacuum chamber, the converter is switched on and the measurements are shown in Figure 89. Partial discharges like pulses only appear when the PWM voltage magnitude (channel 1 and 2) is maximum. When the voltage is decreased, no more discharges are observed. No differences are observed compared to the tests at atmospheric pressure. The behaviour of the discharges being the same, it may be noticed that the occurrence of the pulses is not constant. It happens sometimes that, even at the maximum voltage, no discharge occur during some ten of seconds. This phenomenon is related to the complex behaviour previously mentioned. It's getting worst with time and temperature. This point will be discussed in chapter 4.3.6.

c) Converter in the low pressure environment (115mbar)

As it could have been expected after the first tests, the measurements when the converter in a low pressure environment do not show results different to the ones obtained at atmospheric pressure. High magnitude pulses are measured at the maximum voltage and no discharge occur when the converter is running at its rated voltage.

The previous results outline that if partial discharges occur in the power chain they do not depend on the pressure. This could have been a good indicator to estimate the location of the discharge. In order to try to locate the discharges area, the setup Figure 90 has been used.

d) Pulses localization

Two coaxial sensors, separated by 2m of cabling, are used to identify pulse locations: one situated near the motor, the other near the converter (Figure 90).

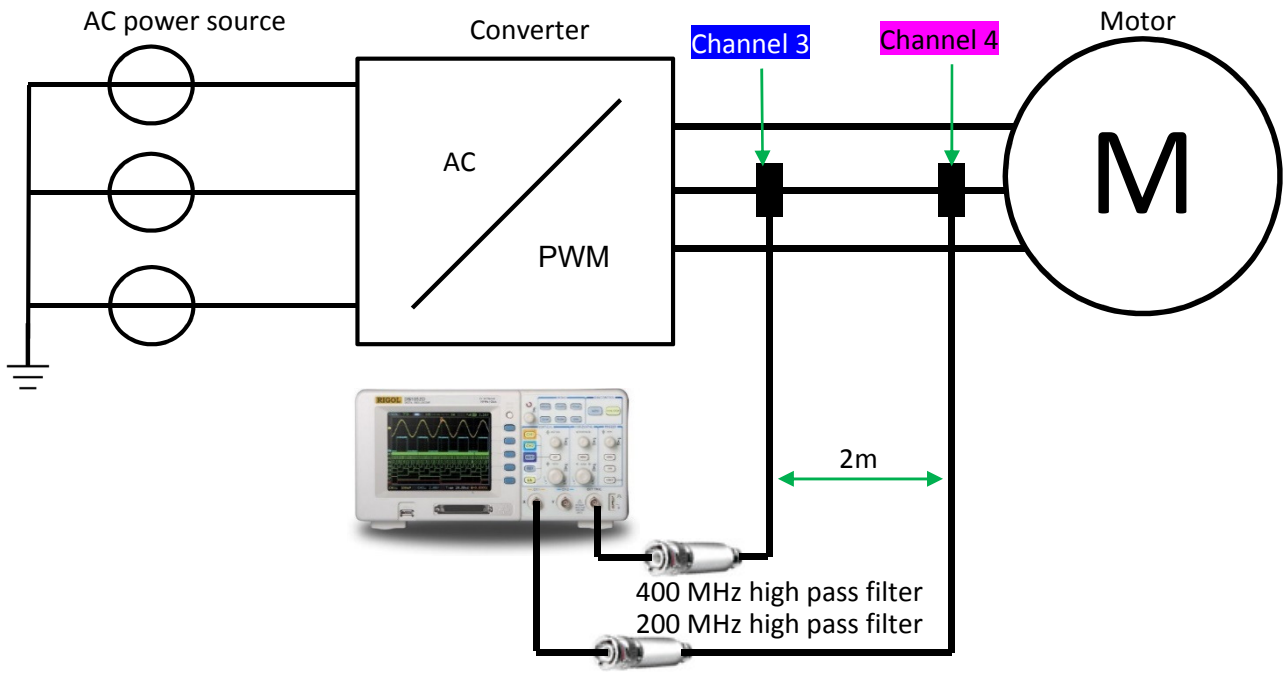

Figure 90: Test setup to locate the most likelihood source of the pulses

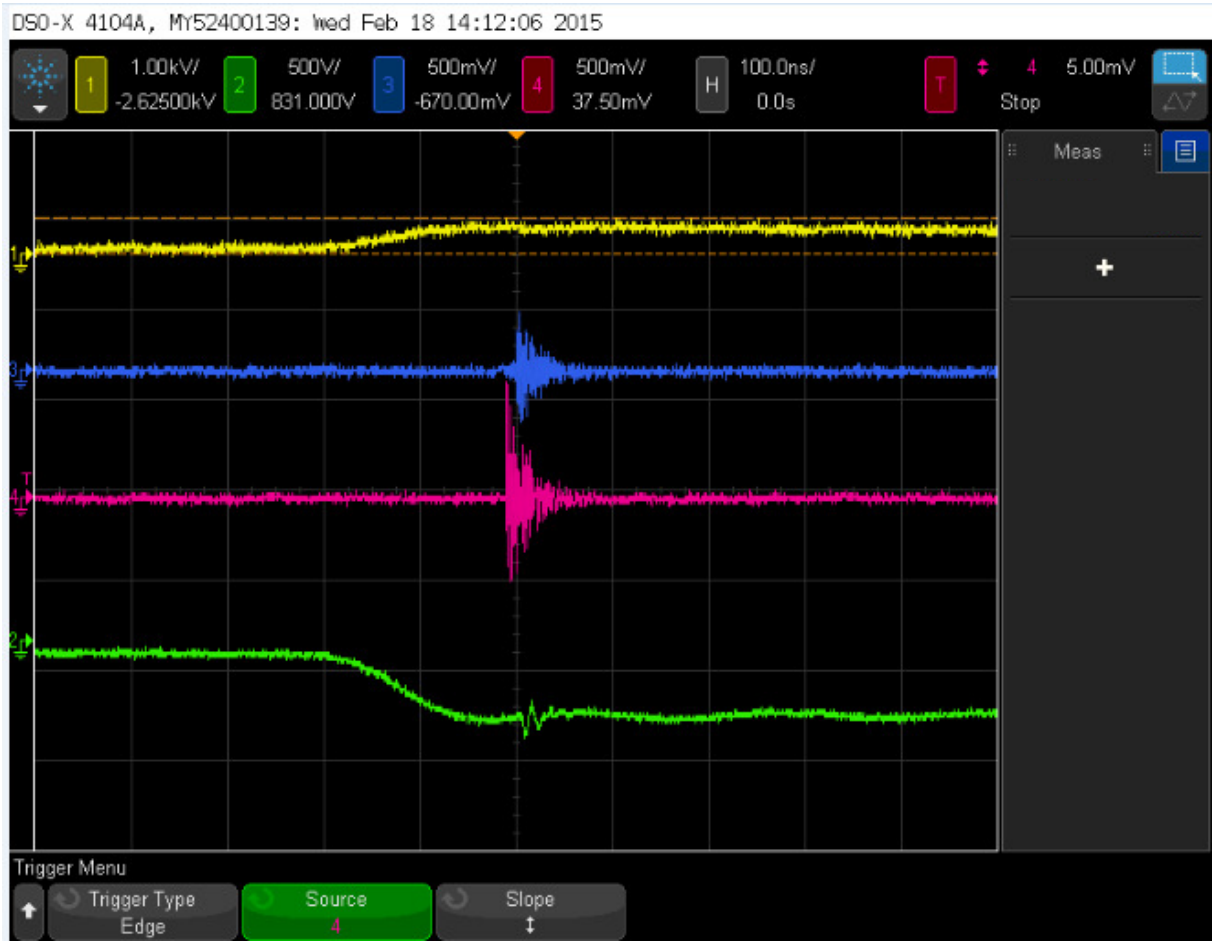

Figure 91: Pulse location measurement. Channel 1: Phase to phase voltage (A and B). Channel 2: Phase to phase voltage (B and C). Channel 3: Partial discharges detection on phase B using a 400MHz filter. Channel 4: Partial discharges detection on phase B using a 200MHz filter.

Figure 91 shows that the pulse observed on channel 4 is detected before the pulse observed on channel 3 if the assumption is made that these two pulses have the same origin. Since channel 4 being on the motor side, this means that the pulse source is in the motor.

If these measurements are correct, the delay between the two pulses should correspond to the time required by the signal to travel the distance between the two sensors at the speed of light divided by $\sqrt{\varepsilon}$. Since $n^2=\varepsilon$. With ε being the permittivity of the cable (~2.2).

$$t = \frac{d}{\frac{c}{\sqrt{\varepsilon}}}$$

With t being the time needed by the signal to travel the inter-sensor distance, d the inter-sensor distance, c the speed of light. It means that the speed of an electrical signal is:

$$\frac{c}{n} = 2.02 * 10^8 \text{ m/s}.$$

Consequently, the time required by the signal to travel a distance of 2m is:

$$t = \frac{2}{2.02 * 10^8} = 9.9\ ns$$

The graph shows a time difference around 10ns which is relatively close to 9.9ns. In order to assert that the time difference which is measured is not due to same problems related to the use of two different filters (200MHz and 400MHz), the same test has been repeated by reversing the filters.

The results were exactly the same, namely pulses are first detected on the motor side. We can therefore consider that our measurements are correct and conclude by saying that the partial discharges are located in the motor.

As a conclusion of this section, partial discharges have been detected in the power chain during on-line testing. These discharges are most likely located in the motor and show a complex behavior (This point will be detailed in chapter 4.3.6). We can therefore assume that the converter, in the conditions of test, is partial discharge-free. The next section describes more tests achieved on the power chain in order to make some comparisons to the results obtained in the previous sections devoted to constituents and components.

4.3.5 SPECIFIC TESTS

This section describes complementary tests. Some of them bring support to the conclusions made in the previous sections, some others bring additional information.

4.3.5.1 Investigations using a twisted pair of enamelled wire

Since no partial discharge has been detected in the converter, a twisted pair of enameled wire is used to validate the sensing method and to confirm that it is able to make the distinction between partial discharges and switching noise. A twisted pair of enameled wire is connected between two phases (as shown in the test setup in Figure 96) and the voltage is increased until partial discharges are observed. The twisted pair is placed first at the output of the converter, and is enduring a PWM voltage. Then, the twisted pair is connected at the input of the converter and support an AC voltage. The tests are performed in the vacuum chamber and the pressure is set to 115mbar.

a) Twisted pair on the PWM side

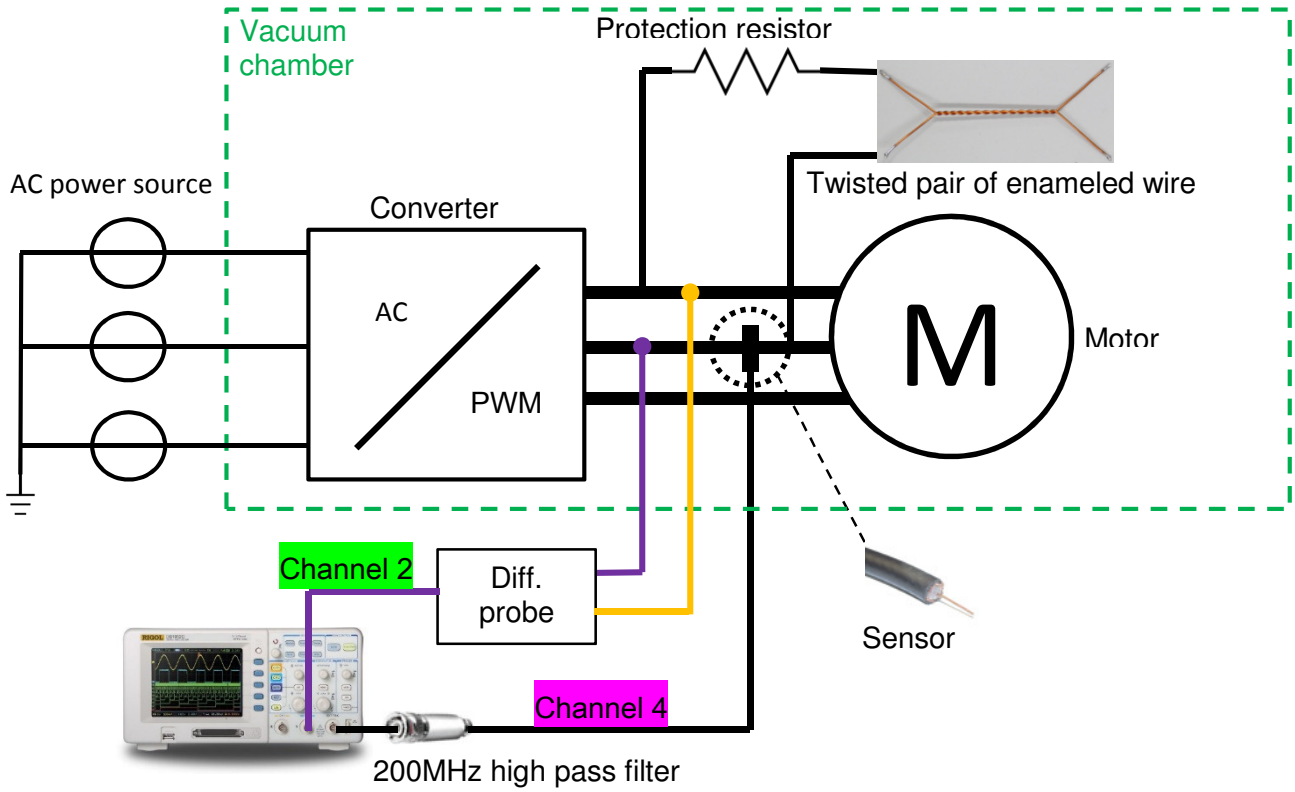

Figure 92: Setup with twisted pair of enameled wire connected at the output of the converter. Channel 2: Phase to phase voltage (A and B). Channel 4: Partial discharges detection on phase B using a 200MHz filter.

Figure 93 shows PDs occurring at low pressure (~115mbar). A persistency effect is applied on the oscilloscope display.

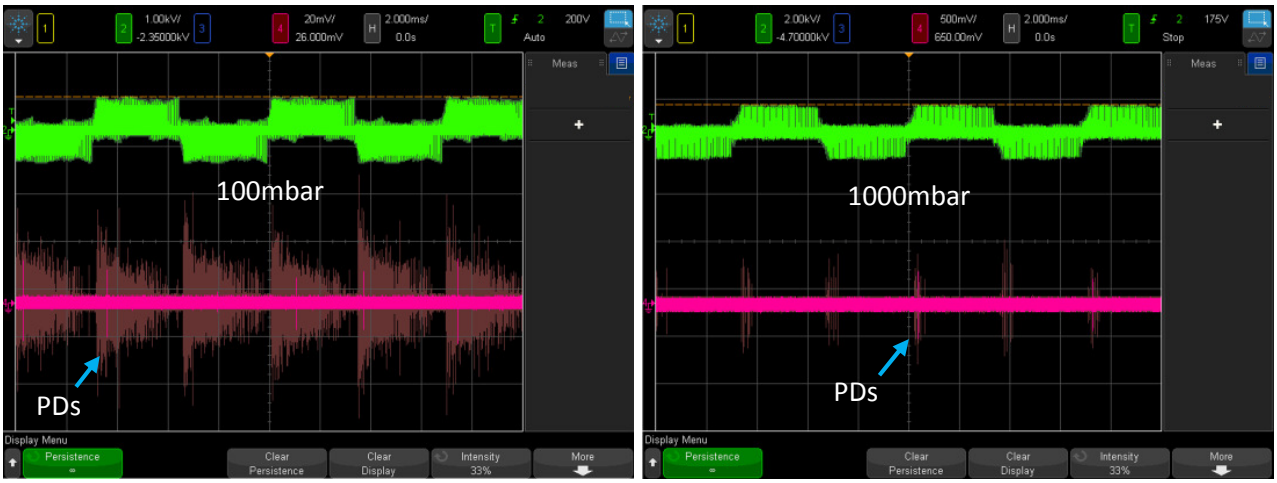

Figure 93: PD on a twisted pair of enameled wire at low pressure (~115mbar). Channel 2: Phase to phase voltage (A and B). Channel 4: Partial discharges detection on phase B using a 200MHz filter.

First of all, partial discharges occurring in the twisted pair of enameled wire are clearly observed. Thanks to the sensor and the filter, the switching noise are removed whereas the partial discharges are still detected.

Some questions arise from the previous observations. The first one concerns the position of the discharges with respect to the power source: Why do PDs mainly occur after the polarity reversal?

[Densley1] explained that the voltage across a defect has a pronounced effect if the polarity of the pulses are reversed. Let us consider the following voltage waveform (Figure 94), reaching inception voltage of a device under test. This graph uses the abc model (Figure 21).

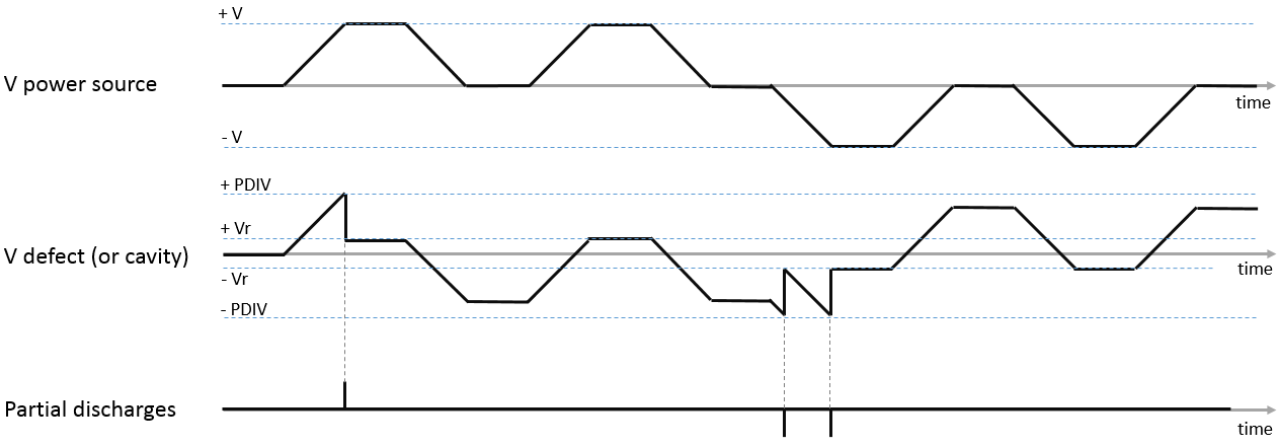

Figure 94: Discharge sequence for bipolar pulses at the inception voltage level

When the voltage at the terminal of the cavity reaches the inception level, a first discharge occurs and the voltage falls to Vr, which is the residual voltage. Afterwards, no more discharges can occur until there is a polarity change. At that moment, two discharges occur.

If the voltage is increased above the inception level, below two times its value, the position of the discharges stays the same, namely at the polarity's reversal. It means that, at PD inception voltage and up to two times the inception voltage, discharges can only occur when there is a voltage reversal, thus explaining our previous observations at 1000mbar since this sample at 1000mbar has an inception voltage around 850Vpeak.

By increasing the voltage by a factor of 2, the voltage across the defect behaves as described in Figure 95.

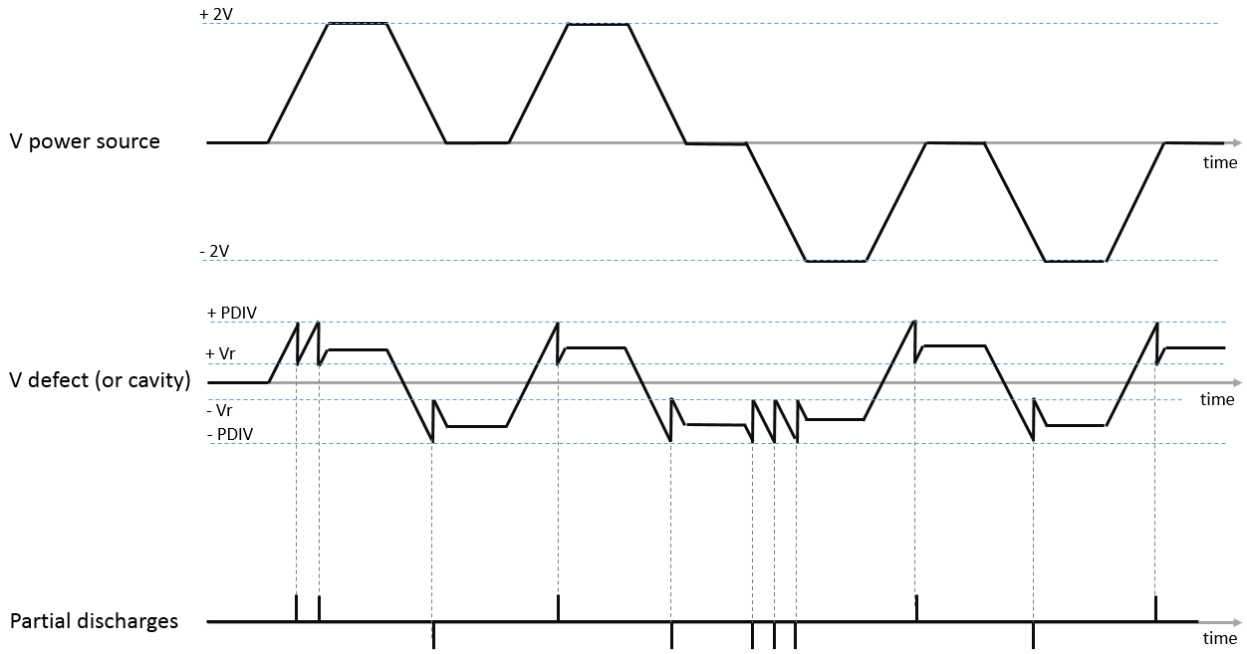

Figure 95: Discharge sequence for bipolar pulses at twice the inception voltage level

When increasing voltage at twice the inception voltage, partial discharges occur during every rising or falling edge of the power signal. This may explain why discharges also occur after polarity changes in Figure 93 at 115mbar since the inception voltage of this sample at 115mbar is between 350Vpeak and 400Vpeak.

Another key issue is related to the magnitude of the discharges. The results show that their magnitude at 115mbar is lower than at 1000mbar.

The magnitude of the discharges, measured on the oscilloscope, is a voltage that depends on the discharge current. This current depends on the quantity of charge flowing during avalanche. When the pressure is low (115mbar), the density of gas molecules is low, and consequently the number of gas molecules available for ionization is reduced. Therefore, a lower number of charges (electrons and ions), coming from the ionization and leading to the avalanche, is created. Therefore, the magnitude of the discharges at low pressure should be lower than at high pressure.

Tests with the twisted pair of enameled wire confirm that the proposed sensing method is able to detect partial discharges above the switching noise of the converter. In the next test, the twisted pair of enameled wire is connected at the input of the converter.

b) Twisted pair on the AC side

To determine if partial discharges can be measured on the AC side and over the noise of the converter, tests have been done using setup in Figure 96. A twisted pair of enameled wire is placed between two phases at the input of the converter and the sensor is placed on the same side.

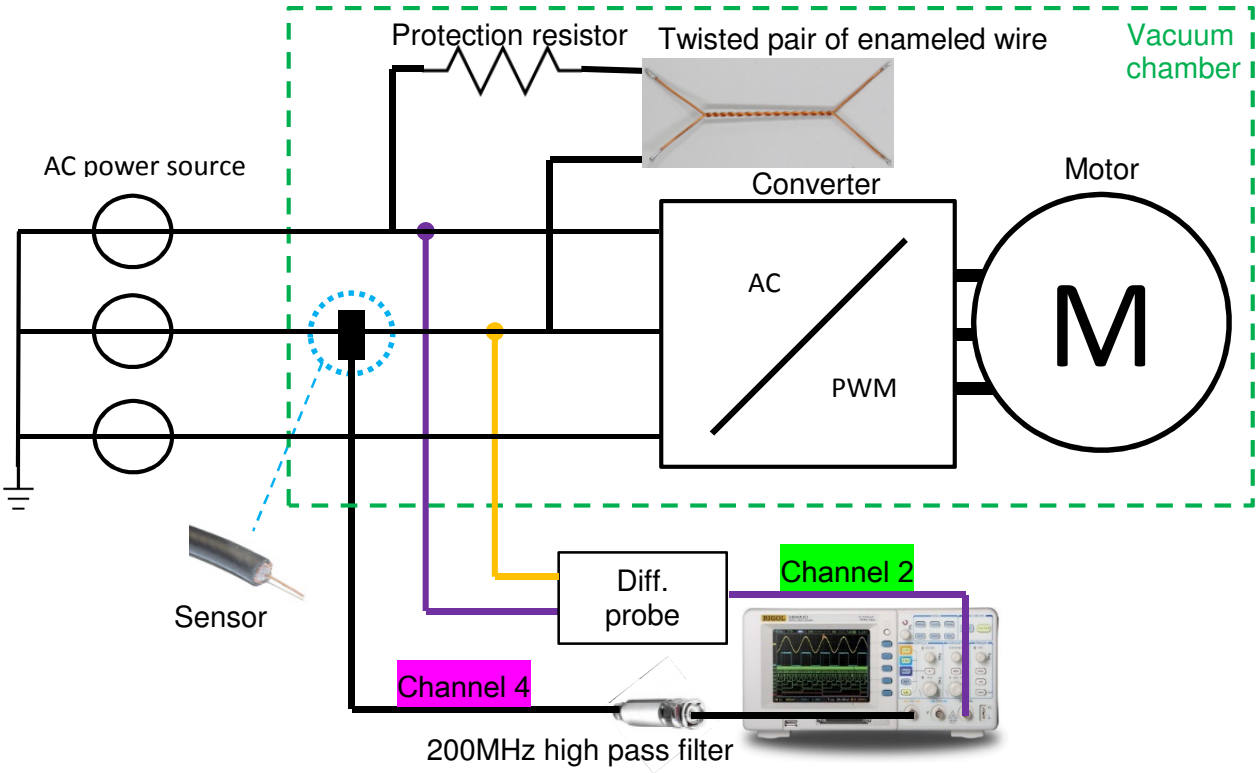

Figure 96: Setup with twisted pair of enamelled wire connected at the input of the converter

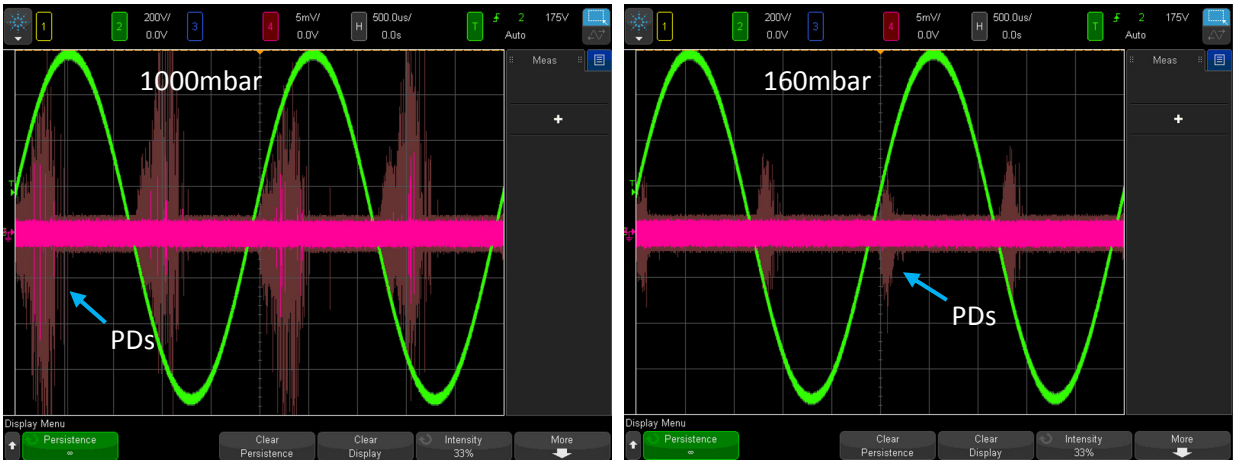

Figure 97: Partial discharges measurement on a twisted pair of enameled wire at the converter input. Channel 2: Phase to phase voltage (A and B). Channel 4: Partial discharges detection on phase B using a 200MHz filter.

Figure 97 shows that many discharges with significant magnitudes are detected despite converter noise.

The main conclusion on the measurements using the twisted pair of enameled wire is the ability of the sensing method to distinguish partial discharges from the noise of the converter.

4.3.5.2 Detection of partial discharges through the converter

In order find out whether the discharge current is able to flow from the converter input to the converter output, and vice versa, we decided to perform measurements as described in the following setup (Figure 98).

a) Sensor on the AC side

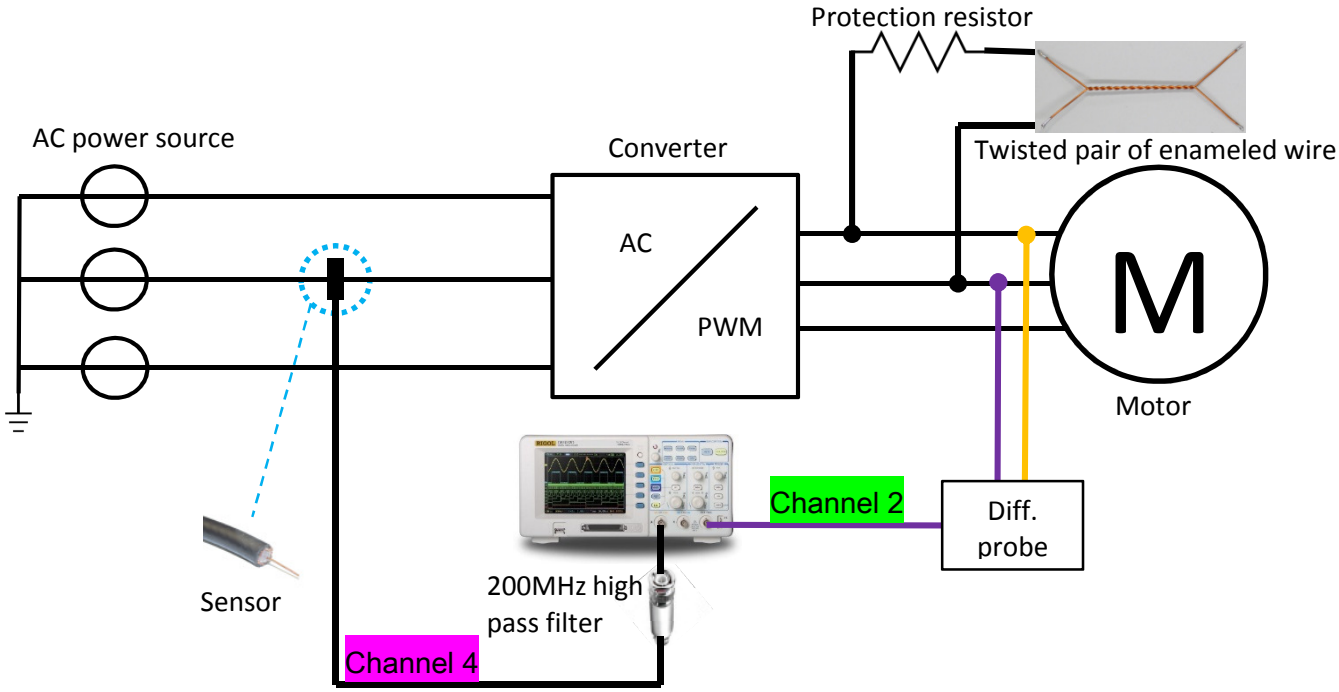

Figure 98: Setup to detect at the input of the converter partial discharges occurring at its output

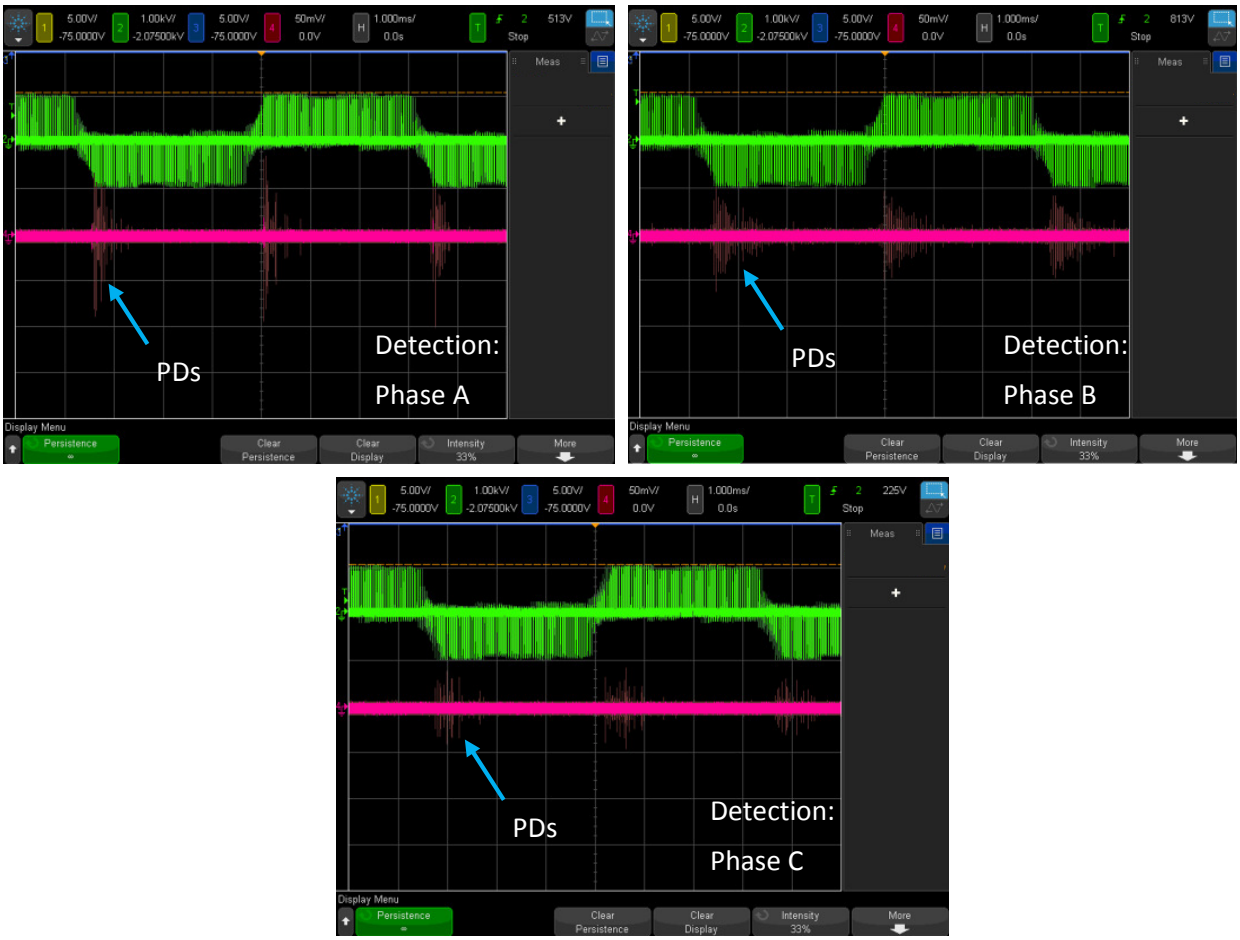

Figure 99: Measurements at the input of the converter when partial discharges occur at its output. Channel 2: Phase to phase voltage (A and B). Channel 4: Partial discharges detection on phase B using a 200MHz filter.

The measurements in Figure 99 shows that partial discharges are detected even if the sensor is placed at the input of the converter.

b) Sensor on the PWM side

The twisted pair of enameled wire is now connected to the converter input (AC voltage), while partial discharges sensing is performed at the converter output as shown in Figure 100. Voltage is increased above the PDIV level of the twisted pair (>700Vpeak), and the results are shown Figure 101.

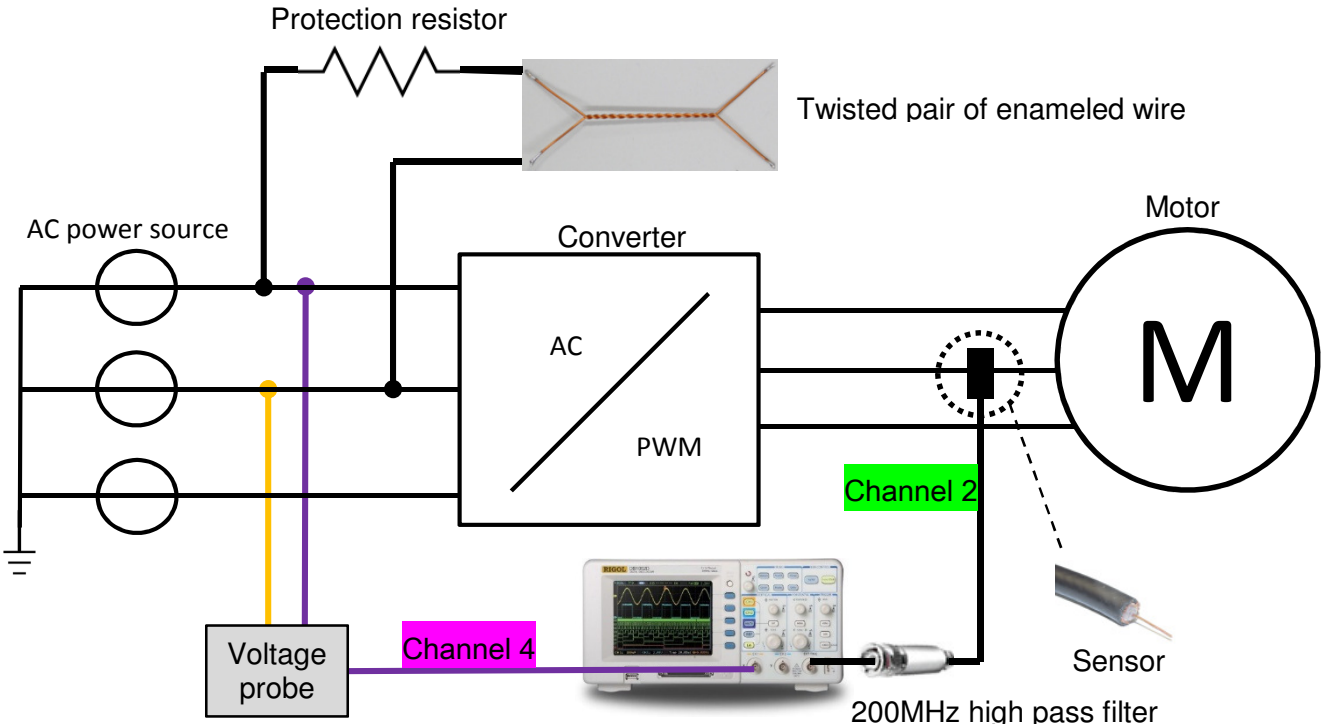

Figure 100: Setup to detect at the output of the converter partial discharges occurring at the input

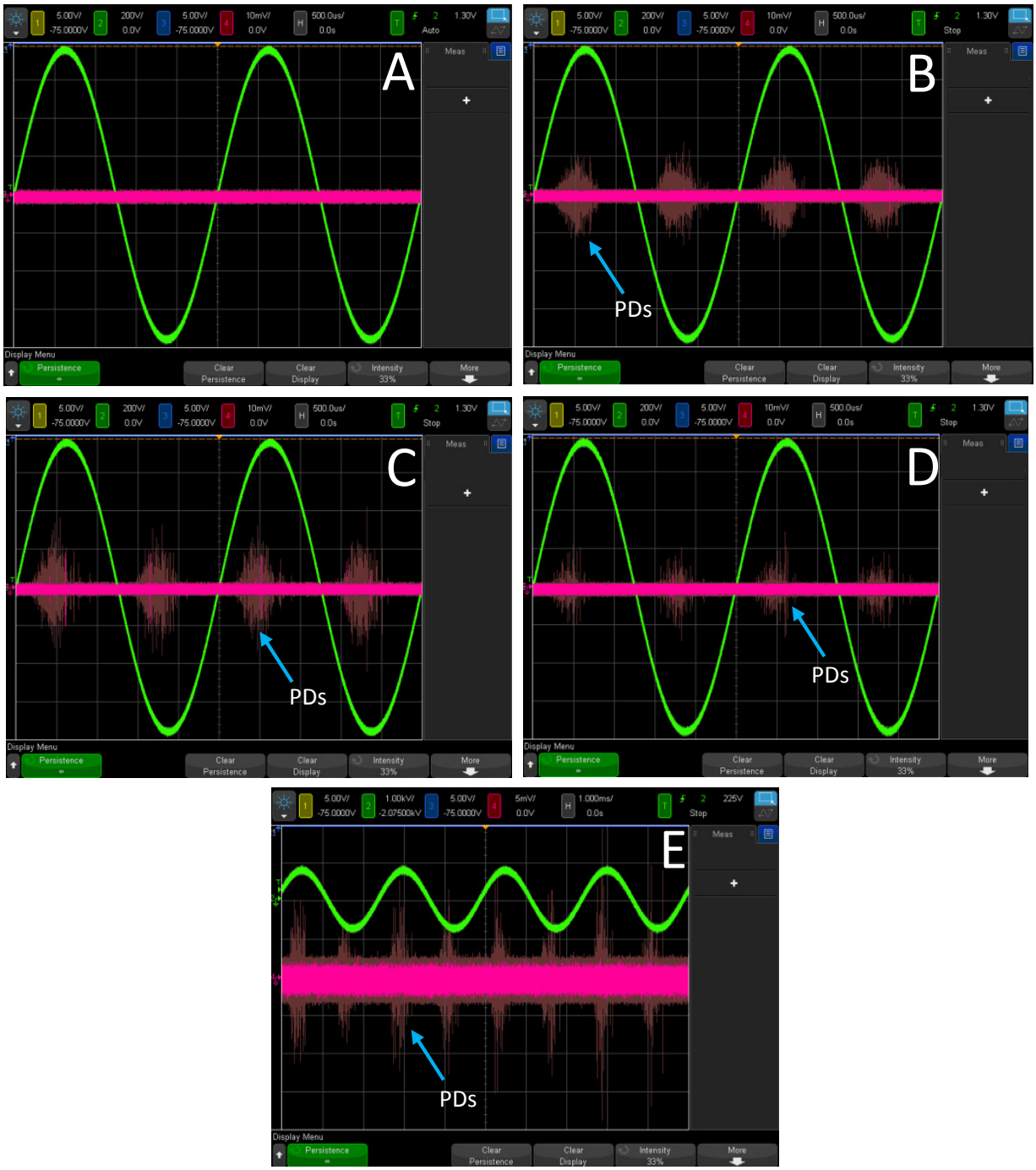

Figure 101: Measurements at the output of the converter when partial discharges occur at the input. Channel 2: Phase to phase voltage (A and B). Channel 4: Partial discharges detection on phase B using a 200MHz filter.

Picture A: Twisted pair: Not connected ; Inverter: Off ; Detection: Phase A
Picture B: Twisted pair: Connected ; Inverter: Off ; Detection: Phase A
Picture C: Twisted pair: Connected ; Inverter: Off ; Detection: Phase B
Picture D: Twisted pair: Connected ; Inverter: Off ; Detection: Phase C
Picture E: Twisted pair: Connected ; Inverter: On ; Detection: Phase C

These pictures shows that the sensor is able to detect partial discharges wherever they occur (at the input of the converter by sensing at the output of the converter by example).

This investigation demonstrates that, on this converter, no matter where the discharges occur inside the converter, they can be detected by the proposed sensing method. The only limitation may be the magnitude of the discharges that can be reduced over a certain distance.

4.3.5.3 Ozone detection

For purposes of comparison with the previous results, it is interesting to use the chemical detection in order to comfort us in one of our main conclusion: the converter is partial discharges-free. Ozone sensing paper [Macherey] has been used. This paper shows at its extremity a white square whose color varies from white to brown (depending on ozone concentration) when ozone is detected.

The converter is placed inside the vacuum chamber, and the motor stays outside since, as shown in previous sections, it is supposed to produce partial discharges (only ozone coming out from the converter is intended to be measured). One of this sensor is placed at the bottom of the chamber, below the converter. The ozone being heavier than air, we would expect to find a higher concentration of ozone at the bottom of the chamber than at the top. The vacuum is created in the chamber and the converter is started. The system ran in this configuration during two hours. Figure 102 shows the results: the ozone tester A is still white, which means that no ozone has been detected.

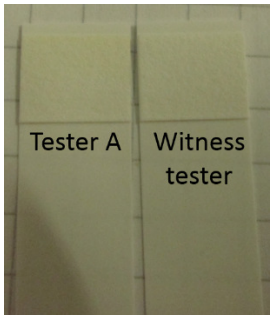

Figure 102: Ozone test in the vacuum chamber, with only the converter running. No PD detected.

Afterwards, we connected the twisted pair of enameled wire to the converter output (PWM voltage), then the voltage is increased to the maximum value allowed by the AC power source (312Vrms), and the pressure is decreased. A photo is taken in the darkness (Figure 103).

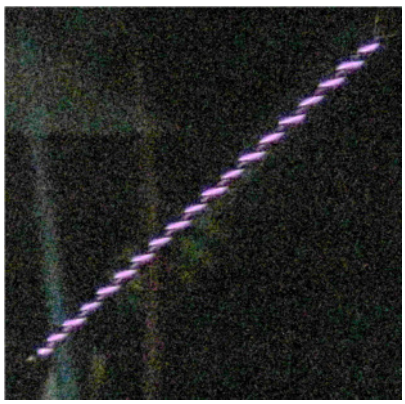

Figure 103: Glowing discharges from a twisted pair of enameled wire connected to the convert output, at low pressure

Glowing discharges can be observed, as was also the case, under PWM voltage, during our investigation of the constituents (c.f.4.1.2.4). This highlights intensive partial discharges activity. During this test, an ozone paper was also put in the chamber, close to the glowing twisted pair. Figure 104 shows the result after waiting only 5 minutes.

Figure 104: Ozone test in the vacuum chamber, with converter running and twisted pair of enameled wire

Regarding the datasheet of the ozone paper, the darker is the color, the higher is the ozone concentration. A legend allows to give an estimation value. Here, it seems that ozone was detected by tester B at a level between 150 and 210 µg/m³. As a comparison, above 180 µg/m³, the ozone concentration may cause eyes irritation and respiratory problems.

4.3.6 LONG TERM EFFECTS

The large magnitude of the pulses described in chapter 4.3.3 showed a complex behavior. The firsts tests did not reveal any pulse, or sometimes only very briefly. After several minutes of testing, an increasing numbers of pulses appeared. After a while, it was no longer possible to count them and at the end of the day no more discharges were measurable. We therefore suspected an effect related to motor temperature. Fortunately, the motor is equipped with internal temperature sensors. We decided to perform a long-term measurement starting at the beginning of the day. We also measure the relative humidity surrounding our system. The voltage is set to the rated value of the converter during the overall test. Figure 105 shows the results that we obtained from this experiment.

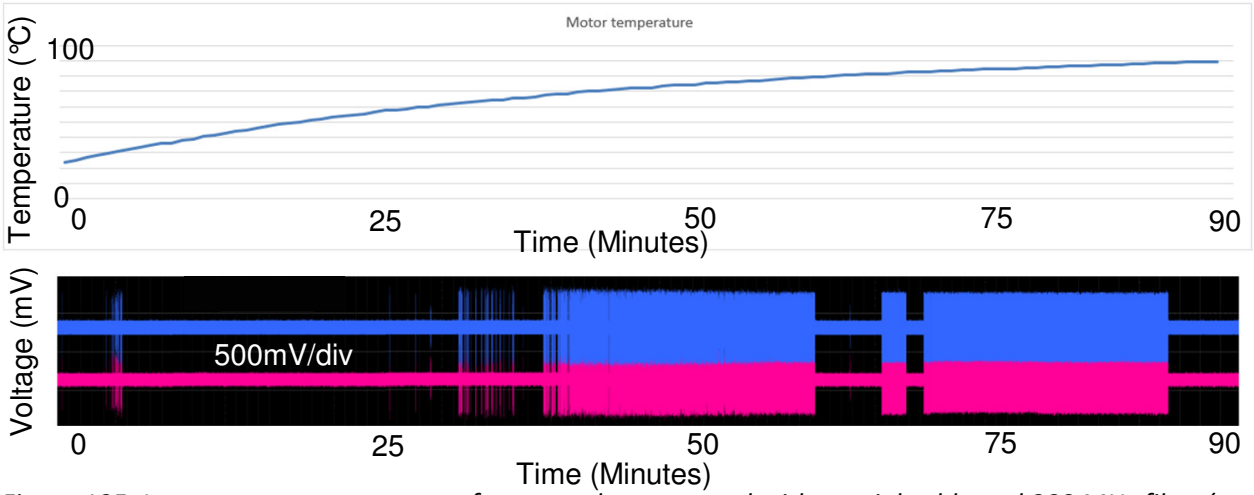

Figure 105: Long-term measurements of motor pulse measured with coaxial cable and 200 MHz filter (total test duration: 90 minutes) on day 1

Two sensors are used, the first using the 200MHz high pass filter (blue curve) and the second using the 400MHz high pass filter (pink curve). The pulses being so large, no differences are measurable between the two filters.

The first remark is that the temperature increases with no noticeable disruption. Moreover, the progression of the curves is logical: over time, the motor heats and the temperature increases. Then, looking at the pulse graph, we observe very irregular behavior: at the beginning of the test, almost no pulses appear. After half an hour, a group of pulses appears very scattered. After 40 minutes, the number of pulses increases drastically. This would seem to indicate that pulses start at a certain temperature threshold. We could then assume that temperature has an effect on the occurrence of these pulses. However, after one hour, the pulses stopped suddenly. Then, they reappeared for a period of 20 minutes before stopping definitively.

The behavior described here above appears to be repeatable from one day to the following one. Figure 106 shows the same test the day after.

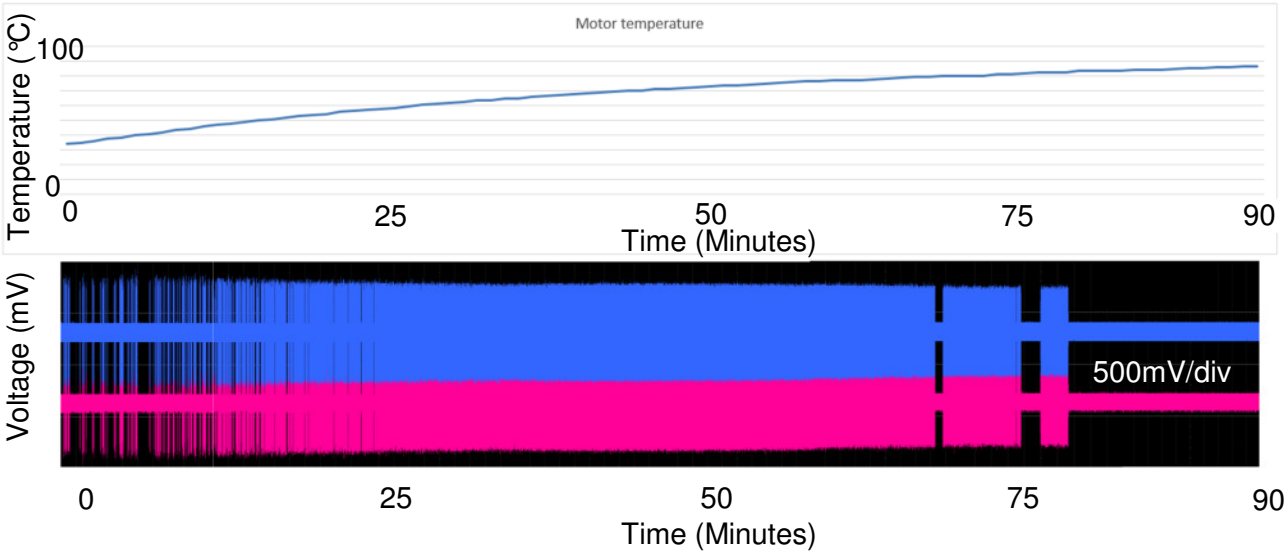

Figure 106: Long-term motor pulse measurements, measured with coaxial cable and 200MHz filter (total test duration: 90 minutes) on day 2

We observe that the temperature thresholds at which the pulses start or stop are relatively similar during both tests. In the first measurement, pulses start at around 30°C and stop completely at 90°C. In the second measurement, pulses start at around 33°C and stop completely at 82°C.

	Pulse start temperature	**Pulse stop temperature**
Test 1	30°C	90°C
Test 2	33°C	82°C

Table 15: Summary of pulse ignition and extinction as a function of temperature

Even if the start and stop thresholds seem to be quite similar, pulses behavior is absolutely not the same during the tests. One hypothesis could be that the increase in temperature slightly modifies irreversibly the structure of the insulating material in the motor. This would induce defects in the material that allow discharges to occur and stop irregularly. Over time, the material would continue to be modified randomly. Therefore, from one test to the other, the occurrence of the pulses would not be the same. If this explanation is correct, it means that the discharges measured inside the motor are internal. Making this assumption, since temperature increases with time (and thus pressure increases within the defect), no more discharges can occur at a certain temperature threshold. Consequently it is most likelihood that the huge discharges measured in the motor are internal discharges. This assumption is supported by the fact that the discharges behavior does not change with pressure variations.

4.3.7 CONCLUSION ON THE MEASUREMENTS ON THE POWER CHAIN

Measuring partial discharges on a system in operation is a challenging task, as it involves many parameters. We encountered some difficulties, not only regarding detection, but also with respect to analyzing our observations. However, by moving forward one step at a time, we reach some important conclusions.

First of all, and not the least, the sensing method proposed in this thesis allows for the first time on-line partial discharges sensing under PWM voltage and low pressure.

Second, the partial discharge sensing method proposed in this thesis proved its efficiency in the harsh environment of an aeronautical converter (switching noise, low pressure). Even if no discharge has been detected on the system itself, using the twisted pair of enameled wire shows that the method is fully able to detect partial discharges if they occur.

Third, we proved the existence of partial discharges in the motor. Even if it was not among our initial objectives, we decided to pursue this point. These discharges have very complex behavior. We showed that they are probably internal discharges, and that they are not influenced by pressure. The effect of temperature on these discharges is not well understood at this time, but proof of their existence was made.

Fourth, the investigation in chapter 4.3.5.2 shows that, no matter where the discharges occur, we are able to detect them using this method.

Lastly, the results show that partial discharges cannot occur in the converter either at ambient or at low pressure. The discharges detected on components, during the component analysis phase, are suppressed when the components are mounted into the system.

5 CONCLUSIONS AND PERSPECTIVES

5.1 CONCLUSIONS

Looking for designing partial discharge-free systems for aerospace applications, Liebherr Elektronik Lindau undertook a study to develop a method for on-line partial discharges detection in aeronautics power electronics converters.

For this study, a relationship between Liebherr and the Laplace Laboratory in Toulouse has been established. The Laplace laboratory offering expertise in the partial discharges field, and Liebherr being an aeronautical manufacturer, this relationship was an ideal opportunity to perform original partial discharges measurements on actual aeronautics power systems.

The goal of Liebherr is to make PD free converter per design. The main difficulty when measuring partial discharges with such a device is to make the distinction between converter switching noise and the discharges' signal. For many years, experiments have been performed with numerous detection methods to overcome this challenge. However, none of the experiments yielded workable results until the work of Thibaut Billard and Thierry Lebey [Billard], in partnership with Renault in France. Using a stripped coaxial cable, they succeeded to perform partial discharges measurement despite the switching noise. Following their works, LEG decided to apply this detection method, on-line, to their aeronautics products. This thesis describes a study conducted to reach these objectives. The study was divided into three steps.

- First, the method was tested on basic samples (twisted pairs of enameled wires, vented samples, and needle-to-plane), which were made with materials used in the aerospace industry. In order to be representative of the field we are studying, tests were all performed at both 1000mbar and 115mbar. The aim of this step was to establish the limits of the detection method, and to confirm or invalidate that it is able to detect partial discharges of different natures, occurring in different defects. The results of this first investigation showed that the method is indeed able to detect discharges occurring internally (vented samples), externally (twisted pair), or in the vicinity of a magnified electric field (needle-to-plane). During this phase, a particular phenomenon was observed, called a pseudo-glow discharge, in which it was no longer possible to detect discharges, but a glowing effect continued to be present at the surface of the sample. Though the studied detection method does not detect this type of discharge, an analysis of the effects revealed its existence.

- Secondly, we continued deeper into the converter study. We chose to study the converter supplying the motor that controls the FLAP parts on the A350 aircraft. A list of components used in this converter was provided, and the components were then tested with the new detection method. Once again, the components were tested at 1000mbar and 115mbar. By testing the components separately, we were able to identify weak points and reach a conclusion regarding the influence of system assembly on partial discharges. Indeed, partial discharges may not occur on a component and occur inside the system and vice versa. Mainly, the investigation showed two weak points: the first is the converter's male output connector, which showed an inception level reachable when transients occur; the second is the input filter, which showed an inception level reachable by nominal voltage.

- Lastly, the complete converter was tested. The system was also tested at 1000mbar and 115mbar. Still using the proposed method, we measured some pulses on the PWM side and none on the AC side. It was quite difficult to reach a conclusion regarding their nature. Indeed their random occurrence made it difficult to distinguish between partial discharges and external noise. Finally, day after day, we observed that the phenomenon was repeatable and depended on voltage magnitude. Therefore, we concluded that these pulses were partial discharges. The next step was to establish the origin of these discharges. Furthermore investigations taught us that discharges were coming from the motor. It was therefore possible to assert that the converter is partial discharges-free. Additional measurements showed that it is possible to measure discharges through the converting chain.

Completing the third step of our investigation, we are able to conclude that the detection method, can be used to detect on-line partial discharges in an aeronautics environment. The method is efficient and enables detecting discharges occurring in various defects (external, internal, corona). Most significantly, the method makes it possible to distinguish between partial discharges and switching noise.

During this investigation, Liebherr Elektronik GmbH desired to develop a PD-free PWM generator for representative PD tests. This system was built and tested using the proposed method, and was then proven to be PD free. (c.f. 6)

5.2 PERSPECTIVES

From the overall investigation, the striped coaxial cable method appears to be able distinguishing between partial discharges signals and switching noise. However, the way the coaxial cable senses discharge current is not well understood at this time. Proper understanding of the sensor is required to optimize sensing. This means that additional investigations have to be carried out to specify the characteristics of the detection method and its application limits.

A particular phenomenon was observed during the first phase of the measurements (constituent study). The tests on a twisted pair of enameled wire, subject to pulse-like waveform at low pressure, revealed that some discharges may exist with a glowing form, but it is not possible to detect them with our method. This phenomenon was already been observed and described a few decades ago by [Bartnikas1]. It means the sensing method fails to detect nature of discharge. Further investigation must be carried out to better understand this glowing phenomena and to find a way to detect them.

Another particular case was been observed on a point-to-plane sample. This sample showed an asymmetrical pattern on the oscilloscope at ambient pressure. Some discharges were visible on the negative polarity of the sinus curve. Once pressure was decreased to 115mbar, the discharges changed position and occurred on the positive polarity of the sinus curve. It is still not well understood why this happened. Furthermore, investigations should be undertaken to understand the behavior of corona discharges under various conditions (pressure, temperature, humidity), but also to modify the shape of the samples and their constitution. For example, this could include modifying the distance between electrodes and applying coating at different places (on the plane,

on the needle, on both). The objective would be to answer these questions clearly: “Why does a point-to-plane sample show an asymmetrical pattern,” and “is that always the case?”

Lastly, it would be very interesting to apply this detection method on various converters using different IGBT in order to validate that the method is applicable, regardless of the IGBT switching dV/dt, or simply to define its limitations. Additional work needs to be carried out in this direction.

6 ANNEXE A: PARTIAL DISCHARGE-FREE CONVERTER DESIGN

Recently, a commercial partial discharges detection system, made by Omicron, has been purchased by Liebherr Elektronik GmbH. This device is designed to detect partial discharges off-line, and under AC or DC voltage. The company decided to invest in buying a partial discharge free AC power source to use this detecting device.
The company develops converters using AC voltage and generating pulse width modulation (PWM) voltage. This means that investigations, regarding partial discharges, must also be carried out using PWM voltage. However, no partial discharge-free PWM power source was available from the company. Therefore it was decided to develop such a system. This section describes the system and its characteristics.

6.1 SYSTEM DESCRIPTION AND REQUIREMENTS

The requirements of the power source were defined as follow: the device shall be partial discharge free. It shall generate PWM voltage up to 2kV with a 10kHz switching frequency. The topology used is H-bridge.

To answer the first requirement, some precautions are taken:

- Any distances between high voltages conductors are defined above two times those found in Paschen's law minimum.
- Sharp edges are avoided on the layout or on the assembly to prevent any corona effects.
- High voltage components are chosen with a maximum voltage at least 1000V above the maximum voltage of the system, namely 3000V.
- In order to validate the partial discharge-free design, a partial discharge test is performed using the partial discharges detection method presented in the work.
- The AC input voltage must be partial discharge-free. Therefore the purchased partial discharges-free AC power source is used as the input source.

Once the system is assembled, it is inserted into the safety box. To set output voltage, the user must set the AC voltage.

Figure 107 shows the architecture of the PD-free PWM power source.

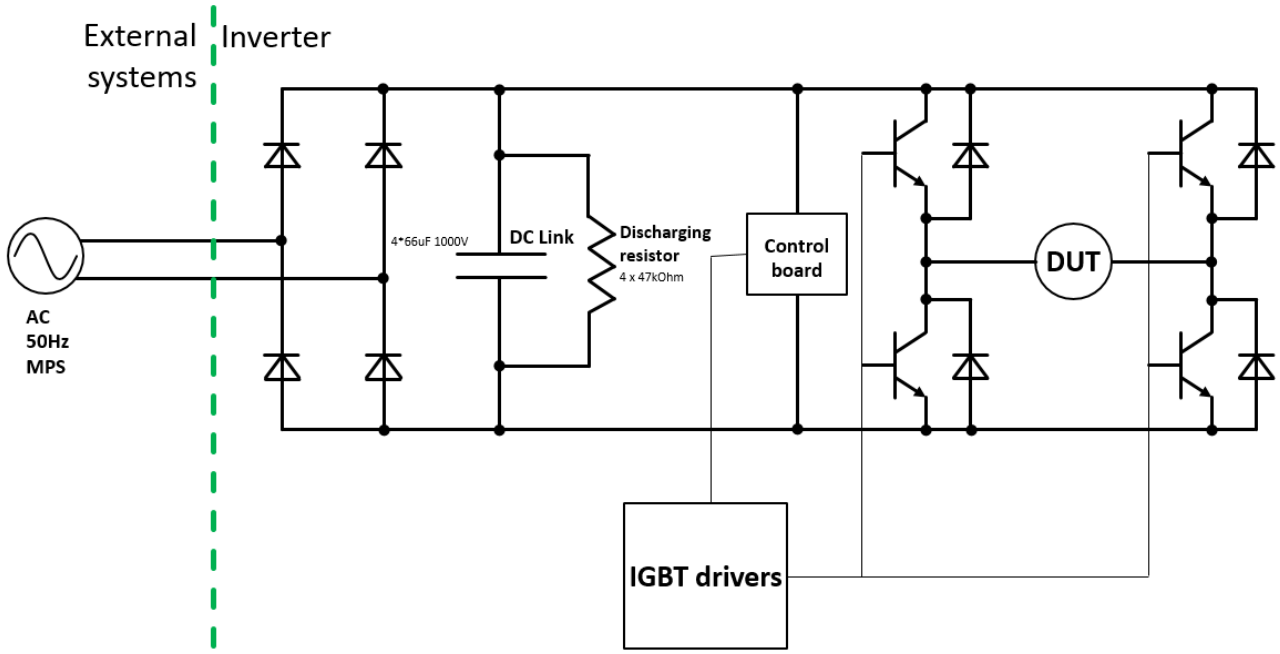

Figure 107: Architecture of the PD-free inverter

The partial discharges-free AC power source is first rectified by a diode bridge. Afterwards, voltage is smoothed by coupling capacitors. The parallel resistors control the capacitor discharge when voltage is off. The calculation of the discharge time, until reaching 50V, is shown below.

$$t = \mathrm{R} * \mathrm{C} * \ln \frac{\mathrm{Vtarget} - \mathrm{Vinit}}{\mathrm{Vfinal} - \mathrm{Vtarget}}$$

Equation 4: Calculation of the capacitor discharging time

R = 188kΩ
C = 16.5uF
Vtarget = 50V
Vinit = 2000V
Vfinal = 0V

The time required to discharge the capacitor from 2kV to 50V is: **t = 11.36 s**. It means that the safety box must not be opened until this time is elapsed. A red lamp warns the user. Afterwards, DC voltage is monitored by the control board. This board is also used to control the IGBT drivers. It uses a microcontroller which generates a pulse width modulation representative of an aeronautics system. Lastly, the DC voltage is used by the IGBTs, which generate the PWM voltage to supply the device under test.

6.2 PERFORMANCE EVALUATION

Once built, the converter underwent a series of tests to validate its characteristics and efficiency. The tests are described in this section.

First of all, the maximum voltage value was reached and the voltage waveform, which is supposed to be a PWM, was verified. The voltage is indeed a PWM, reaching 2000Vpeak as shown in Figure 108.

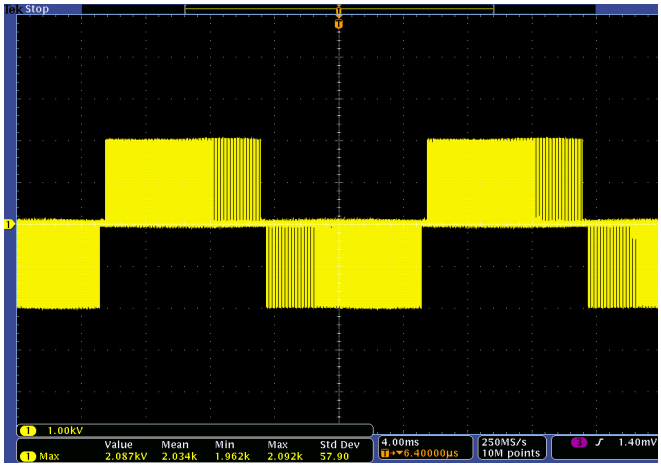

Figure 108: Output voltage of the converter

The most important characteristic of this converter is that it is intended to be partial discharge-free, and thus appropriate for use in partial discharges tests. To validate this point, the setup Figure 109 is used.

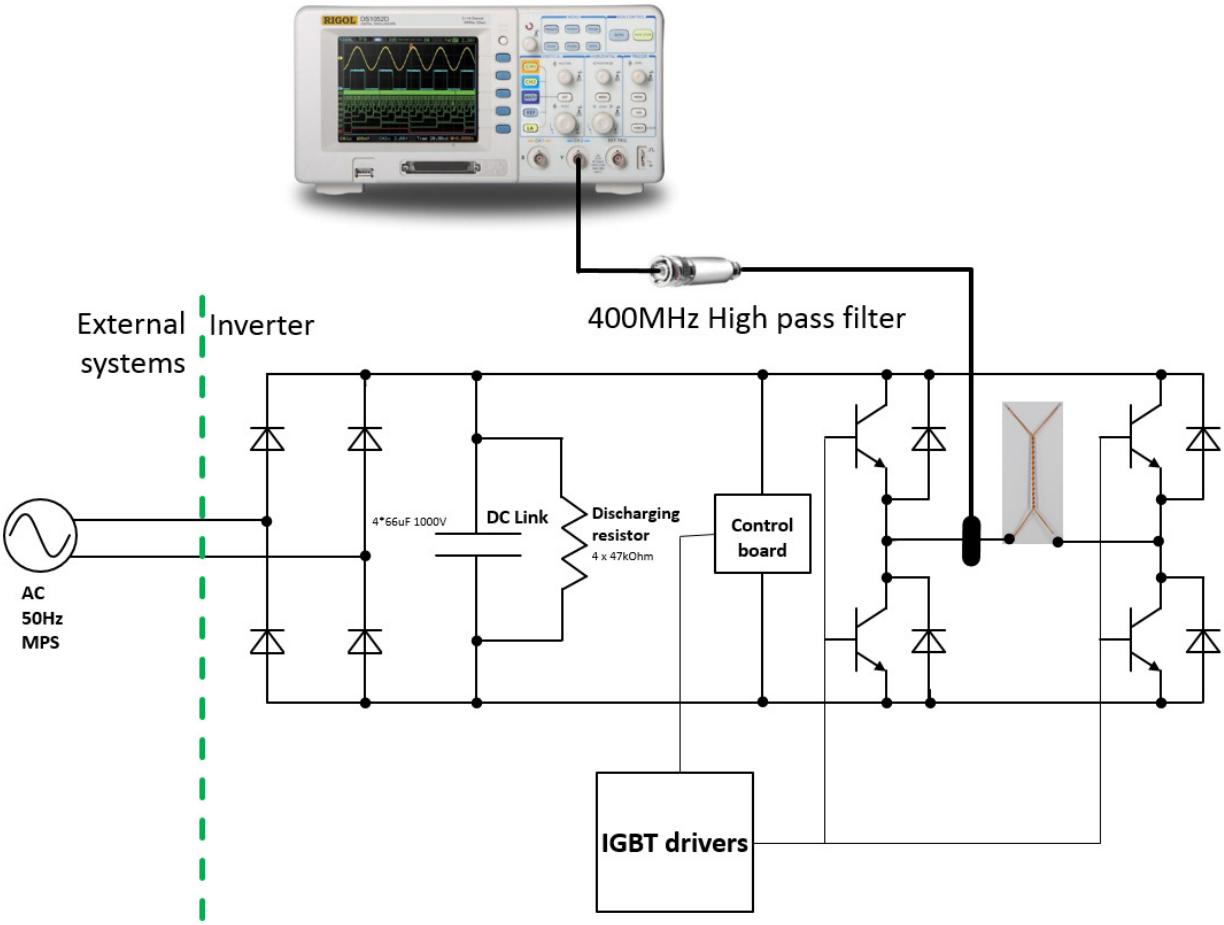

Figure 109: Setup for partial discharge test on the PD-free converter

a) Without sample

First of all, the twisted pair of enameled wire is not connected, and voltage is increased to 2000V (Figure 110).

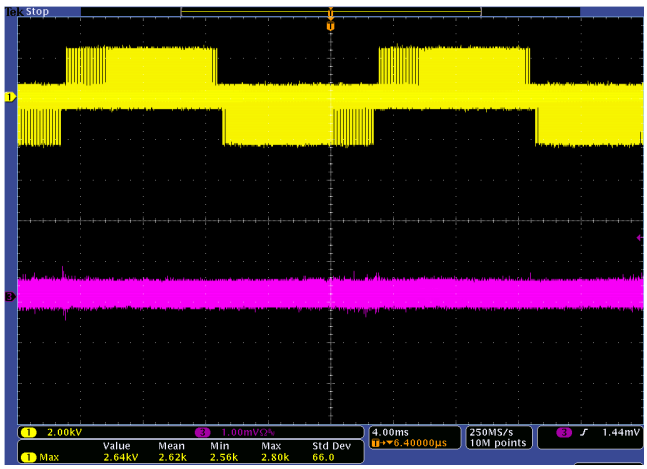

Figure 110: Measurement of signal from the sensor at 2000V

Some small pulses can be observed at the voltage polarity change. Their linear behaviors with voltage allow us to conclude that these pulses are not partial discharges, but switching noise. Figure 110 shows that no partial discharge are detected.

b) With the twisted pair of enameled wire

The twisted pair of enameled wire is added, as shown in Figure 109. The voltage is increased until partial discharges occur and the inception voltage is measured at about 700Vpeak.

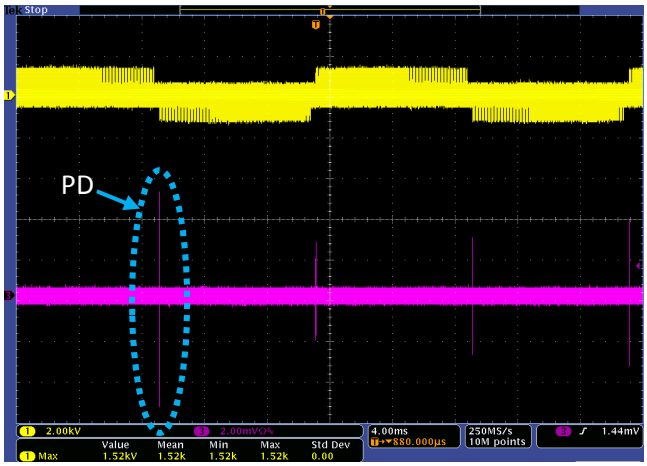

Figure 111: Partial discharges measured on a twisted pair of enameled wire slightly above PDIV

Some pulses can be observed at polarity change. These pulses did not exist before 700Vpeak, and they suddenly occur at 700Vpeak. This non-linear behavior is typical of partial discharges. Moreover, the pulses can be distinguished clearly from background noise.

During the test, the voltage is increased until some changes are perceptible. No changes are visible on the pulses up to 1300Vpeak, except their magnitudes, which is increased. Around 1400Vpeak, new types of discharges are measurable between the polarity changes (Figure 112).

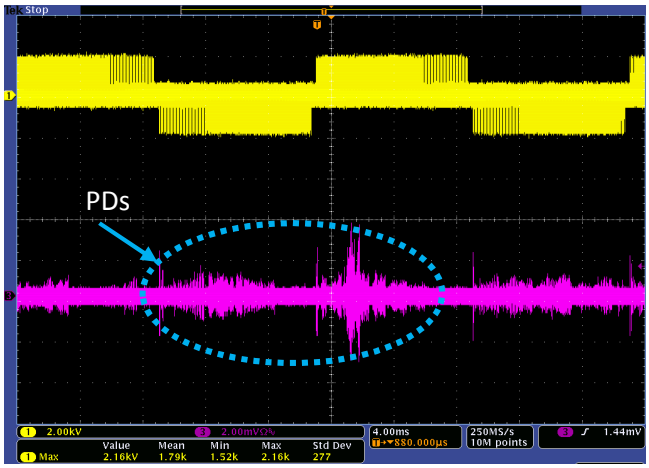

Figure 112: Partial discharges measured on a twisted pair of enameled wire at 2 x PDIV

The measured numerous impulses have a magnitude lower than the ones measured at PDIV. We can assume that the nature of the discharges has changed with the increase of the voltage. At twice

the inception voltage, a glowing phenomenon started to be visible on the sample, as shown in Figure 113.

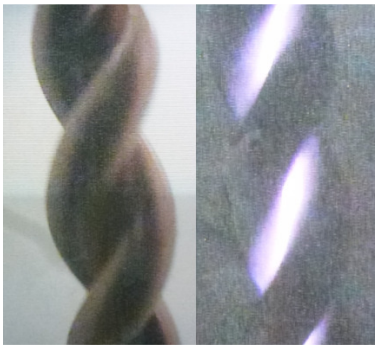

Figure 113: Glowing effect on the sample at 2 x PDIV

c) With a point to plane sample

The twisted pair of enameled wire is now replaced by a point-to-plane sample in order to create corona discharges (Figure 114). This sample is expected to show an asymmetrical pattern when discharges occur.

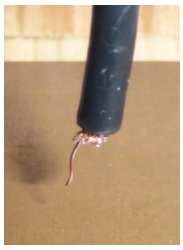

Figure 114: Point-to-plane sample to create corona discharges

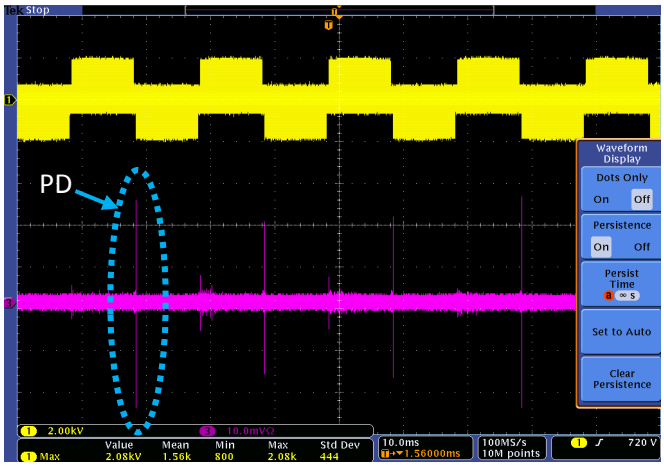

Figure 115: Partial discharges occurring on a point to plane sample

Some pulses are measurable at 1.7kV when the voltage switches from positive to negative. Some pulses are also visible when the voltage switches from negative to positive, but their magnitudes are well smaller. This pattern is clearly asymmetrical and is characteristic of corona discharges.

d) A350 high voltage connector

The next test focuses on the male part of high voltage connector used in the studied converter. These components showed partial discharges with a corona shape (asymmetrical shape) at about 910Vpeak. The test has been repeated with the partial discharges-free PWM generator. The results are shown Figure 116.

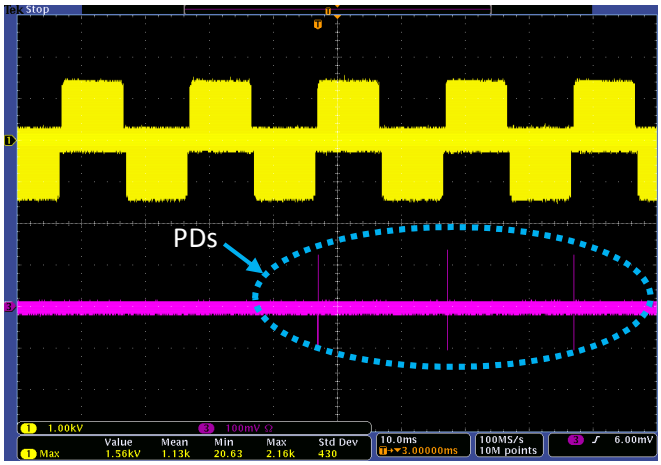

Figure 116: Partial discharges measurements on the male part of the output connector from ADGB converter

Partial discharges are detected with an asymmetrical pattern, which implies that corona discharges are occurring. However, the inception voltage in this case is about 1.1kVpeak, which is above the PDIV measured at the Laplace laboratory (910Vpeak). This difference may be due to environmental parameters (humidity and temperature) that may have been different during the tests at the Laplace laboratory in February, 2015. Tests at Liebherr were performed in July, 2015. However, the results are similar to those obtained at the Laplace laboratory.

6.3 CONCLUSION

The series of tests described in this annex outlines the characteristics of the partial discharge-free converter. First, no partial discharges were measured when no samples is connected. This means that the converter is partial discharge-free. Then, the series of tests demonstrate good consistency with previous tests which were performed at the Laplace laboratory. The twisted pair of enameled wire has the same inception level (+/- 50V). The point-to-plane sample shows an asymmetrical pattern. The A350 connector showed the expected behavior regarding the measurements obtained at the Laplace laboratory. Therefore it can be concluded that this PWM power source can be used to perform partial discharges investigations.

7 ANNEXE B: INVESTIGATION OF THE INPUT FILTER

During the components' investigation, one particular component showed partial discharges at a level reachable by the converter at rated voltage (230Vrms): the input filter. This result was expected to be found in the measurement of the system since, during our tests, this latter reached 312Vrms. However, as shown in Figure 83, no partial discharges have been measured on the AC side.

This result being surprising, we decided to perform the same measurement as in Figure 83, but this time, the component after the filter (ATRU) being disconnected from the input filter. By this way, only the input filter is tested.

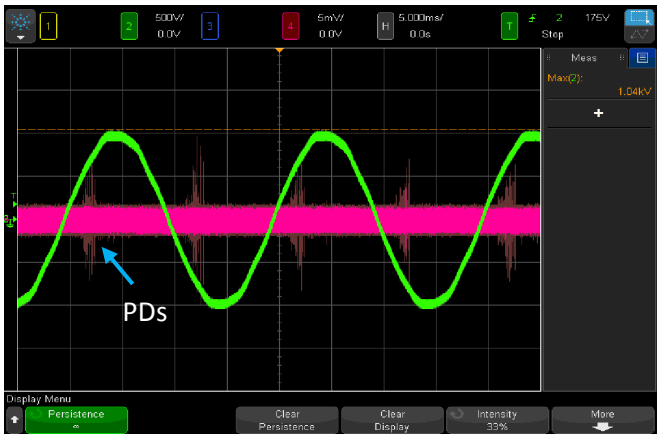

Figure 117: PD measurements at the converter input, ATRU disconnected from input filter (115mbar). Channel 2: Phase to phase voltage (A and B). Channel 4: Partial discharges detection on phase B using a 200MHz filter.

After disconnecting the ATRU from the input filter, partial discharges occur. An inception voltage of about 720Vpeak is measured, which is coherent with components' measurements.

In summary, when the input filter is tested alone, it shows partial discharges, but when it is connected to the converter via the ATRU, no discharges are measurable.

This behavior may be explained by the voltage distribution inside the input filter once this one is connected to the converter. The place where the discharges occur in the input filter, gets a lower voltage once the input filter is connected to the system. This is due to the choke (Figure 71) inside the filter which creates voltage drops when a current get through them. These voltage drops reduce the electric field inside the filter and finally suppress the discharges. Consequently, we can conclude that partial discharges cannot occur at the AC side of the converter, either at ambient or at low pressure. This, despite the fact that the input filter has been identified has a weak point during the components' investigation.

8 LIST OF FIGURES

9 LIST OF TABLES

10 LIST OF EQUATIONS

11 REFERENCES

[Rosero] Rosero J., "Moving towards a more electric aircraft", IEEE aerospace and electronic systems magazin, Volume 22, Number 3, p. 3-9, 2007

[Roboam] Roboam X.,"More Electricity in the Air: Toward Optimized Electrical Networks Embedded in More-Electrical Aircraft", Industrial Electronics Magazine, IEEE, Volume 6, Issue 4, 2012

[Billard] Billard T., "Off-line and On-line Partial Discharges Detection in Low Voltage Motors of Electrical Vehicle fed by a PWM inverter using Non-Intrusive Sensor", 2014

[IEC60270] "High Voltage Test Technique: Partial Discharge Measurements Standard", 1968

[Cella] Cella B. "Partial discharges measurements at the constituents' level of aerospace power electronics converters", More Electric Aircraft Conference, Tolouse, 2015

[Bartnikas1] Bartnikas R., "Engineering dielectrics – Volume 1 – Corona measurements and interpretation", American Society for Testing and Materials - STP669, p53-56, 1979

[Meek] Meek J.M, "A theory of spark discharge" Physical Review, Volume 57, Issue 8, p722-728, 1940

[Bartnikas2] Bartnikas R., "Engineering dielectrics – Volume 1 – Corona measurements and interpretation", American Society for Testing and Materials - STP669, p53-56, 1979

[Austen] Austen A. E. W. and Hackett W., Journal, Institution of Electrical Engineers, Volume 91, Part I, p298-322, 1944

[Densley1], Densley R. J., "Engineering dielectrics – Volume 1 – Corona measurements and interpretation", American Society for Testing and Materials - STP669, p468-503, 1979

[Densley2], Densley R. J., "Engineering dielectrics – Volume 1 – Corona measurements and interpretation", American Society for Testing and Materials - STP669, p409-467, 1979

[ASTM1] "standard Method for Detection and Measurement of Discharge Pulses in Evaluation of Insulation Systems", D 1868-73

[ASTM2] "Standard test method for thermal endurance of film-insulated round magnet wire", D2307-05

[FC72] 3M™ Fluorinert™ Electronic Liquid, clear, colorless, fully-fluorinated liquid

[ABD] "Electrical characteristics of A350 AC and DC equipement", ABD0100.1.8.1, 2008

[Lebey] Lebey T., Patent, "Method and a device for testing a power module", Patent Number 6836125, 2004

[Liebig] Liebig S. "Characterisation and evaluation of 1700V SiC-MOSFET modules for use in an active power filter in aviation", International Conference on Power Electronics (PCIM), Nuremberg, May, 2012

[Povey] Povey E. H., "Engineering dielectrics – Volume 1 – Corona measurements and interpretation", American Society for Testing and Materials - STP669, p264-265, 1979

[Kreuger1] Kreuger F.H, "Industrial High Voltage", Volume 2, p141, 1992

[Kreuger2] Kreuger F.H, “Partial Discharge Detection in High-Voltage Equipement”, p134, 1989

[Macherey] Ozone test strips, 907 36, Macherey-Nagel